8-1985

Investigation of the dynamic behavior of soybean plants during cutting

Steve Shoulders

To the Graduate Council:

I am submitting herewith a dissertation written by Steve Shoulders entitled "Investigation of the dynamic behavior of soybean plants during cutting." I have examined the final electronic copy of this dissertation for form and content and recommend that it be accepted in partial fulfillment of the requirements for the degree of Doctor of Philosophy, with a major in Mechanical Engineering.

B. L. Bledsoe, Major Professor

We have read this dissertation and recommend its acceptance:

Robert Krane, James Euler, Fred Allen, Ray Holland, Fred Tompkins, Luther Wilhelm

Accepted for the Council:

Carolyn R. Hodges

Vice Provost and Dean of the Graduate School

(Original signatures are on file with official student records.)

To the Graduate Council:

I am submitting herewith a dissertation written by Steve Shoulders entitled "Investigation of the Dynamic Behavior of Soybean Plants During Cutting." I have examined the final copy of this dissertation for form and content and recommend that it be accepted in partial fulfillment of the requirements for the degree of Doctor of Philosophy, with a major in Agricultural Engineering.

B. L. Bledsoe, Major Professor

We have read this dissertation
and recommend its acceptance:

James A. Eiler

Robert G. Kroone

Luther R. Wilhelm

Ray W. Holland

Fred L. Allen

Accepted for the Council:

Vice Provost
and Dean of The Graduate School

INVESTIGATION OF THE DYNAMIC BEHAVIOR OF SOYBEAN PLANTS DURING CUTTING

A Dissertation

Presented for the

Doctor of Philosophy

Degree

The University of Tennessee, Knoxville

Steve Shoulders

August 1985

To my parents, for their patient support ...

and for all those times they had to answer

a question with "He's still in school."

ACKNOWLEDGEMENTS

The author wishes to express his sincere appreciation to the following:

Dr. Bobby Bledsoe for his support, guidance, and encouragement while serving as my major professor.

Dr. Robert Krane, committee member, for his advice and classroom instruction throughout my graduate program.

Dr. James Euler, another committee member, for his advice and assistance in completing my graduate program.

Dr. Fred Allen, Professor Ray Holland, Dr. Fred Tompkins, and Dr. Luther Wilhelm, the other members of my committee, for their help during my graduate program.

Paul Elliot and Walker Garner for their advice and help in constructing experimental apparatus.

John Wilkerson and Robert Freeland for their assistance with experimental hardware and software.

Fellow Graduate Students of the Agricultural Engineering Department for their assistance and friendship during the many hours of work and study.

ABSTRACT

Shatter losses of soybeans are still a substantial percentage of potential profits despite extensive research of the problem. Previous efforts have tended to be concerned with the design and operating aspects of harvesting machinery rather than the dynamic characteristics of the plant. In contrast, this study focused on the dynamic behavior of soybean plants during cutting.

Mathematical models were developed for the dynamics of the components of the soybean plant: the stalk and pod. The Euler-Bernoulli beam appeared to be a satisfactory model for the stalk, predicting modes of vibration with corresponding natural frequencies. The simple pendulum with a torsional spring was adequate for modeling some aspects of pod motion. The coupled stalk-single pod model showed the effect of the pod on the motion of the stalk to be due to: the added mass of the pod, the motion of the pod, and collisions between the pod and stalk. The model also predicted that the pod and stalk tended to move out of phase for vibration at most frequencies, and that the response of the pod to stalk vibration was frequency dependent, the most significant pod response occurring at lower frequencies.

The notion of a cutting function was introduced to represent the aspects of cutting that cause motion of the plant. For the type of cutting device used in this study, a multi-tooth circular saw blade, a sequence of pulses appeared to be an adequate mathematical model cutting function. Experimental determination of cutting functions using stalks with pods attached was hindered by the nonlinearities

caused by friction between pods and collisions between pods and the stalk.

Data collection was accomplished with accelerometers and an analog-to-digital data acquisition system. The presence of the accelerometers and cables affected the response of the plant and the instrumentation would very likely be damaged by severe plant motion; therefore, another method of sensing plant response would be more appropriate.

Digital signal analysis using Fast Fourier Transform methods proved to be an effective method of data analysis. The application of this technology to the study of crop dynamics appears as promising as it has been for other areas of vibration research.

TABLE OF CONTENTS

LIST OF FIGURES

FIGURE PAGE

FIGURE PAGE

CHAPTER I

INTRODUCTION

Background and Statement of Problem

Harvest losses have been a concern since ancient times, when crops were harvested manually. Losses were controlled by dividing the laborers into two groups: gleaners and reapers. The gleaners followed the reapers as the harvest progressed, gathering whatever was missed or dropped.

More recently, harvest losses in soybeans (Glycine max (L.) merr.) have received considerable attention. The reason for this attention is primarily financial: losses have been estimated to be as much as one third of the farmers' potential soybean profit (Quick, 1973) representing several hundred million dollars annually nationwide (Hummel, 1984).

Of all soybean losses that are incurred during harvesting, the majority occur as shatter losses due to the action of the cutterbar. Machine shatter losses, as defined by Quick and Buchelle (1974), are free beans or beans in pods that are detached from the plant as a result of machine action. Quick (1972), in laboratory tests, found that of the 9 percent of the total crop lost during harvesting, 84 percent was lost at the combine header. Of this, 61.2 percent was in the form of shatter. Furthermore, the majority of the total header loss, 79.6 percent, was attributable to the action of the cutterbar. Dunn et al. (1973) obtained similar results. In field tests, 64.1

percent of the header loss was in the form of shatter of which 81.1 percent was caused by the cutterbar.

Attempts to reduce soybean losses have generally fallen into one of four categories (Lamp et al., 1961): "(a) development of plants better adapted to harvesting; (b) harvesting when losses are less likely to occur; (c) optimum machine operation; and (d) improved harvester design."

Plant breeders have had some success in developing varieties with improved pod height, lodging resistance, and shatter resistance. However, their success in the area of shatter resistance has been limited to preharvest shatter that occurs naturally while the plant is in the field. The "shattering index" used by agronomists to indicate the natural shatter resistance of a variety has not been found to be a good indicator of that variety's resistance to machine-induced shattering. In fact, any attempts to develop soybean varieties that are machine-shatter resistant would probably be hindered by the fact that no accepted measure of this property exists at present other than the collection of actual harvest loss data (Quick, 1973).

Harvesting soybeans at high moisture content can reduce losses (Lamp et al., 1961). However, harvesting at high moisture content is not always possible due to poor field conditions. Even when possible, subsequent post-harvest drying of the crop may be required.

The selection of optimum machine operating parameters has also been investigated. Lamp et al. (1961) suggested optimum ranges for ground speed, reel index, reel height, and cutting index. However,

even optimum machine operation has not been successful in consistently reducing losses to acceptable levels.

Improvements in existing harvester designs have resulted in some reductions of soybean harvest losses. The floating cutterbar, which can follow ground contours more closely than conventionally mounted cutterbars, is one such improvement. Nave and Hoag (1975) investigated the use of narrow guard and sickle spacings, high sickle frequencies, and the use of shear bars without guards. Quick and Mills (1978) conducted tests on a floating cutterbar with narrow-pitch knife sections and multi-prong guards. Both teams reported that lower losses were possible with these arrangements. Quick and Mills, in particular, reported some loss levels as low as one percent. These experimental reductions in soybean harvest losses have not been realized in practice, however, prompting some researchers to look at new cutting devices to replace the cutterbar.

The design of new cutting devices has, by far, received the most research attention. Included among the list of candidates that have been nominated to replace the cutterbar: a high speed rotary sickle (Bledsoe, 1969), a row crop puller header (Williams and Richey, 1973), multi-tooth rotary disk blades (Hummel and Nave, 1979), a continuous band blade (Walker, 1979), flexible blade impact cutters (Hummel, 1983), and rotary disk mowers (Hall et al., 1983). However, to date, only one manufacturer has offered an alternate cutting device commercially.

Soybean harvest losses still remain high despite all of these efforts; Hummel (1984) now estimates loss levels to be around four

percent of the total crop. Therefore, the search continues for a cutting device that will reduce harvest losses to acceptable levels.

Research Approach

In the research efforts expended to date on the problem of soybean harvest losses, the soybean plant itself has been treated somewhat superficially. In effect, the plant has been replaced with a "black box." Various cutting devices and operating conditions are applied as inputs to this black box, and losses, primarily in the form of shatter, are the resulting output. Little investigative attention has been given to the particulars of how this happens.

Shatter, or more precisely, the phenomenon of the opening of pods and the resulting release of beans, has received similar treatment. Nowhere in the literature is there a step-by-step account of the mechanics of shatter. Hoag (1972) states: "There is presently a lack of basic information about the mechanics of pod failure by shattering and about what types of knowledge concerning plant properties of soybeans could be used in machine design or plant breeding programs to prevent or reduce shatter." Hoag then goes on to investigate physical properties of the soybean pod, neglecting the mechanics of exactly how shatter occurs.

One has to wonder if the knowledge that will ultimately be required to reduce soybean harvest losses to acceptable levels is not inextricably dependent on an understanding of the plant itself as a dynamic system; how it moves as it is cut and how that motion results in the shatter of pods.

If an investigation of the dynamic aspects of the plant is to be made, how should it be accomplished? The engineering approach to such a problem is to replace the physical system of interest with an appropriate (and often simplified) mathematical model. An understanding of the physical problem is achieved during the development, analysis, and solution of its mathematical equivalent. Thus, mathematical modeling of the dynamic behavior of the soybean plant seems appropriate.

No analysis of plant motion would be complete, however, without also considering the cutting mechanism. For it is the cutting device that forces the plant to move. Therefore, modeling the cutting device also seems appropriate.

Finally, mathematical efforts must be guided by some physical knowledge of the system being modeled. This knowledge, as well as validation of the model, is often obtained by experimental testing. In a problem of this nature, where previous modeling attempts do not exist, experimental testing is especially important. The acquisition of such experimental evidence is by no means a trivial process, and therefore must be considered as much a part of the problem as the derivation of the mathematical models.

Research Objectives

The specific objectives of this study were:

1. Determine appropriate mathematical models for the dynamic behavior of the soybean plant during cutting.

2. Determine appropriate mathematical models for the forces applied to the soybean plant by the cutting device that cause motion of the plant.
3. Determine appropriate methods for obtaining the experimental data necessary to develop and verify these mathematical models.

CHAPTER II

EXPERIMENTAL EQUIPMENT

Review of Literature

Experimental research in the laboratory offers several advantages over field research. Experimental conditions can be better controlled, and factors such as weather and field conditions can be eliminated. Moreover, laboratory experiments allow the use of instrumentation and high speed photography that would be impossible in the field.

Several investigators have used laboratory setups to investigate soybean harvest losses. Quick (1973) simulated the harvesting operation with a stationary header and a mobile carriage that moved soybean plants into the cutterbar. The performance of the header was evaluated by measuring the amount of crop left unharvested.

Nave and Hoag (1975) used a similar arrangement in their experiments. They used high speed film to determine the accelerations of stalks during cutting in addition to collecting the unharvested crop.

Bledsoe (1969) used a laboratory test stand to evaluate a rotary sickle. Measured variables included the input torque to the rotor shaft, shaft angular displacement, and carriage forward velocity. High speed film was also used to study the effects of the cutting device on the plants.

Laboratory arrangements have also been used to investigate the harvest of other crops. For example, McRandal and McNulty (1978)

developed a laboratory test rig to study the effect of blade velocity on energy consumption during forage harvesting. The blades were instrumented with strain gauges and the outputs from these gauges were used to calculate the work done on forage stems during cutting.

Laboratory Test Stand

A photograph of the test stand used in this study is shown in Figure 1. A schematic drawing is shown in Figure 2. The test stand can be discussed in four general parts: (1) the plant holding table, (2) the cutting device carriage and carriage track, (3) the forward velocity system, and (4) the cutting device and power supply.

Plant Holding Table

The plant holding table (Figure 3) consisted of a plywood platform into which an eight-inch diameter hole was cut. The rim of this hole was surrounded by tubular foam padding. The construction of this arrangement was such that an eight-inch diameter pot, containing soil and a soybean plant, was held firmly when placed in the hole.

The height of the platform could be varied using a handcrank. This allowed for adjustment of the level of the plant relative to the cutting device. The platform and elevating mechanism were supported by a metal framework that was bolted to the laboratory floor. The plant holding table was located relative to the cutting device carriage such that cutting of the plant and subsequent retraction of the blade were possible.

An adjustable bar was attached to the table for use in tests that

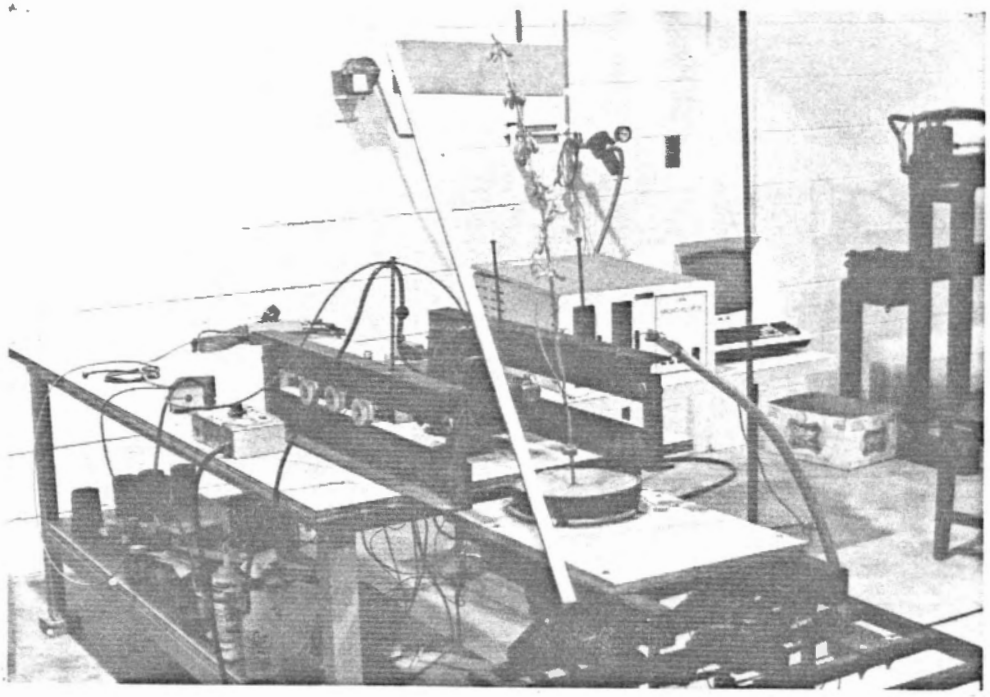

Figure 1. Laboratory test stand.

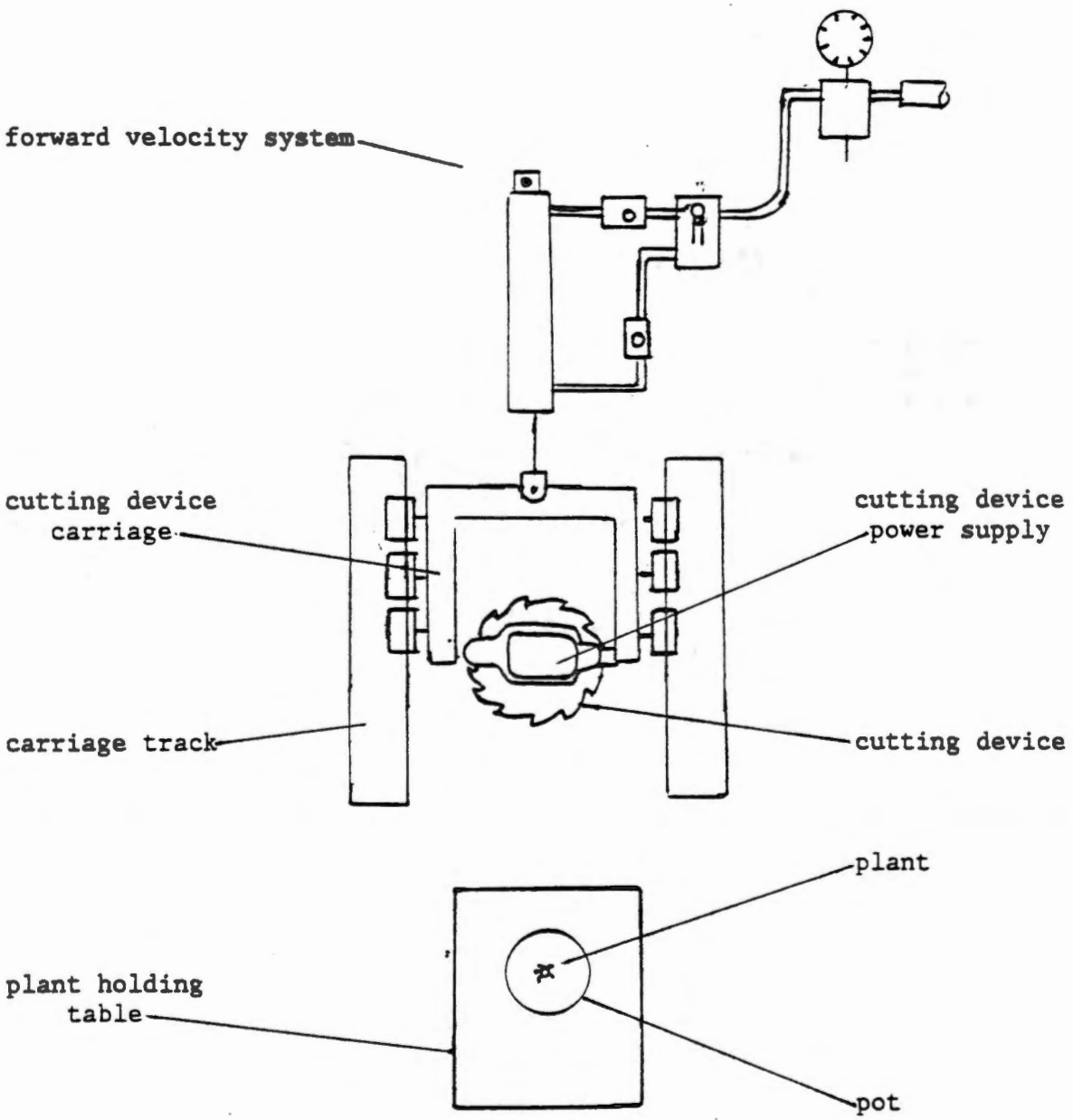

Figure 2. Schematic of the laboratory test stand.

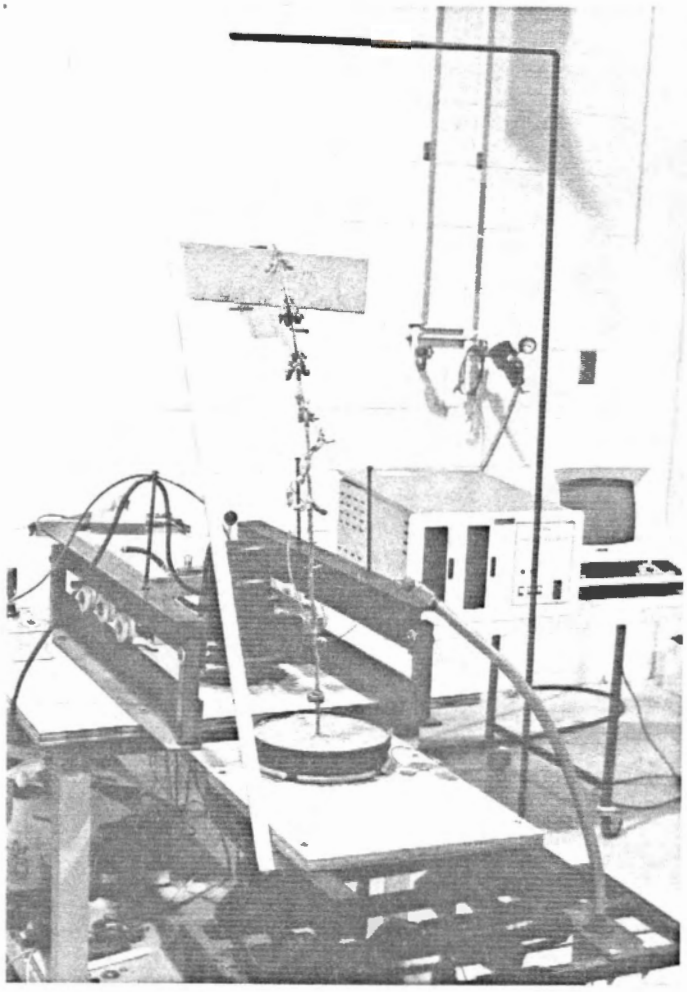

Figure 3. Plant holding table.

involved simulating the action of the reel on the plant. A bent steel rod was attached to the table frame such that it could be located over the plant. Nylon string, attached to this rod and the plant with sufficient slack for free plant motion, prevented the plant from falling into the blade after being cut.

While the frequency response of the plant holding table would ideally be low in the frequency range of interest, testing after construction revealed that the table had a natural frequency at 46 hz (hertz). In practice, this presented problems only when the table itself was directly excited by (inadvertant) contact just prior to testing.

Instrumentation of a pot revealed that some motion was transmitted from the plant to the pot during cutting tests. However, this transmitted motion was small relative to the motion of the plant itself.

Despite these problems, it was felt that this method of holding the plant was a better approximation of actual field conditions than a mechanical clamping device would have offered. However, future improvements in test equipment could certainly be made in this area.

Cutting Device Carriage and Carriage Track

The cutting device carriage and carriage track (Figure 4) provided the means to support the cutting device during its motion. The cutting device carriage was constructed of angle iron. Three nylon track wheels were attached to each side of the carriage. The offset arrangement of the wheels provided positive control of carriage motion.

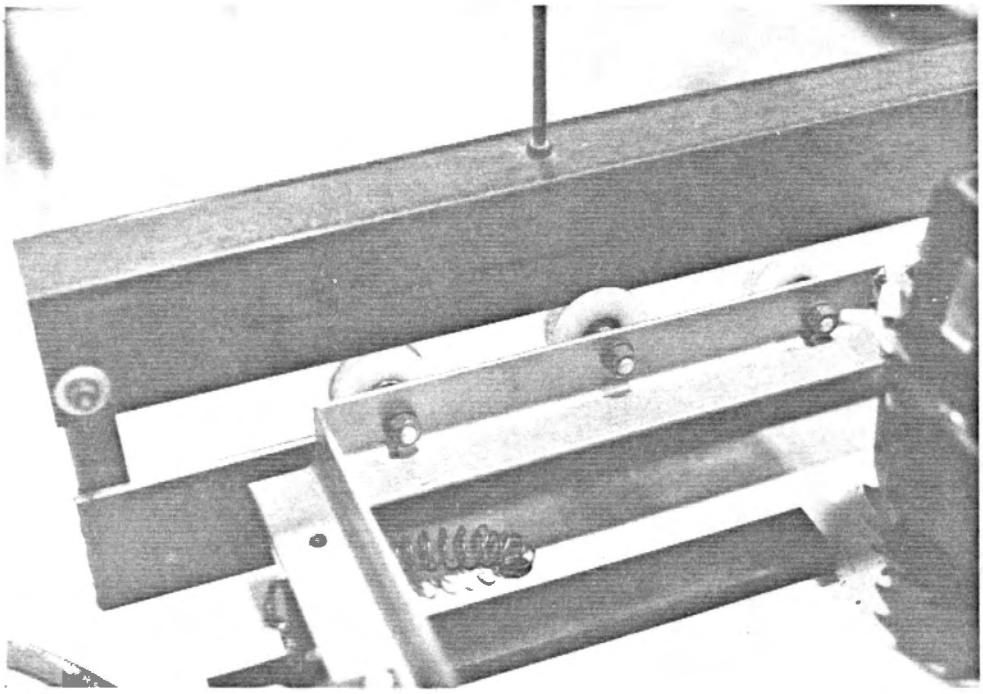

Figure 4. Cutting device carriage and carriage track.

Removable sections at the front of the carriage allowed for attachment of the cutting device.

The carriage track consisted of four sections of angle iron: two top sections and two bottom sections. Relative alignment between top and bottom sections to permit only linear motion of the cutting device carriage was possible. The two bottom sections of track were securely fastened to a supporting table.

Forward Velocity System

The forward velocity system is shown in Figure 5. A 12-inch stroke pneumatic cylinder imparted forward motion to the cutting device carriage. One end of the cylinder was attached to the rear of the carriage and the other end was attached to the supporting table.

A two-way two-position pneumatic control valve and a flow control valve were used to actuate the cylinder and control its speed. A flow control valve in the return line prevented the high speed retraction of the cylinder and carriage that occurred otherwise.

An 80-psi (pounds per square inch) air supply, readily available in the laboratory, was used to power the cylinder. Connection between the supply and the two-way control valve was made using hydraulic hose and a pressure regulator at the supply outlet.

Cutting Device and Power Supply

The cutting device and its power supply are shown in Figure 6. The cutting device chosen for this study was a multi-tooth rotary saw blade. This type of cutting device was selected because it was representative of one type of experimental cutter that had been used by

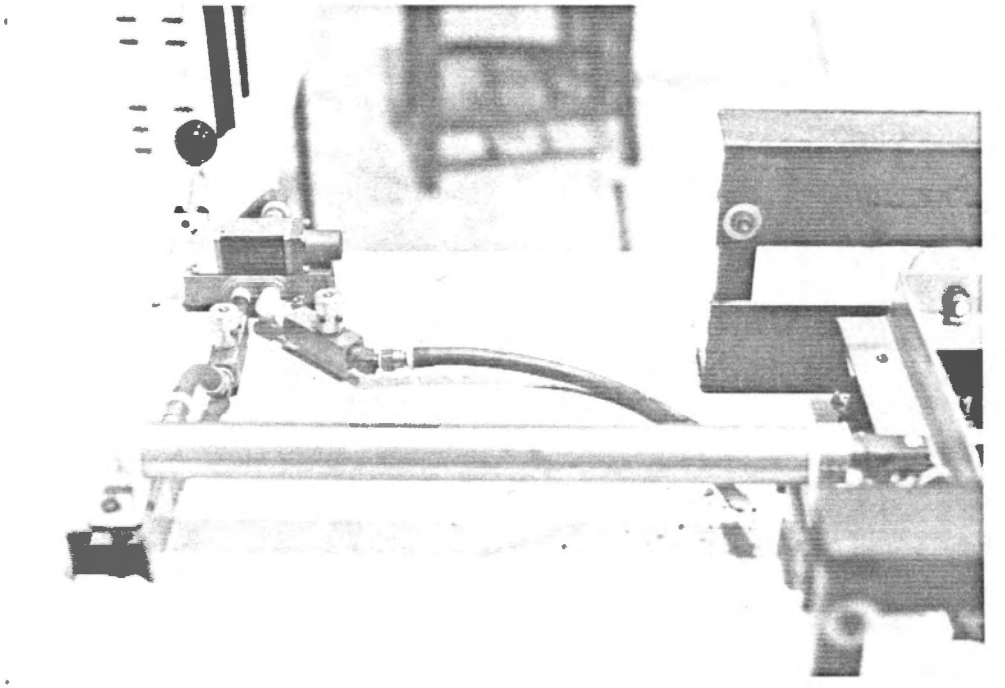

Figure 5. Forward velocity system.

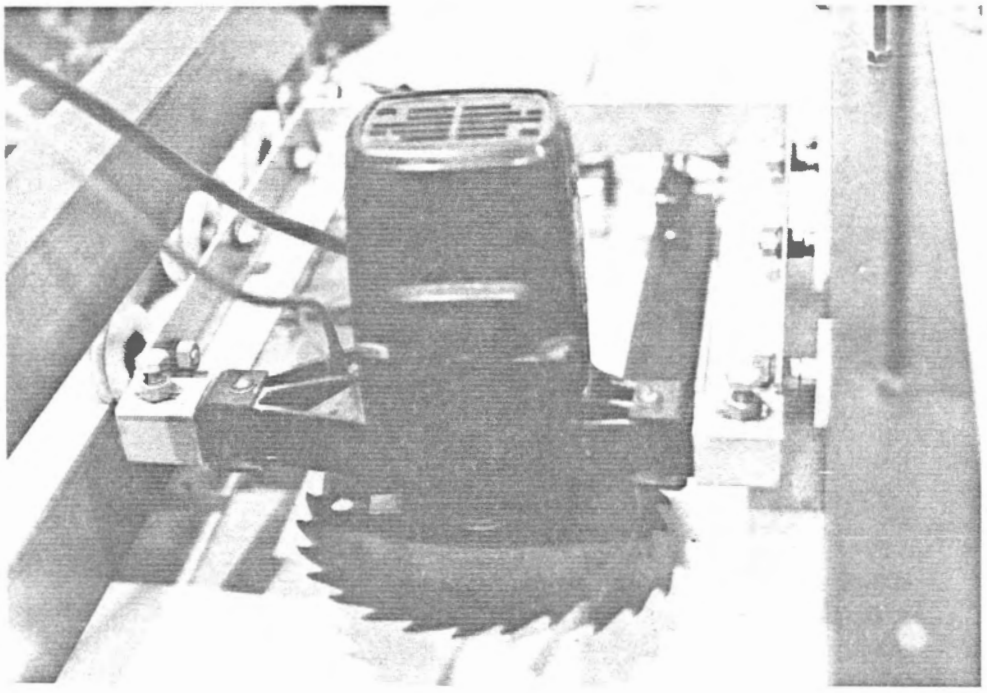

Figure 6. Cutting device and power supply.

other researchers and because it was easy to implement in the laboratory.

Power was supplied to the blade using a 4800-rpm (revolutions per minute), 110-volt, 8.5-amp motor unit of a commercial circular saw. Speed of the blade was regulated using a speed controller designed for use with Universal brush-type motors.

Instrumentation

Prior to this study, the primary methods of obtaining data in studies of soybean harvest losses have been high speed photography and the collection of unharvested crop.

High speed photography was also used in this work, mainly to provide an understanding of the mechanics of plant motion. Because plant motion in general, and cutting in particular, are transient phenomena lasting often only a few milliseconds, the ability to visually observe the motion of the plant is an invaluable asset that is only possible using high speed film. High speed photography was particularly useful for studying the motion of individual pods since these could not be instrumented.

In this study, the primary method of obtaining data was with the use of miniature accelerometers mounted on the stalk of the soybean plant. The necessary instrumentation therefore consisted of: (1) the accelerometers; (2) their associated signal conditioners and power supply; (3) the data acquisition system; (4) the impulse gun used to excite the plant; and (5) a transducer for monitoring the speed of the cutting device.

Accelerometers

Three Endevco model 2222b microminiature accelerometers were used for this study (Figure 7). The nominal frequency response for this type of accelerometer as stated by the manufacturer was plus or minus five percent below 6000 hz. (Endevco, 1979). The weight of each accelerometer was 0.5 gram excluding cable. Additional specifications of the accelerometers are available in the manufacturer supplied manual.

Mounts were specifically designed and constructed for use with the accelerometers (Figure 8). The main body of the mount was constructed of aluminum to reduce weight. The base of the mount was drilled to accept the shaft of a number 12 sewing needle, which was fixed in place using a high strength glue. The same glue was also used to fix the accelerometer to the mount as per manufacturer recommendations. The accelerometer cable was then secured to the tail of the mount to minimize motion of the cable relative to the accelerometer. Plastic-coated flexible steel hose was used to support and protect the accelerometer cables.

Charge Amplifiers and Power Supply

Three Endevco model 2721a charge amplifiers were purchased for conditioning the accelerometer signals. These charge amplifiers allowed each signal conditioner to be matched to the charge sensitivity of its respective accelerometer. Gain adjustments were also possible. The accelerometers were connected to the charge amplifiers using cables supplied by the manufacturer for this purpose. Capacitors were

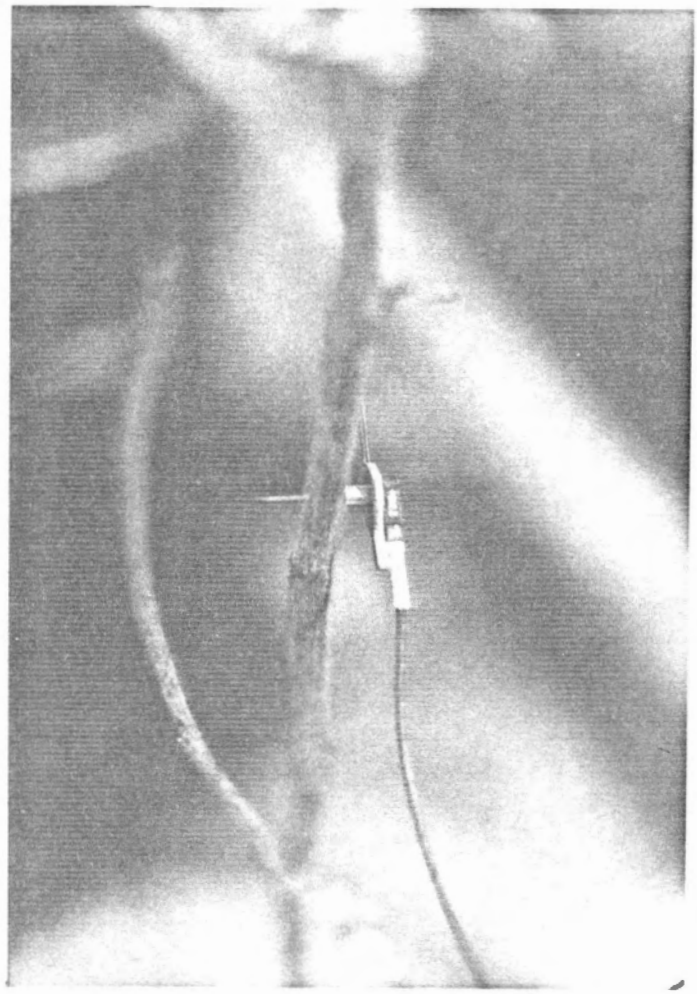

Figure 7. Accelerometer positioned on the stalk of a soybean plant.

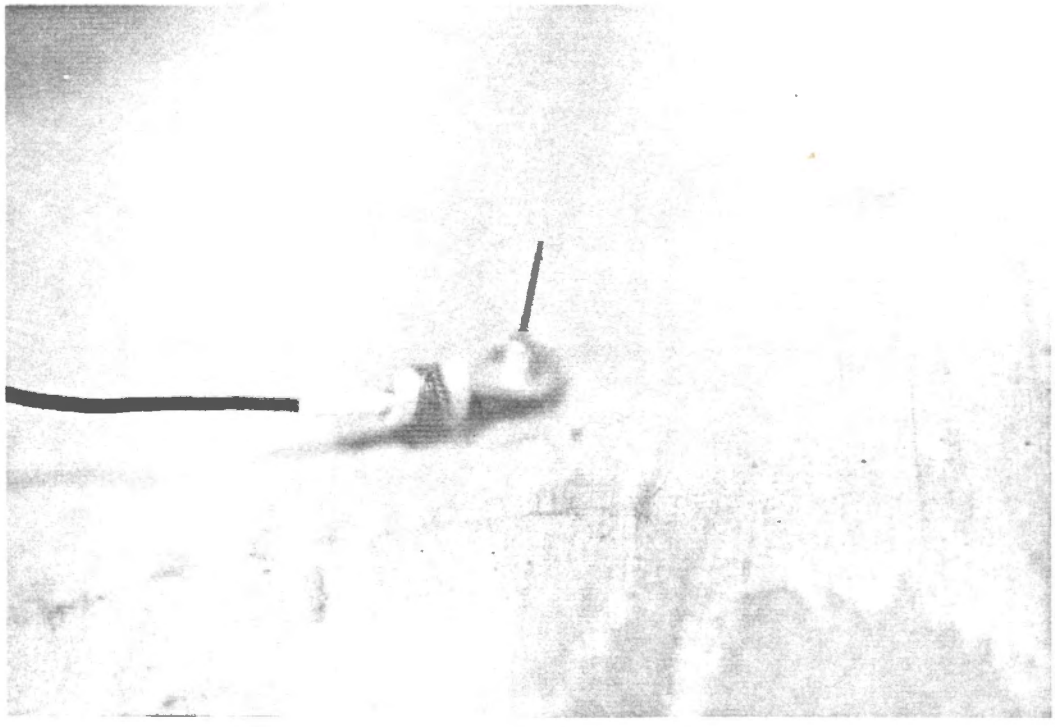

Figure 8. Accelerometer mount. The mount is shown from the underside with accelerometer and cable attached.

installed in each charge amplifier, following manufacturer instructions (Endevco, 1979), to adjust the low-pass frequency to 5000 hz. The charge amplifiers were powered with an Endevco model 4221 power supply (Endevco, 1978).

Data Acquisition System

Accelerometer data were collected with a Data Translation model DT1761-DI-C-DMA data acquisition system (DT1761). This system, consisting of an analog-to-digital converter and associated circuitry, resided in the backplane of a Charles Rivers LSI-11 microcomputer. The DT1761 provided a maximum of eight differential-ended data acquisition channels with a single channel throughput rate of 100,000 hz.

The eight channels of the DT1761 were connected by ribbon cable to an interface box that provided for four inputs: one for each of the three accelerometers used and one for the blade speed transducer. Thus, the analog signals from each of the accelerometers and the blade speed transducer were sampled twice during an eight channel sequential sampling cycle. The sampling rate was therefore 100,000 hz divided by four channels, or 25,000 hz.

Control of the DT1761 was accomplished using an assembly language subroutine linked with a FORTRAN calling program. The details of data acquisition for a particular test, such as the number of samples to be taken and the number of the file on floppy disk the data was to be stored in, were specified through the FORTRAN calling program and passed to the assembly language subroutine. These programs are listed in Appendix A.

The initiation of data acquisition was accomplished using the external trigger feature of the DT1761. Trigger switches, located on the impulse gun and the cutting device carriage (Figures 9 and 10), were used to begin data acquisition at the proper time. Additional circuitry was necessary to provide the proper trigger signal to the DT1761 and to prevent multiple triggering. The electronic and control features of the DT1761 are explained in the Data Translation, Incorporated DT1760 Series User Manual (1978).

Cutting Device Blade Speed Transducer

The speed of the cutting device was determined using a photodiode, associated signal conditioning circuitry, and either a DynaScan model 812 frequency counter or one of the channels of the DT1761. A light source that excited the photodiode at the frequency of blade rotation was provided by a bulb located below the blade and in line with the diode (Figure 11). A hole in the blade allowed light to strike the diode once during every revolution of the blade. The frequency of the resulting signal was measured with the frequency counter before each test to set the initial blade speed. The signal line was then connected to the interface box so that the actual blade speed during cutting could be measured. a 12-volt lantern battery was used to power the bulb.

Impulse Gun

The impulse gun was used to excite the soybean plant during impulse response tests. A .177 calibre air pistol (Daisy model 188) was used for this purpose. The only modification made to the gun was

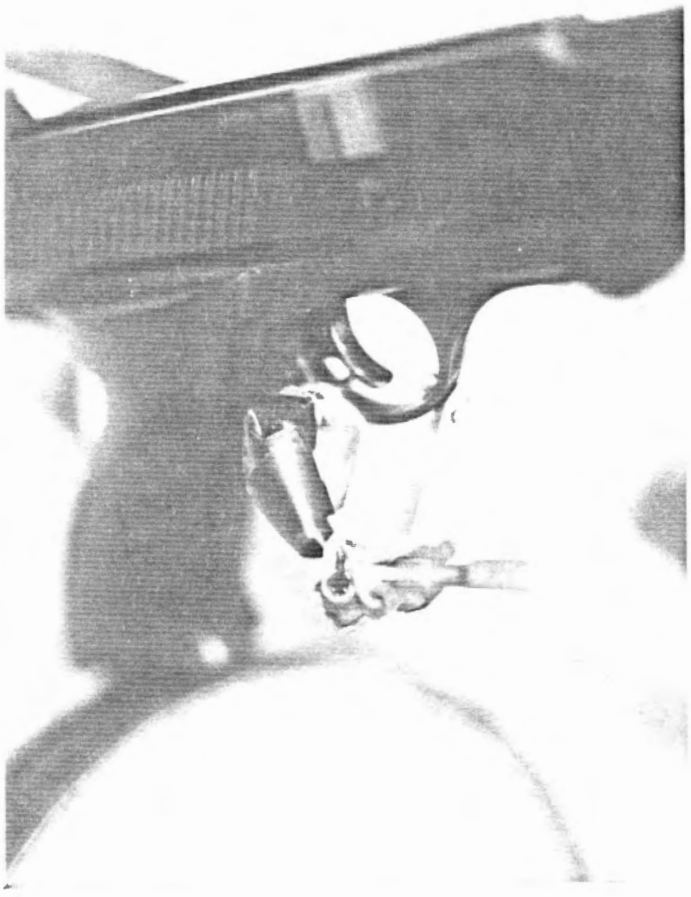

Figure 9. Impulse gun data acquisition trigger switch.

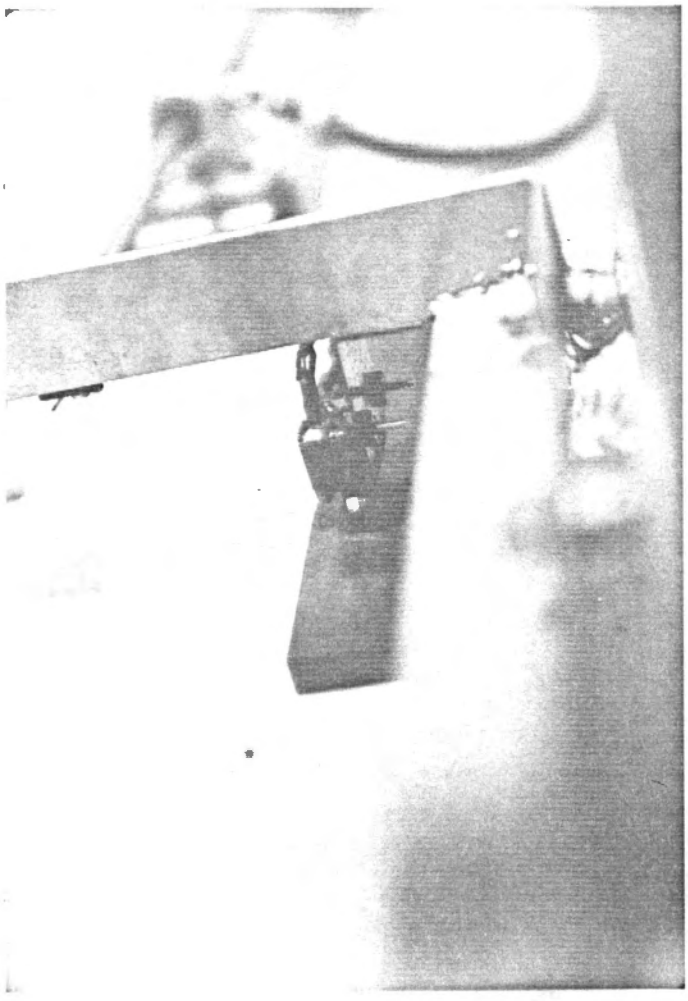

Figure 10. Cutting device carriage data acquisition trigger switch.

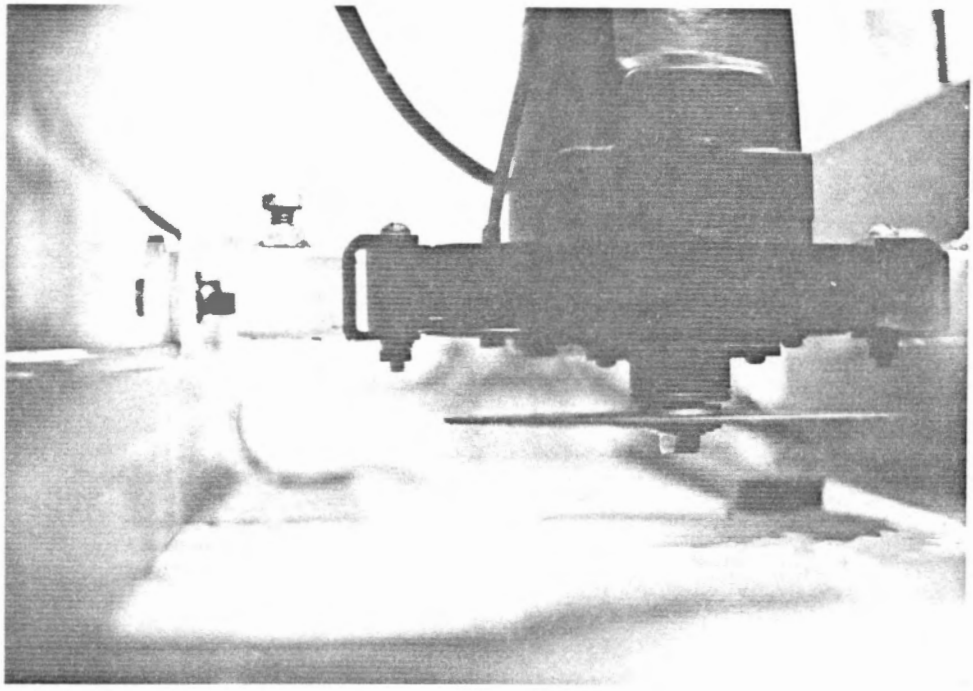

Figure 11. Light source and photodiode used for sensing blade speed.

the addition of the data acquisition trigger switch described in a previous section. The trigger switch was located on the gun such that it was depressed as the gun trigger was pulled. The impulse gun is shown in Figure 12.

The BB from the impulse gun was fired into a clay target (Figure 13) located on the stalk at the point of excitation. The purpose of the target was to prevent damage of the stalk that would otherwise occur and to provide a more consistent excitation pulse than would be obtained if the BB was allowed to ricochet.

Figure 12. Daisy model 188 .177 calibre air pistol used to excite the plant.

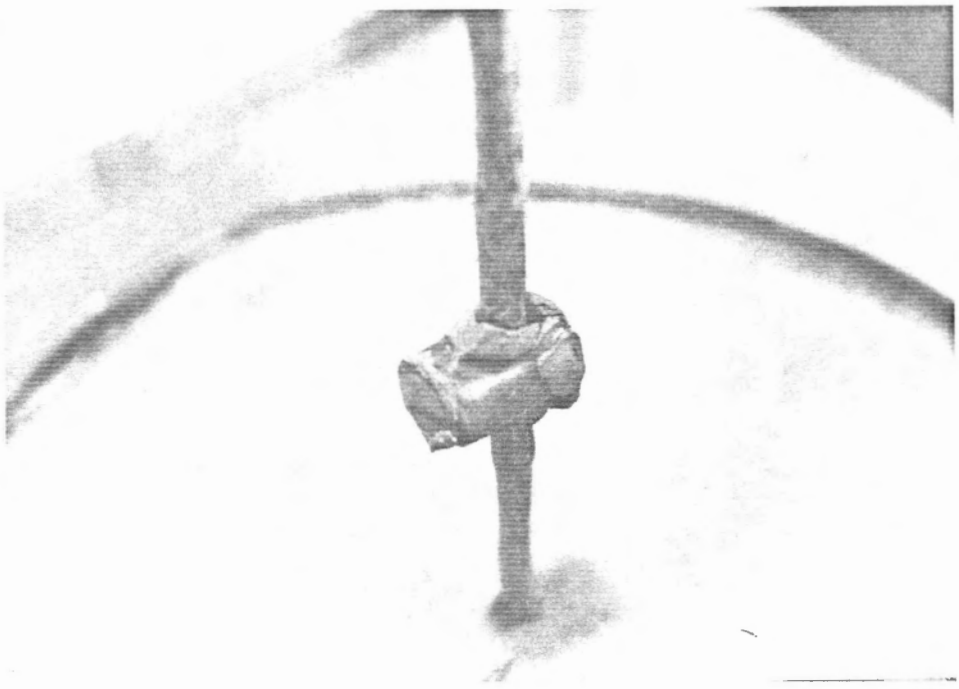

Figure 13. Clay target.

CHAPTER III

EXPERIMENTAL PROCEDURES

Two types of experimental tests were conducted in this study: impulse response tests and cutting response tests. Impulse response tests were performed to: (1) verify the mathematical models chosen to represent the plant, and (2) investigate the effects of the reel on plant motion. Cutting response tests were performed in conjunction with impulse response tests to verify the mathematical models chosen to represent the cutting device.

Impulse Response Tests

Plant Preparation

Soybean plants were taken from a field planting and the soil was removed from the roots. Soil was also taken from the same field and placed in eight-inch diameter pots. Both plants and soil were transported to the laboratory.

Each plant was "replanted" in a separate pot by packing moist soil firmly around the roots. The potted plants were then stored in the lab for later use.

One or two days prior to testing, the soil surrounding the plant to be tested was thoroughly rewetted so that it would swell around the main root of the plant. The plant itself was also misted so that its moisture content would be closer to normal plant conditions at the time of harvest.

For tests requiring only the plant stalk, the pods and secondary

stems were removed at this time. Just before a test, the pot containing the test plant was placed in the plant holding table and a snug fit was ensured.

Accelerometer Placement

The locations of the three accelerometers on the stalk were, to some extent, arbitrarily chosen, though consistency was maintained for a series of tests. For tests conducted early in the study, the accelerometers were distributed fairly uniformly along the length of the stalk. For later tests, the accelerometers were placed lower on the stalk in an effort to reduce the effect of the instrumentation on the frequency response of the plant at higher frequencies. After attaching the accelerometers, the distances from the soil at the base of the stalk to the points of accelerometer attachment and the total height of the stalk were measured and recorded.

Actual attachment was accomplished by pushing the needle of the accelerometer mount through the stalk at the desired location until the base of the mount contacted the stalk. The direction of needle travel was parallel to the direction in which the impulse was to be applied since this ensured the proper alignment of the accelerometer.

Clay Target Placement

The clay target was attached to the stalk by spreading the flanges of its Tygon tubing case and sliding the target into place. The location of the target was chosen to be representative of typical cutting heights; that is, between one and two inches above the soil surface. If a subsequent cutting test was to be performed, then target

location was also chosen to coincide with the site on the stalk at which cutting would occur. The target height was measured and recorded.

Modeling clay was pressed firmly into the barrel of the target case until the target was securely positioned on the stalk. The target was aligned such that its barrel was parallel to the direction in which the impulse would be applied. When a cutting test was to follow, this direction coincided with the direction of cutting as the blade passed through the stalk.

Impulse Application and Data Acquisition

The data acquisition program was executed. The number of samples taken was normally 16,384 as this was close to the maximum number that could be stored in computer memory.

The gain of each charge amplifier was adjusted to an appropriate level. Next, the trigger of the (unloaded) impulse gun was pulled, initiating the acquisition of data to be used in "zeroing" the output of each charge amplifier. The impulse gun was then loaded and cocked. When the data acquisition program signaled that the system was ready for data acquisition, the impulse was applied to the plant by shooting a BB into the clay target. Data acquisition and transfer to floppy disk occurred automatically under program control.

After data transfer was complete, a visual check of the data was made to ensure that the charge amplifier signals did not exceed the plus-or-minus-ten-volt limits of the DT1761. If these limits were exceeded, the gain settings of the charge amplifiers were adjusted and the test was repeated.

Normally, between two and four impulse response tests were conducted for each experiment. Between each of these tests, the BB was removed from the clay target and the clay was repacked in the target case. Then, the impulse response test procedure was repeated.

High Speed Film

Several high speed films were made during impulse response tests involving a stalk with a single attached pod. The Hycam model K2004E-115 high speed motion picture camera was used for this purpose. Procedures recommended by Hizer (1959) and the Hycam Instruction Manual (1968) were followed. The film speed used was 1500 frames per second.

Cutting Response Tests

Preliminary Preparations

Cutting response tests involved the acquisition of data from the accelerometers mounted on the plant stalk as the stalk was cut. Since cutting tests were always preceded by impulse response tests, the clay target had to be removed from the stalk prior to cutting.

The desired forward speed of the cutting device carriage was selected prior to the placement of the test plant on the plant holding table. If the response of the plant to cutting was expected to be severe, the gain controls of the charge amplifiers were adjusted lower accordingly. These settings were recorded at this time. The impulse gun data acquisition trigger switch was disconnected from the interface box and the trigger switch on the cutting device carriage was connected in its place. The approximate blade speed was selected by adjusting

the dial of the speed control and using the frequency counter to read the ouput of the blade speed transducer.

Data Acquisition

The data acquisition program was executed and the carriage was moved down the track by hand until the data acquisition trigger switch "tripped," causing the collection of data for zeroing the charge amplifier output. The carriage was then returned to its original position. The initial blade speed and data file number were recorded.

Next, the forward speed system was connected to the air supply and the pressure regulator was adjusted to maintain the supply at approximately 40 psi.

The cutting device carriage was propelled down the carriage track using the cylinder control valve. The plant holding table was located such that cutting occurred just before carriage motion ceased. Data acquisition, initiated by the carriage trigger switch just before cutting began, was completed automatically under program control.

The handle of the control valve was released, returning the carriage to its initial position, and the blade and air supply were turned off. Finally, a measurement of the stalk diameter at the site of cutting was made and recorded.

High Speed Film

High speed films were also made during some of the cutting response tests. The procedure followed was identical to the procedure used for filming impulse response tests. Film speeds of 2000 and 4000 pictures per second were used.

CHAPTER IV

ANALYSIS OF EXPERIMENTAL DATA

Mathematical Basis

Impulse Response of a Linear System

Discussions of impulse response techniques often begin with a definition of the unit impulse function, or Dirac delta function, $\delta(t)$. The unit impulse function is defined to have infinite height, infinitesimal width, and bounded area of one. Mathematically, this can be expressed as follows:

$$\delta(t)=0, \quad t\neq 0$$
$$\int_{-\infty}^{+\infty}\delta(t)dt=1 \tag{4-1}$$

where: $\delta(t)$ = the unit impulse function, and

t = time.

Impulses of greater magnitude, that is, greater bounded area, can be represented by multiplying the unit impulse function by a constant.

The impulse function is an ideal, physically unrealizable function. However, realistic pulses (having finite height and width) can be used to represent an impulse if the pulse duration is much shorter than the period of the highest response frequency of the system the pulse is applied to.

The response of a linear system (with no initial conditions) to a unit impulse is called the "impulse response" of the system. The response of a linear system to any excitation is the convolution of its

impulse response and that excitation:

$$x(t)=\int_0^t h(t-\tau)b(\tau)d\tau \qquad (4\text{-}2)$$

where: h(t) = the impulse response of the system,

b(t) = the excitation applied to the system, and

x(t) = the system response to excitation.

This mathematical statement is the basis of impulse response techniques. Once the impulse response of a system is known, the response of that system to any excitation can be predicted (assuming the system behavior remains linear).

Fourier Transform

The impulse response and excitation response of a system, as well as the excitation itself, are functions of time, but they can also be considered as functions of frequency. The function of frequency, H(f), that corresponds to a function of time, h(t), is the Fourier transform of h(t). The Fourier transform can be determined by evaluating the Fourier integral:

$$H(f)=\int_{-\infty}^{+\infty} h(t)e^{-j2\pi ft}dt \qquad (4\text{-}3)$$

where: $j=\sqrt{-1}$,

e = 2.718...,

f = frequency, hz,

t = time,

h(t) = a function of time, and

H(f) = the Fourier transform of h(t).

The Fourier transform is, in general, a complex quantity. That is, its value at every point in frequency has a real part and an imaginary part. An equivalent representation of the Fourier transform in terms of its magnitude and phase is also possible:

$$H(f)=R(f)+jI(f)=|H(f)|e^{j\theta(f)}$$
$$|H(f)|=\sqrt{R^2(f)+I^2(f)} \qquad (4\text{-}4)$$
$$\theta(f)=\tan^{-1}\left[I(f)/R(f)\right]$$

where: R(f) = the real part of H(f),

I(f) = the imaginary part of H(f),

/H(f)/ = the magnitude or amplitude of H(f), and

θ(f) = the phase of H(f).

/H(f)/ is often referred to as the "amplitude spectrum" of h(t), and θ(f) is referred to as the "phase spectrum." It should be noted, however, that /H(f)/ is actually an amplitude density rather than an amplitude. A check of the units of H(f) will confirm this.

When the function h(t) is the impulse response of a system, then H(f), the Fourier transform of h(t), is termed the "frequency response function," the "sinusoidal transfer function," or simply the "transfer function" of the system.

The Fourier transform pair h(t) and H(f) are just two ways of depicting the same signal, but in system response analysis, the important aspects of the system are often much clearer in the frequency domain than in the time domain. This fact is one of two reasons the Fourier transform is so widely used.

The second reason for widespread use of the Fourier transform is the ease with which convolution can be performed in the frequency domain. Convolution in the time domain,

$$x(t)=\int_0^t h(t-\tau)b(\tau)d\tau \qquad (4\text{-}2)$$

corresponds to multiplication in the frequency domain:

$$X(f)=H(f)\cdot B(f) \qquad (4\text{-}5)$$

Thus, convolution, which is difficult to evaluate in the time domain, is simply (complex) multiplication in the frequency domain.

X(t), the system response to excitation in the time domain, can then be recovered from equation 4-5 using the inverse Fourier transform:

$$x(t)=\int_{-\infty}^{+\infty} X(f)e^{j2\pi ft}df \qquad (4\text{-}6)$$

where: x(t) = the system response in the time domain, and

X(f) = the system response in the frequency domain.

Correlation

Correlation is a mathematical operation that is similar in some respects to convolution. Correlation of two signals in the time domain corresponds to multiplication in the frequency domain of one signal's Fourier transform by the complex conjugate of the Fourier transform of the other signal:

$$\phi_{12}(f)=S_1^*(f)S_2(f) \qquad (4\text{-}7)$$

where: $\phi_{12}(f)$ = the Fourier transform of the correlation function, referred to as the "cross-spectral density" of signals 1 and 2,

$S_1(f)$ = the Fourier transform of signal 1,

$S_2(f)$ = the Fourier transform of signal 2, and

$S_1^*(f)$ = the complex conjugate of S (f).

Correlation of a signal with itself in the time domain corresponds to multiplication in the frequeny domain of the Fourier transform of the signal with its complex conjugate:

$$\phi_{11}(f) = S_1^*(f) \cdot S_1(f) \qquad (4\text{-}8)$$

where: $\phi_{11}(f)$ = the Fourier transform of the "autocorrelation" of signal 1, often referred to as the "power spectral density" of signal 1.

Transfer Function Determination

Practical Considerations

Equation 4-5 implies that the transfer function of a system can be determined by applying any known excitation to the system, measuring the system response, and forming the ratio of the two for each value of frequency:

$$H(f) = X(f)/B(f) \qquad (4\text{-}9)$$

where: $H(f)$ = the system transfer function,

$X(f)$ = the Fourier transform of the system

response to excitation, and

B(f) = Fourier transform of the excitation.

While mathematically true, there are practical limitations to this approach. The response of any system at high frequencies will approach zero due to damping. The frequency beyond which little response occurs is called the "cutoff frequency" of the system. The excitation also has a cutoff frequency because its frequency content cannot realistically be infinite. This may also contribute to low system response at high frequencies. Therefore, at high frequencies, equation 4-9 may involve the ratios of very small, unreliable numbers. Additionally, instrumentation, analog-to-digital conversion, and system nonlinearities introduce noise and error into the data that also reduce its reliability, particularly at higher frequencies where the signal-to-noise ratio is already low for reasons just mentioned.

Beyond a certain frequency, then, the computed transfer function will be inaccurate. Thus, there are two important considerations for this type of testing:

1. the extension of the frequency domain for which data are reliable to the extent that it includes the highest frequency of interest;
2. the ability to determine the frequency beyond which data are no longer reliable.

When a pulse is used to approximate an impulse, as in this study, both the duration and magnitude of the pulse are important to determining the domain of reliable data. The pulse must be of

sufficiently short duration to "look like" an impulse to the system being tested, and the magnitude of the pulse must be sufficient to significantly excite the system at the highest frequency of interest.

The first condition is met if the cutoff frequency of the pulse, which is primarily determined by the pulse duration, is higher than the cutoff frequency of the system. The ideal impulse function, which has infinitesimal width, has a cutoff frequency at infinity. Thus, the shorter the duration of the real pulse, the higher its cutoff frequency and the better it approximates an ideal impulse.

The second condition may be difficult to achieve. Because system response is usually less at high frequencies than at low frequencies due to damping, pulse magnitudes that can cause significant high frequency response may also cause excessive (nonlinear) low frequency response or even physical damage to the system.

Coherence Function

The frequency range for which data are valid is determined using the coherence function. The coherence of any two signals can be computed as follows:

$$\gamma_{12}^2(f) = |\phi_{12}(f)|^2_{AVG} / \phi_{11}(f)_{AVG} \phi_{22}(f)_{AVG} \qquad (4\text{-}10)$$

where: γ_{12}^2 (f) = the coherence function,

$|\phi_{12}(f)|$ = the magnitude of the cross-spectral density of signals 1 and 2,

$\phi_{11}(f)$ = the power spectral density of signal 1, and

$\phi_{22}(f)$ = the power spectral density of signal 2.

For noise-free, perfectly repetitive signals

$$\gamma_{12}^2(f) = 1.0$$

over the entire frequency range. Random noise, measurement errors, and system nonlinearity will cause the values of the coherence function to be less than one, particularly in regions where low system response makes the signal-to-noise ratio low. The frequencies for which the values of the coherence function are consistently high (generally 0.9 or greater) are the frequencies for which data are reliable.

For transfer function determination, the two signals for which the coherence function is computed are usually the excitation and the system response to excitation. However, in this study, since the excitation was not measured, the coherence function was computed for two impulse response signals measured simultaneously at two different locations on the stalk.

The computed coherence functions for the impulse response data of a stalk without attached pods are shown in Figures 14, 15, and 16 for 2, 3, and 4 replications of the test, respectively. For two replications (Figure 14), the coherence of the impulse response data is generally above 0.9 from 0 to 5000 hz. One method of improving the reliability of test data is through replication and averaging; therefore, it is interesting to note that in this study averaging adversely affected the coherence of the test data, as seen by comparing Figures 15 and 16 to Figure 14. Presumably, this adverse effect was

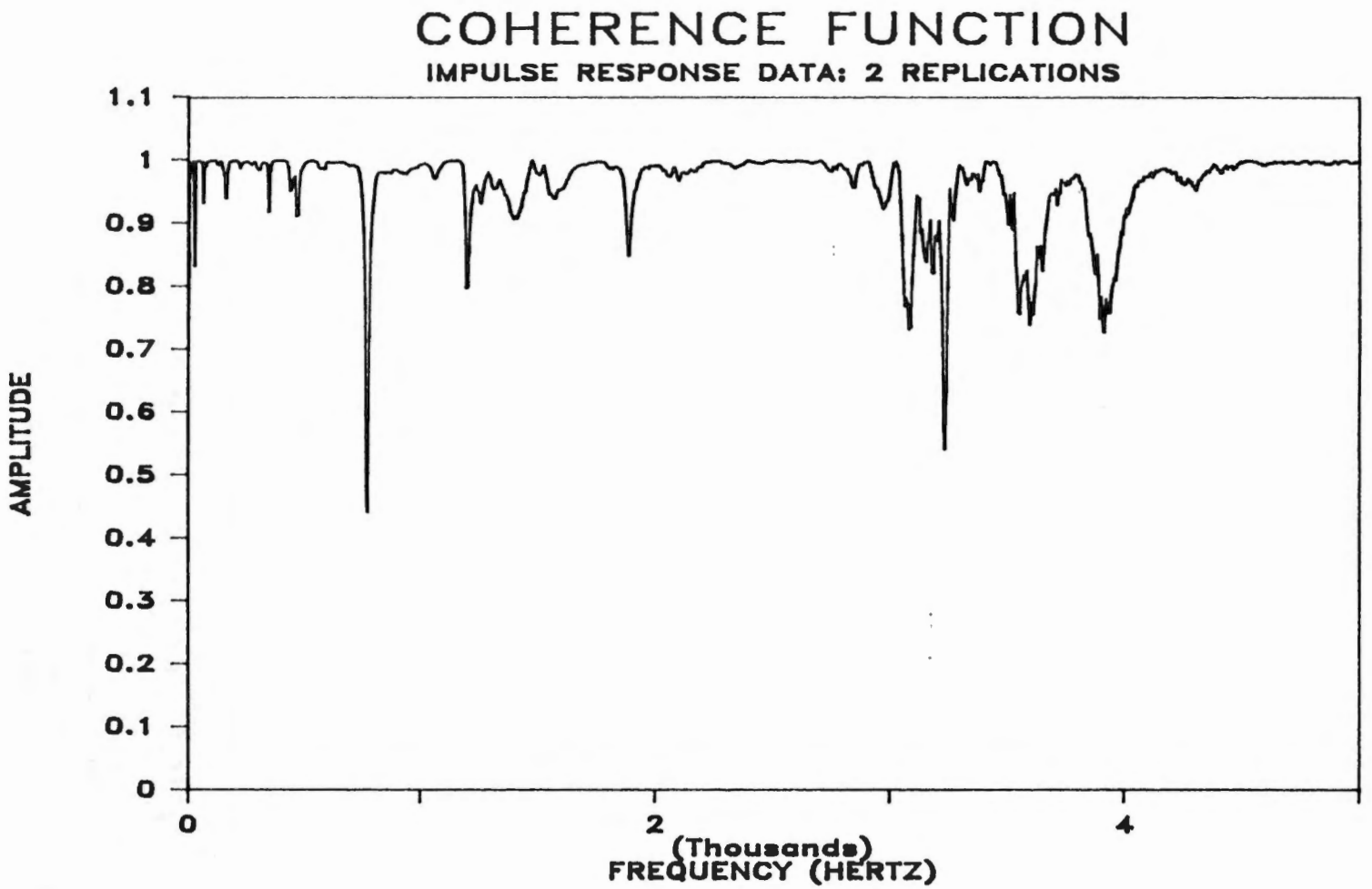

Figure 14. Coherence function computed using two replications of an impulse response test of a bare stalk.

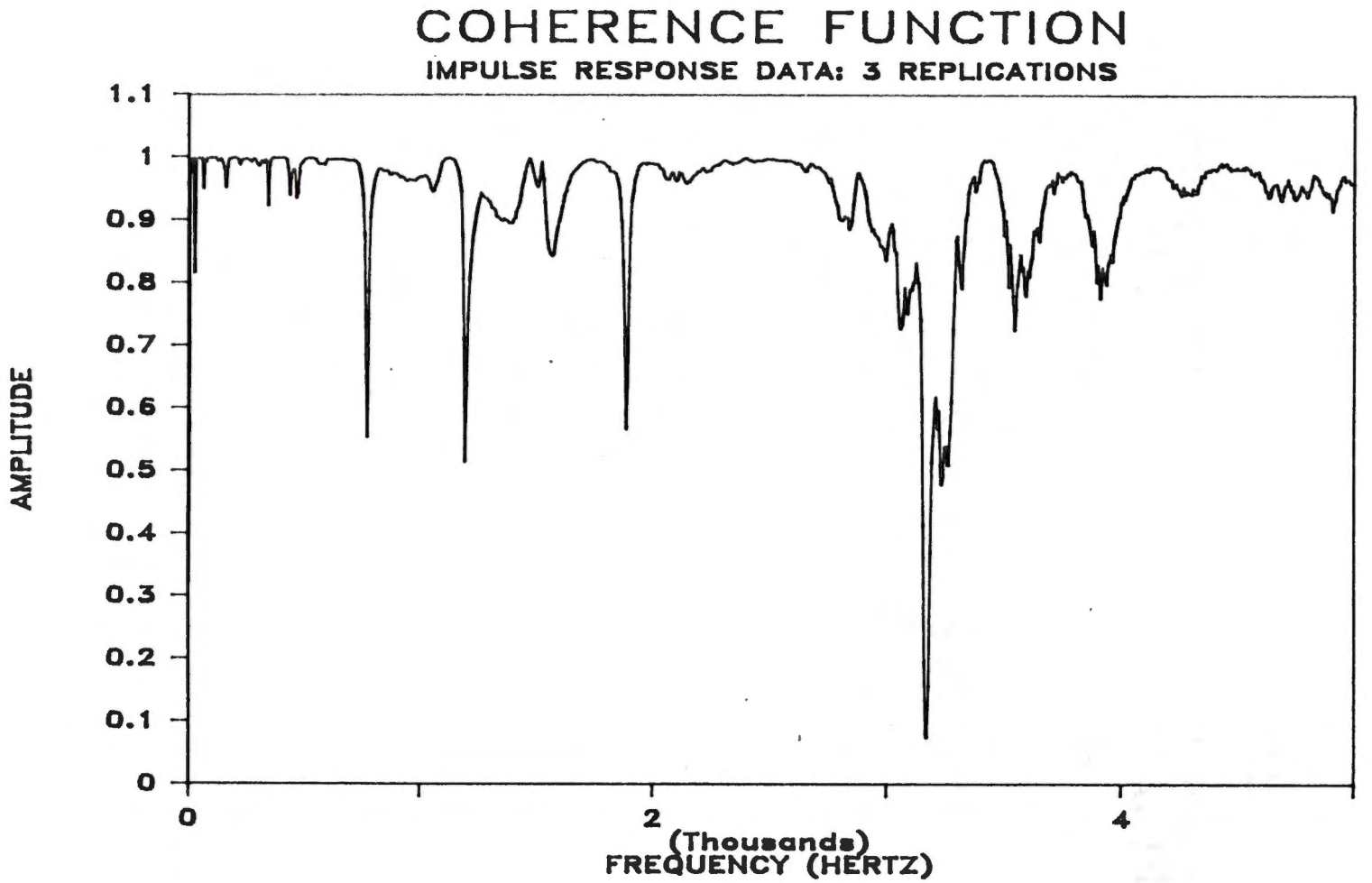

Figure 15. Coherence function computed using three replications of an impulse response test of a bare stalk.

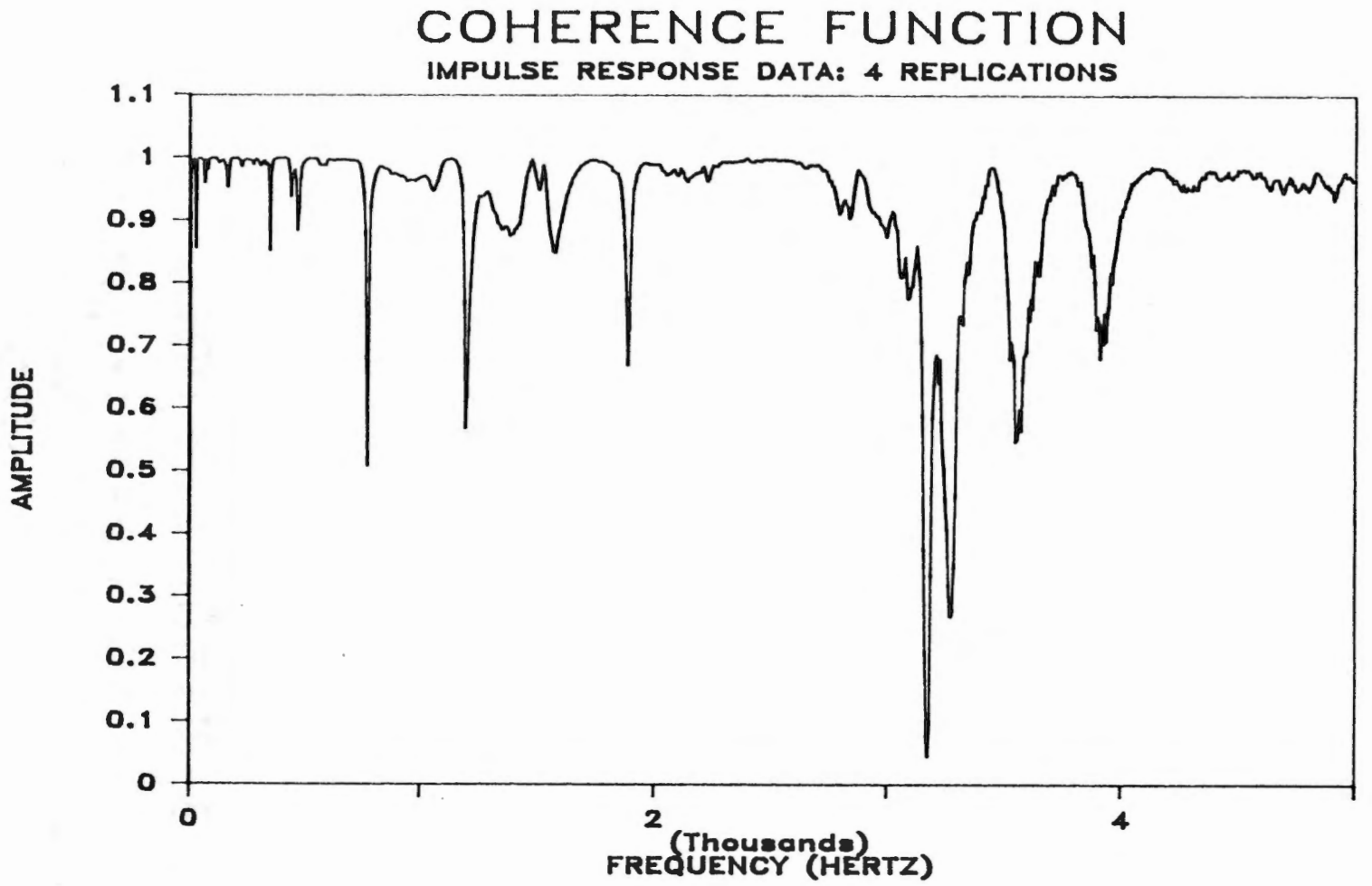

Figure 16. Coherence function computed using four replications of an impulse response test of a bare stalk.

because each replication of a test changed the system slightly. The soil in which the stalk was placed was so well conditioned that each pulse application probably caused the soil surrounding the stalk to be compacted slightly by the stalk's vibration. This problem might have been avoided if the plants had been grown to maturity in the pots.

Figures 17, 18, and 19 show the computed coherence function for impulse response data of a stalk with pods attached but constrained with a light adhesive tape. The pods were constrained to prevent collisions with each other and the stalk during motion because this is a nonlinear phenomenon. Again, the adverse effect of averaging several test replications is evident. Of particular interest is the poor coherence of the data beyond about 3700 hz. As will be shown later, the presence of pods significantly reduces the response of the stalk. Hence, one possible explanation for the poor coherence above 3700 hz is that the magnitude of the pulse was not sufficient to excite the stalk with pods at higher frequencies. Another possible explanation is that, for this particular series of tests, the pulses produced were not of sufficiently short duration to raise their cutoff frequency above 3700 hz.

Evaluation of Pulsing Method

The highly responsive yet fragile nature of the plant, as well as the desire to obtain data from which a cutting function with high frequency content could be reliably computed, set severe standards for the required excitation pulse. The use of the BB gun and clay target for producing pulses was an acceptable, though not completely satisfactory, attempt to meet these standards.

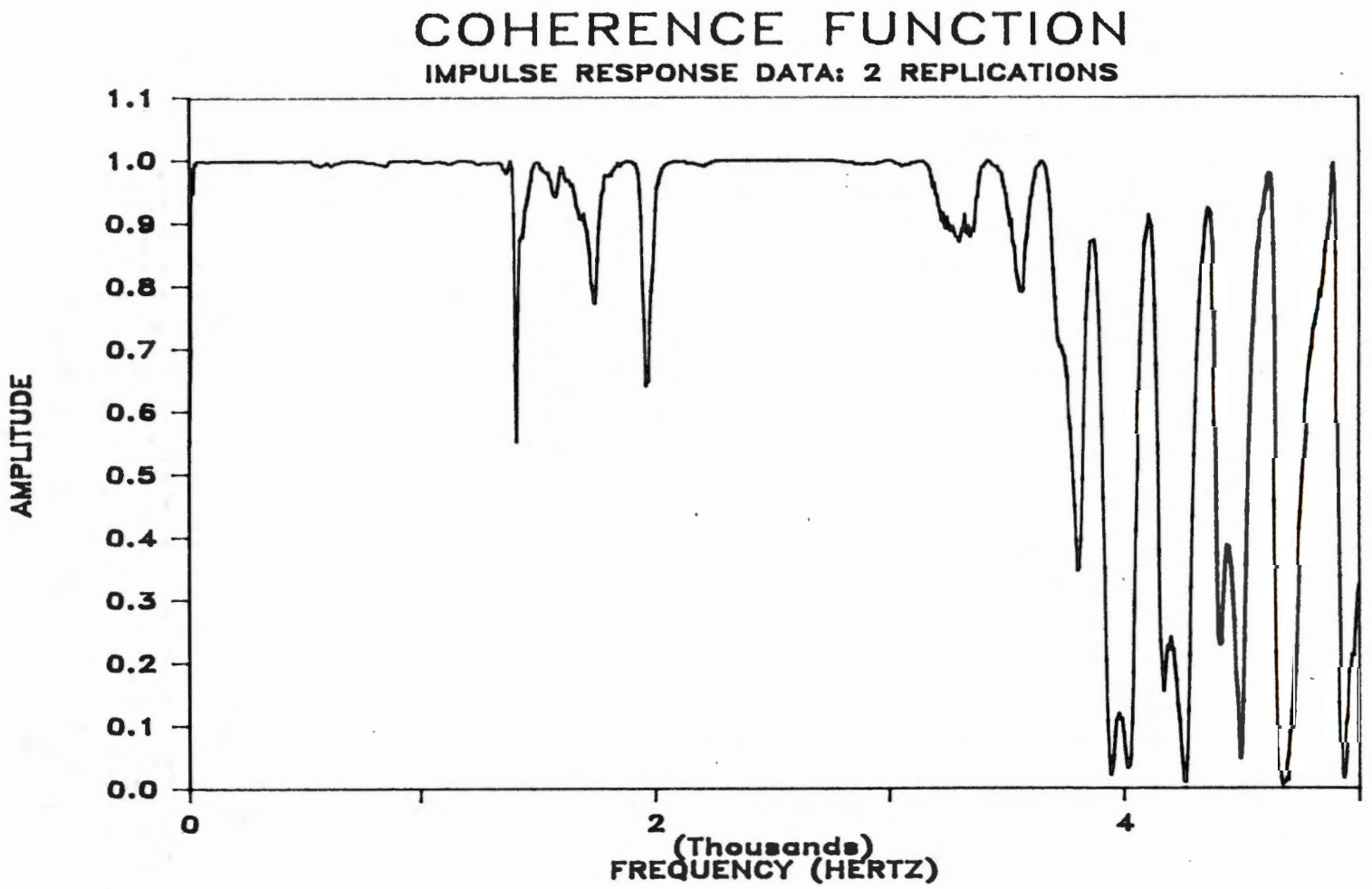

Figure 17. Coherence function computed using two replications of an impulse response test of a plant with restrained pods.

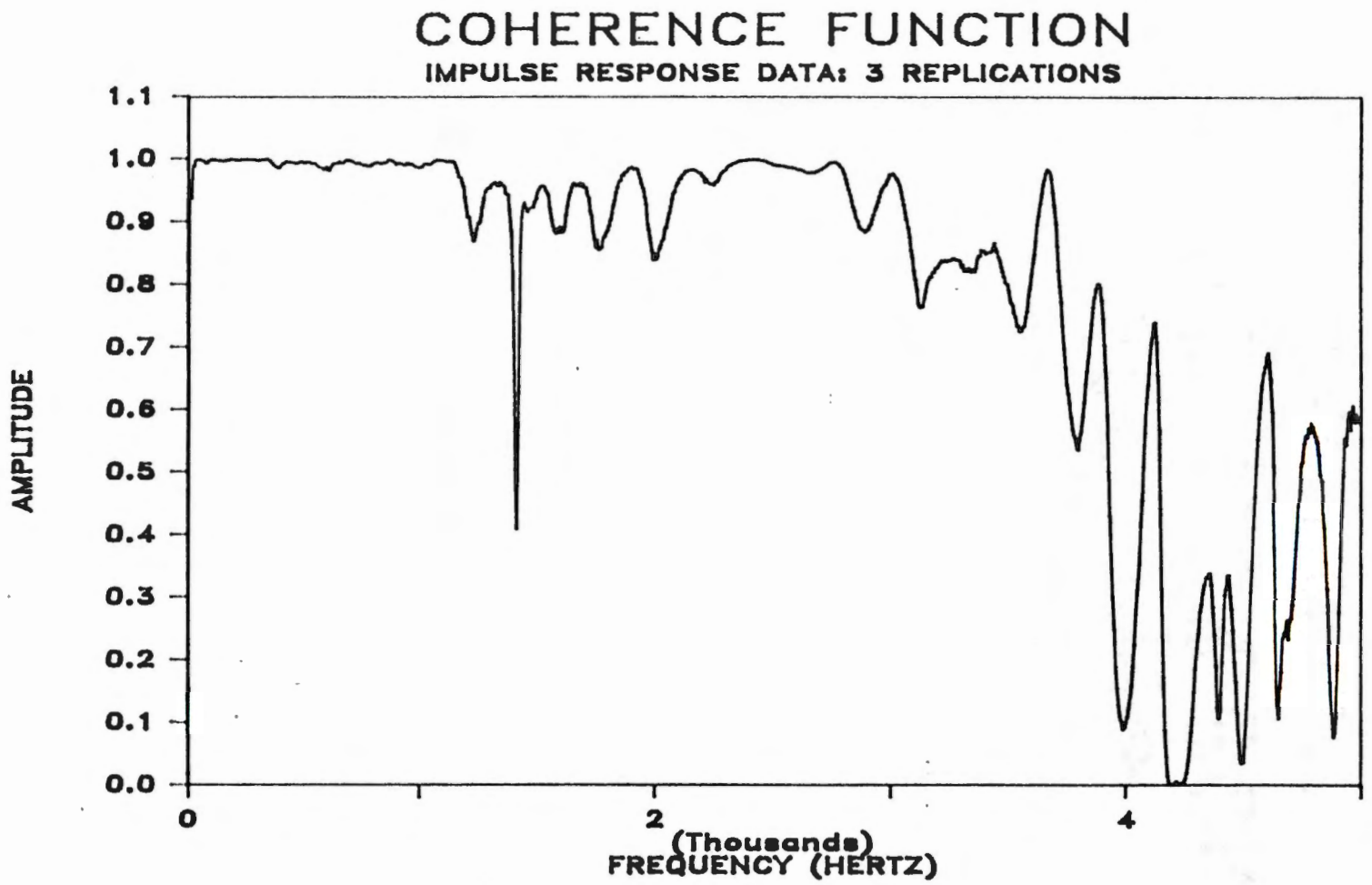

Figure 18. Coherence function computed using three replications of an impulse response test of a plant with restrained pods.

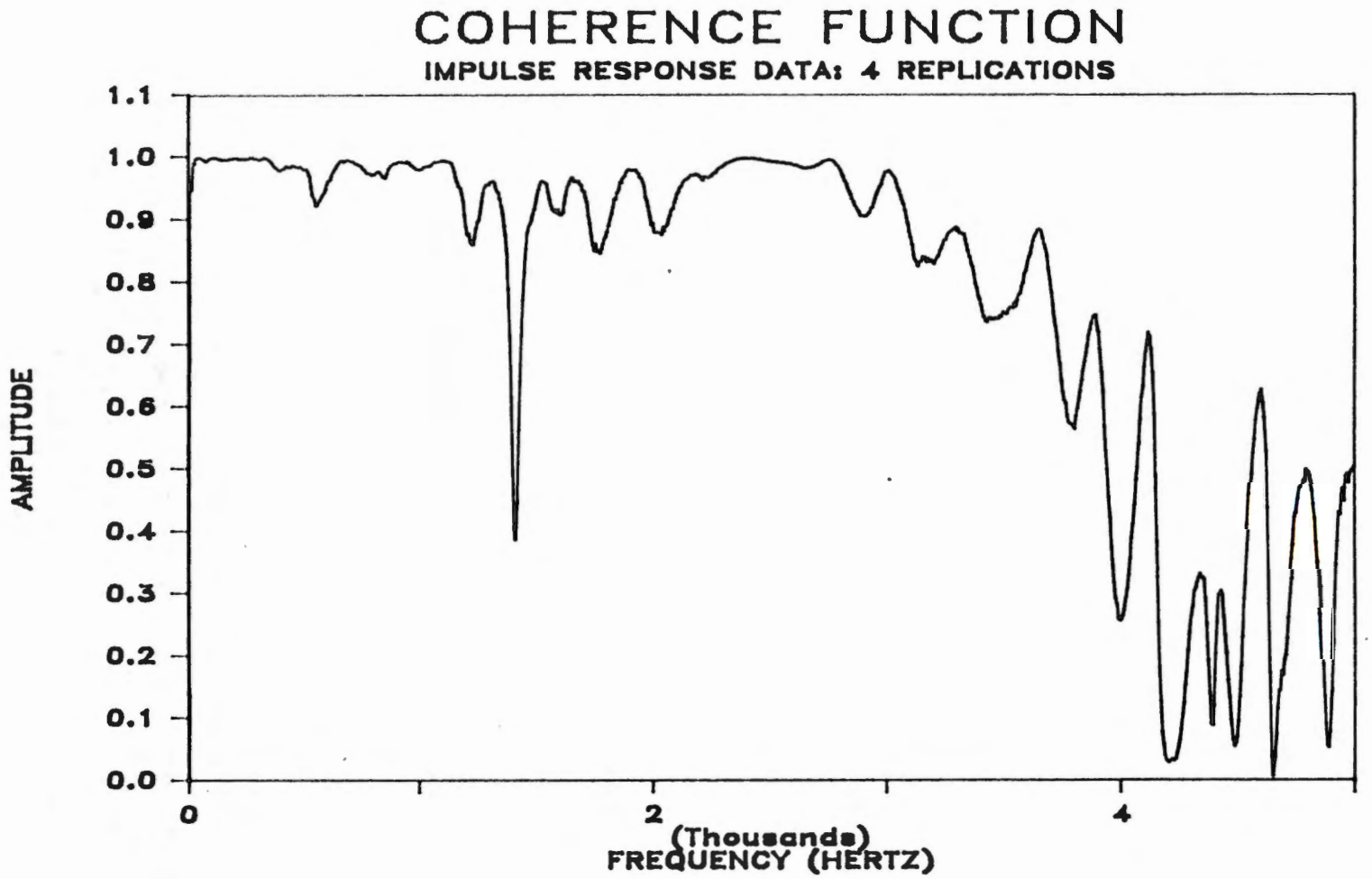

Figure 19. Coherence function computed using four replications of an impulse response test of a plant with restrained pods.

Very short pulse durations were achieved by cooling the target clay with ice. The BB came to rest quickly in the cooled clay, thereby minimizing the duration of the pulse caused by its impact and travel. The magnitude of the pulse provided by this arrangement also seemed satisfactory for most of the tests. As seen from the computed coherence function, the bare stalk was significantly but not excessively excited over most of the linear dynamic range of the accelerometers without suffering physical damage. However, a shortcoming of this method was the fact that no direct measurement of the excitation was possible. Thus, while consistent pulses were obtained, the magnitude of these pulses was undetermined. For the purposes of this study, the magnitude of the approximate impulse provided by the BB and target was designated to be one daisy (dy).

Cutting Function Determination

For the purposes of discussion, the excitation applied to the stalk by the cutting device will be referred to as the "cutting function." Referring to equations 4-2 and 4-9, and solving for the Fourier transform of the cutting function:

$$B(f)=X(f)/H(f) \qquad (4\text{-}11)$$

where: B(f) = the Fourier transform of the cutting function,
X(f) = the Fourier transform of the stalk response to cutting measured at a particular location, and
H(f) = the transfer function for that location on the stalk.

Thus, knowing the transfer function of a location on the stalk and the response to cutting of that location, the Fourier transform of the cutting function can be computed using equation 4-11. For this study, the transfer functions and responses to cutting were obtained for two locations on the stalk. Therefore, equation 4-11 was employed for each location and the results averaged to obtain a better estimate of the Fourier transform of the cutting function.

It should be mentioned that cutting is a very complex phenomenon, more so in this case because the physical parameters of the system under consideration are altered even as the system is excited. Specifically, the cross section of part of the stalk is changed as cutting progresses. Therefore, the "cutting function" is a simplistic view of a less than simple process. Nevertheless, the notion is a useful one, and promises to be even more meaningful for cases, such as the cutterbar, where the stalk undergoes significant deflection before cutting actually occurs.

Digital Implementation of the Mathematics

The computation of the transfer function and the cutting function rely on the ability to determine the Fourier transform of a time series of data. Because the time series is in numerical form, the Fourier transform must be calculated numerically. This is accomplished using an algorithm known as the Fast Fourier Transform or FFT (Brigham, 1974).

Signal analysis hardware and software that implement the FFT are commercially available; however, the software described here was

developed during this study specifically for use with the computing hardware that was available: a Digital Equipment Corporation PDP-11/23 minicomputer, VT100 cathode ray screen, and LA 120 serial line printer.

Two programs that compute the Fourier transform of a time series are listed in Appendix A. FFT4 computes a 4096 point transform and, for cases where greater resolution is desired, FFT16 computes a 16384 point transform. Both programs assume the time series data are evenly spaced in time. Both employ a technique known as "zero filling" whereby the remainder of the record is filled with zeroes for cases where the time series are not 4096 values long (or 16384 values long if FFT16 is used).

In many cases, though, the time series is too long and must be truncated to the correct number of values. The resulting sharp discontinuity at the end and/or beginning of the time series introduces rippling into the computed spectrum which is characterized by side-lobes on both sides of spectrum peaks. This effect can be minimized by using a window function that tapers the beginning and end of a truncated time series. However, the use of window functions can also cause smearing of spectrum peaks. Furthermore, when the time series is a transient signal, such as impulse response data, tapering the beginning of the record can result in the loss of data, particularly in the high frequency range.

Figure 20 shows the amplitude spectrum of the transfer function of a stalk computed both with and without the use of a window function. The window does reduce the amount of side-lobing, a fact that may not be immediately obvious because of the relatively poor (6.1 hz)

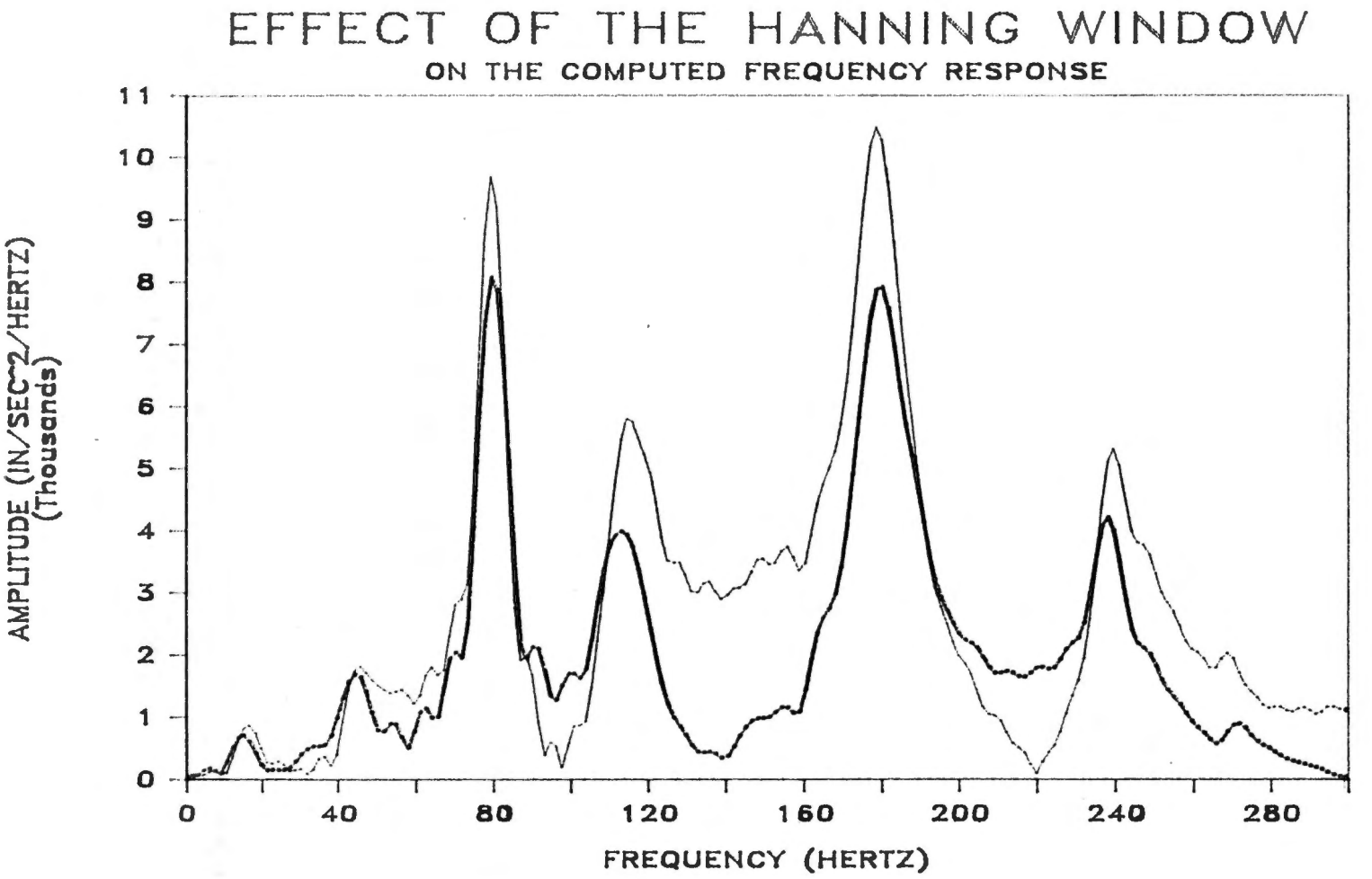

Figure 20. Amplitude spectrum of the impulse response of a location on a bare stalk computed with (bold curve) and without (fine curve) the use of a window function.

resolution of the spectrum. However, the peak amplitudes have also been reduced significantly.

The coherence of two impulse response signals for which the window function was used is shown in Figure 21. Comparison of Figure 21 and Figure 14 shows the adverse effect of the window function on the validity of the data over a wide range of frequencies. For this reason, the window function was not employed and significant degrees of side-lobing were tolerated.

Both FFT4 and FFT16 also compute the inverse Fourier transform, the mathematical description of which is given by equation 4-6.

As shown previously, convolution in the time domain corresponds to multiplication in the frequency domain. Thus, convolution can be accomplished numerically by computing the Fourier transforms of the two signals involved (using FFT4 or FFT16) and multiplying the results for each value of frequency. The Fortran program COMPUT listed in Appendix A can be used to accomplish multiplication. Then, the inverse Fourier transform (using FFT4 or FFT16) yields the desired convolution in the time domain.

Both the cross-spectral density of two signals (equation 4-7) and the power spectral densities of signals (equation 4-8) are required to compute the coherence function. Both can be computed numerically using a program such as COMPUT which is listed in Appendix A, once the Fourier transforms of the signals have been obtained using either FFT4 or FFT16. (When the Fourier transforms of signals are computed for the purpose of performing either convolution or correlation, certain procedures must be followed regarding the addition of zeroes to the

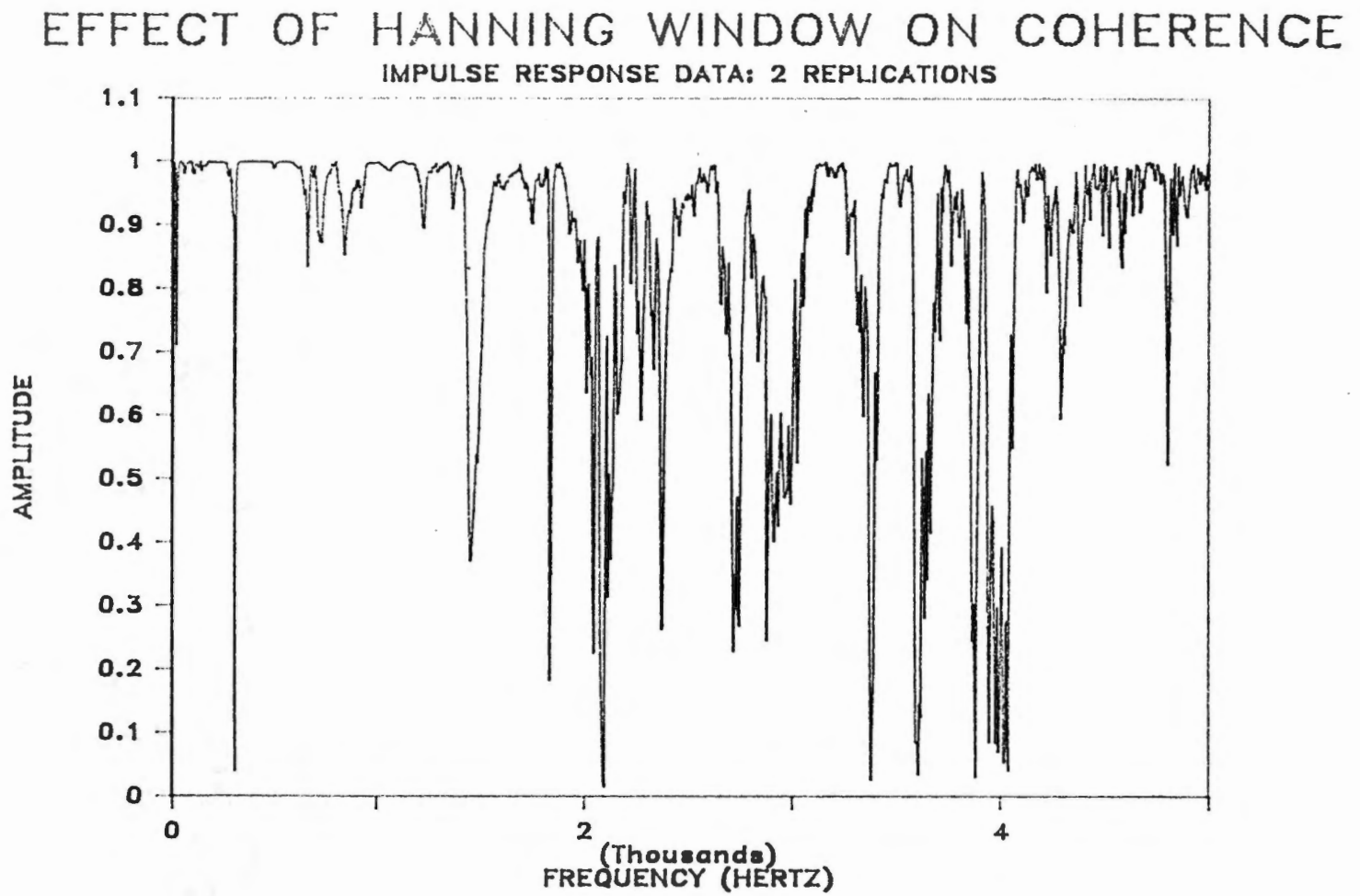

Figure 21. Coherence function computed using two replications of an impulse response test of a bare stalk and with the use of a window function.

beginning or end of the signals prior to transformation. These procedures are listed in several references, Brigham (1974) being one.) Complex division, an operation necessary for computing the cutting function via equation 4-10, is also provided by COMPUT.

In addition to FFT4, FFT16, and COMPUT, several utility programs are also necessary for data analysis. CHOP is useful for truncating the beginning or end of a time series. ADZERO can be used to add a series of zeroes to the beginning or end of a time series. SEPRAT is used to scale the raw data and separate it into individual time series for each accelerometer. LOOK can be used to graphically display one or several time series at a video terminal. A listing of each of these programs is provided in Appendix A.

CHAPTER V

MATHEMATICAL MODELING OF THE SOYBEAN PLANT

Mathematical modeling of physical systems must, to some degree, involve a compromise between the complexity required to adequately describe system behavior and the simplicity necessary to allow solutions. In some instances, simplification, even at the expense of accuracy, can be justified if the results promote a better understanding of the problem.

In this study, such compromise was necessary. No attempt was made to model the dynamics of a complete plant, although experimental data from whole plant motion were obtained. Instead, mathematical models of the components of the soybean plant--the stalk and pod--were developed and investigated, with hopes that knowledge of their dynamics would yield a fuller understanding of the motion of the entire plant.

In this chapter, the dynamic behavior of the soybean plant is discussed in four parts: (1) the mathematical model of the stalk, (2) the mathematical model of the pod, (3) the mathematical model of a stalk-single pod system, and (4) the dynamics of a complete plant, including the effects of the reel on plant motion during cutting.

Mathematical Model of the Stalk

Model Selection

A visual inspection of the stalks of typical soybean plants reveals that each is different. The differences include random variations in: cross section along the length of the stalk, the amount

of tapering along the length, and random curvature of portions of the stalk, particularly near the free end. Another uncertainty is the effect of the soil around the base of the stalk on stalk motion. Observations while deflecting stalks reveal that this soil undergoes elastic deflection.

Certainly, some attempts to consider these factors could be made. Research concerning the effects of such factors on dynamic systems has been conducted. Collins and Thomson (1968) treated the effect of random variations in mass and stiffness on the eigenvalues and eigenvectors of dynamic systems. As a particular case, they concluded that lateral beam vibrations were indeed somewhat sensitive to such variations.

Garland (1939) determined the normal modes of vibration for beams having noncollinear elastic and mass axes. This condition might arise due to unsymmetrical cross sections, unsymmetrical variations of an otherwise symmetric cross section, or curvature of the beam. Results indicated that the normal modes consisted of both a translation and a torsional rotation.

Conway et al. (1964) determined the natural frequencies of a tapered, conical cantilever beam for various amounts of taper. Their analysis presented the solution to the governing Euler beam equation in the form of Bessel functions.

If the soil at the base of the stalk were idealized as a spring-hinge, the effect of soil elasticity on the normal modes of vibration of the stalk could also be considered and would depend on the value of the spring constant of the hinge (Chun, 1972).

For this study, however, all of these factors were neglected. The most important aspects of the stalk were considered to be that its mass and lateral stiffness were approximately uniformly distributed along its length. The cross section of the stalk was assumed constant and symmetrical about a linear axis, and the soil at the base of the stalk was assumed to be perfectly rigid.

The simplest dynamic model possessing distributed mass and lateral stiffness is the Euler-Bernoulli beam. The equation of motion can be found in standard vibrations texts:

$$EI\frac{\partial^4 y(x,t)}{\partial x^4} + M\frac{\partial^2 y(x,t)}{\partial t^2} + C\frac{\partial y(x,t)}{\partial t} = F(x,t) \qquad (5\text{-}1)$$

where: E = the modulus of rigidity of the stalk material,

I = cross section moment of inertia,

M = mass per unit length of the stalk material,

C = damping per unit length of the stalk material,

y(x,t) = the lateral deflection of the stalk,

x = the location along the length of the stalk,

t = time,

F(x,t) = the force distribution on the stalk;

subject to the boundary conditions for a cantilever beam:

y(0,t) = 0 (no deflection at the fixed end),

$\frac{\partial y}{\partial x}(0,t) = 0$ (the slope at the fixed end is 0),

$\frac{\partial^2 y}{\partial x^2}(L,t) = 0$ (no moment at the free end), and

$\frac{\partial^3 y}{\partial x^3}(L,t) = 0$ (no shear at the free end).

Impulse Response of the Stalk

The impulse response of the stalk can be modeled using the Euler-Bernoulli beam equation. An ideal unit impulse can be applied to the beam as shown in Figure 22:

$$EI\frac{\partial^4 y}{\partial x^4} + M\frac{\partial^2 y}{\partial t^2} + C\frac{\partial y}{\partial t} = \delta(t)\delta(x-b) \qquad (5\text{-}2)$$

where: $\delta(t)\delta(x-b) = F(x,t)$ = a unit impulse applied to the stalk at x = b and t = 0.

The solution for the deflection y(x,t) is assumed to be composed of separable functions of space and time:

$$y(x,t) = \sum_{i=1}^{\infty} q_i(t)\phi_i(x) \qquad (5\text{-}3)$$

where:

$q_i(t)\phi_i(x)$ = the ith principal mode of the system,

$q_i(t)$ = a function of time, t, and

$\phi_i(x)$ = a function of position along the length of the stalk, x.

The delta function $\delta(x-b)$ can be expanded in terms of the

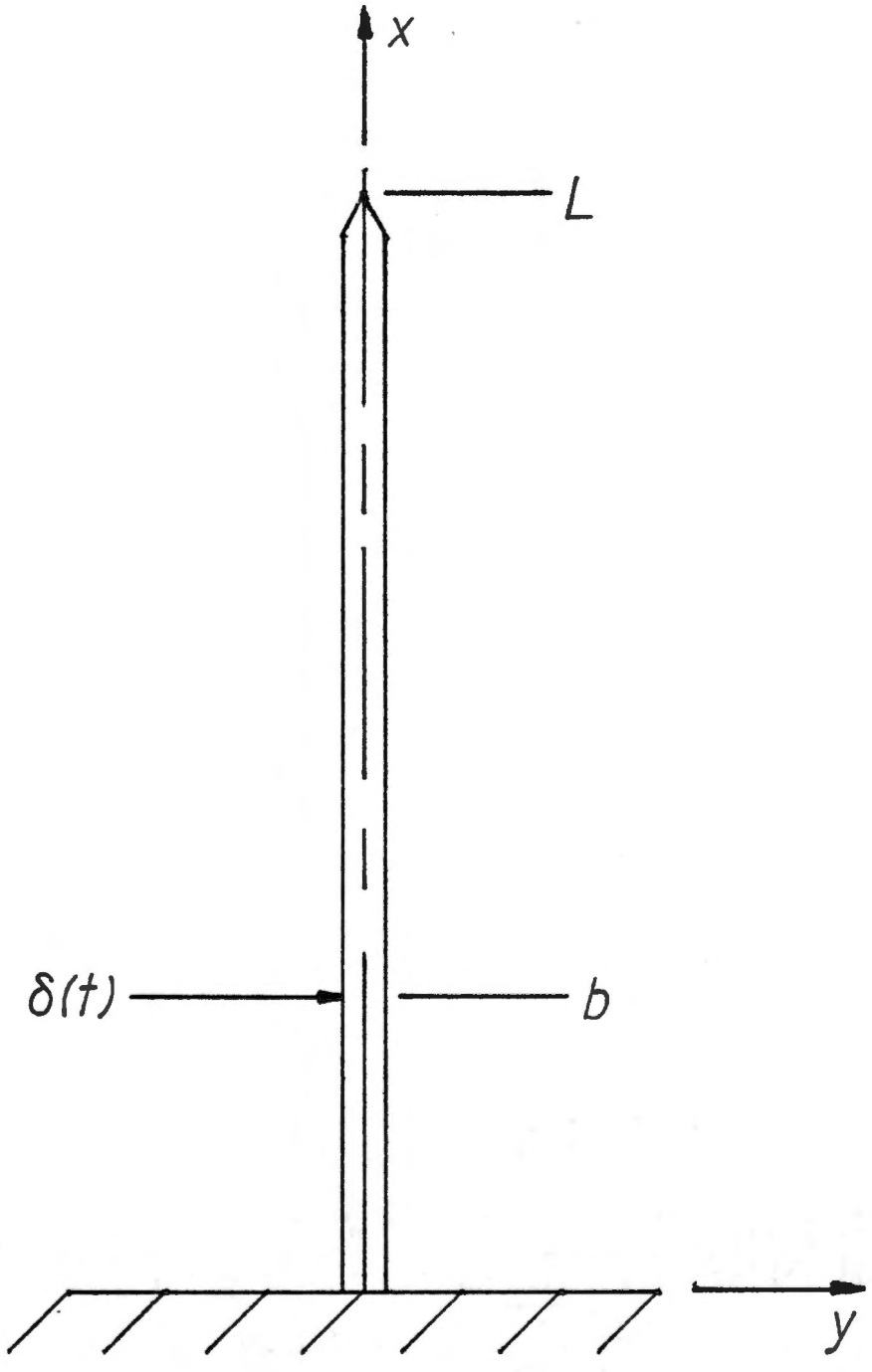

Figure 22. Unit impulse applied to the stalk at x equal b.

eigenfunctions of the system:

$$\delta(x-b)=\sum_{i=1}^{\infty} N_i \phi_i \tag{5-4}$$

where: the N_i = undetermined coefficients.

The orthogonality of the eigenfunctions is used to evaluate the coefficients N :

$$N_i=\frac{1}{\alpha_i}\int_0^L \delta(x-b)\phi_j dx=\frac{1}{\alpha_i}\int_0^L \sum_{i=1}^{\infty} N_i \phi_i \phi_j dx \tag{5-5}$$

where: $$\alpha_i=\int_0^L \phi_i^2 dx \tag{5-6}$$

Equations 5-3, 5-4, and 5-6 can be substituted into equation 5-2 to obtain two ordinary differential equations:

$$\frac{d^4\phi_i}{dx^4}+\beta_i^4\phi_i=0 \tag{5-7}$$

where: $\beta_i^4 = \frac{M\omega_{n_i}^2}{EI}$, and

$$\frac{d^2 q_i}{dt^2}+2\zeta\omega_{n_i}\frac{dq_i}{dt}+\omega_{n_i}^2 q_i=\frac{\delta(t)\phi_i(b)}{M\alpha_i} \tag{5-8}$$

where: $2\zeta\omega_{n_i} = \frac{C}{M}$, and

ω_{n_i} = the natural (undamped) frequency of the i<u>th</u> principal mode.

The solutions $\phi_i(x)$ are tabulated for the particular boundary

conditions of interest or can be calculated:

$$\phi_i = A_i(\cos\beta_i x - \cosh\beta_i x) + (\sin\beta_i x - \sinh\beta_i x)$$
$$A_i = (\cos\beta_i L + \cosh\beta_i L)/(\sin\beta_i L - \sinh\beta_i L) \qquad (5\text{-}9)$$

Representative modes of vibration, the O (x), are shown in Figure 23.

The solutions to equation 5-8 (using zero initial conditions for this particular case) are also available in standard vibrations texts:

$$q_i = \phi_i(b)e^{-\zeta\omega_{n_i}t}\sin\omega_{d_i}t \qquad (5\text{-}10)$$

where: $\omega_{d_i} = \sqrt{1-\zeta^2}\,\omega_{n_i}$ = the damped natural frequency of the ith principal mode of vibration.

The complete solution for the deflection of any point on the stalk due to a unit impulse applied at x equal b is obtained by substituting equation 5-10 into equation 5-3:

$$y(x,t) = \sum_{i=1}^{\infty}\left[\phi_i(b)e^{-\zeta\omega_{n_i}t}\sin\omega_{d_i}t\right]\phi_i(x) \qquad (5\text{-}11)$$

The deflection of any point on the stalk, for example x equal p, can be found from equation 5-11:

$$y(p,t) = \sum_{i=1}^{\infty}\left[\phi_i(b)e^{-\zeta\omega_{n_i}t}\sin\omega_{d_i}t\right]\phi_i(p) \qquad (5\text{-}12)$$

Expressions for the velocity and acceleration of a location on the stalk can be found by differentiating equation 5-12 with respect to

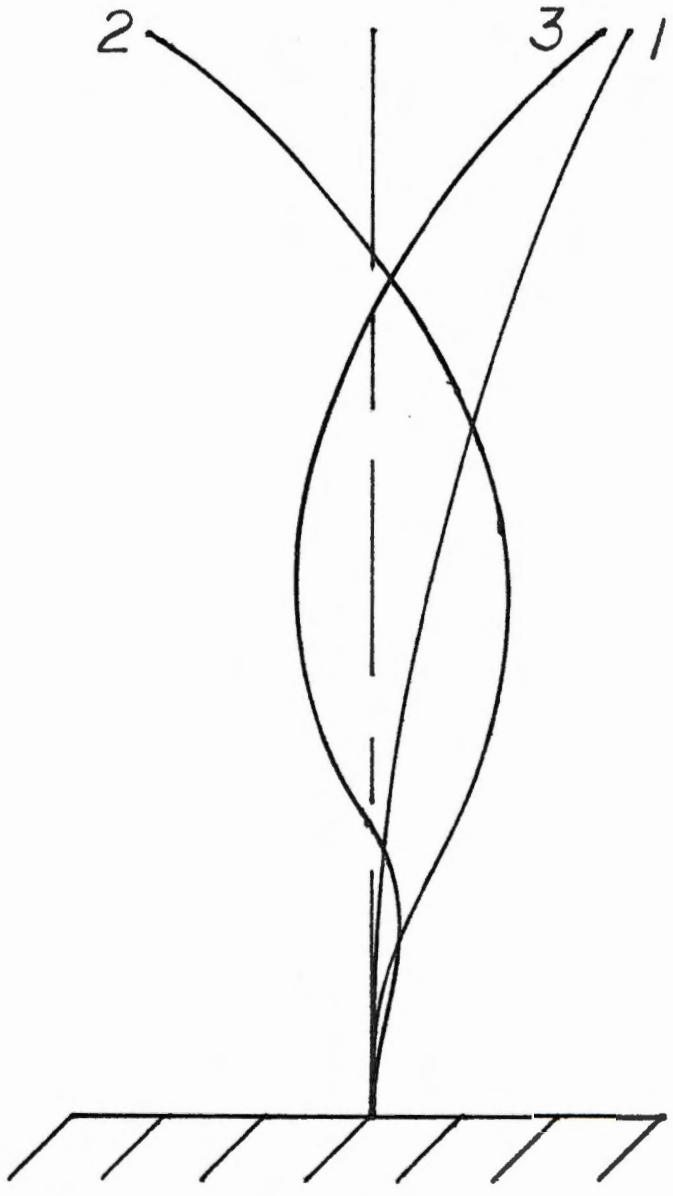

Figure 23. Representative modes of vibration of the Euler-Bernoulli cantilever beam.

time. For example, the expression for the acceleration of a point z is obtained by differentiating twice with respect to time:

$$\ddot{y}(p,t) = \sum_{i=1}^{\infty} \ddot{q}_i \phi_i(p) \qquad (5\text{-}13)$$

Thus, the impulse response of the stalk, measured at any location along the stalk, is seen to be the sum of a series of damped sinusoids, the magnitudes of which depend on the location of impulse application b, the location of measurement z, and the values of the system parameters E, I, M, and C (or ζ and ω_n).

Values for the parameters of a particular stalk were estimated to be:

$EI = 1.044 \times 10^{1}$ lbf-in ,

$M = 6.06 \times 10^{-7}$ lbf-sec /in , and

$C = 5.0 \times 10^{-2}$ lbf-sec/in .

Using these values, equation 5-13, and the Fourier transform program SFFT16, amplitude spectra for the theoretical accelerations of two locations on the stalk were computed. The results are shown in Figures 24 and 25.

Corresponding experimental data for an actual stalk were obtained using the methods described in Chapters III and IV. The average experimental amplitude spectra are shown in Figures 26 and 27. Appendix B contains the amplitude spectra of test replications from which average spectra were computed for all of the experimental results discussed in this chapter.

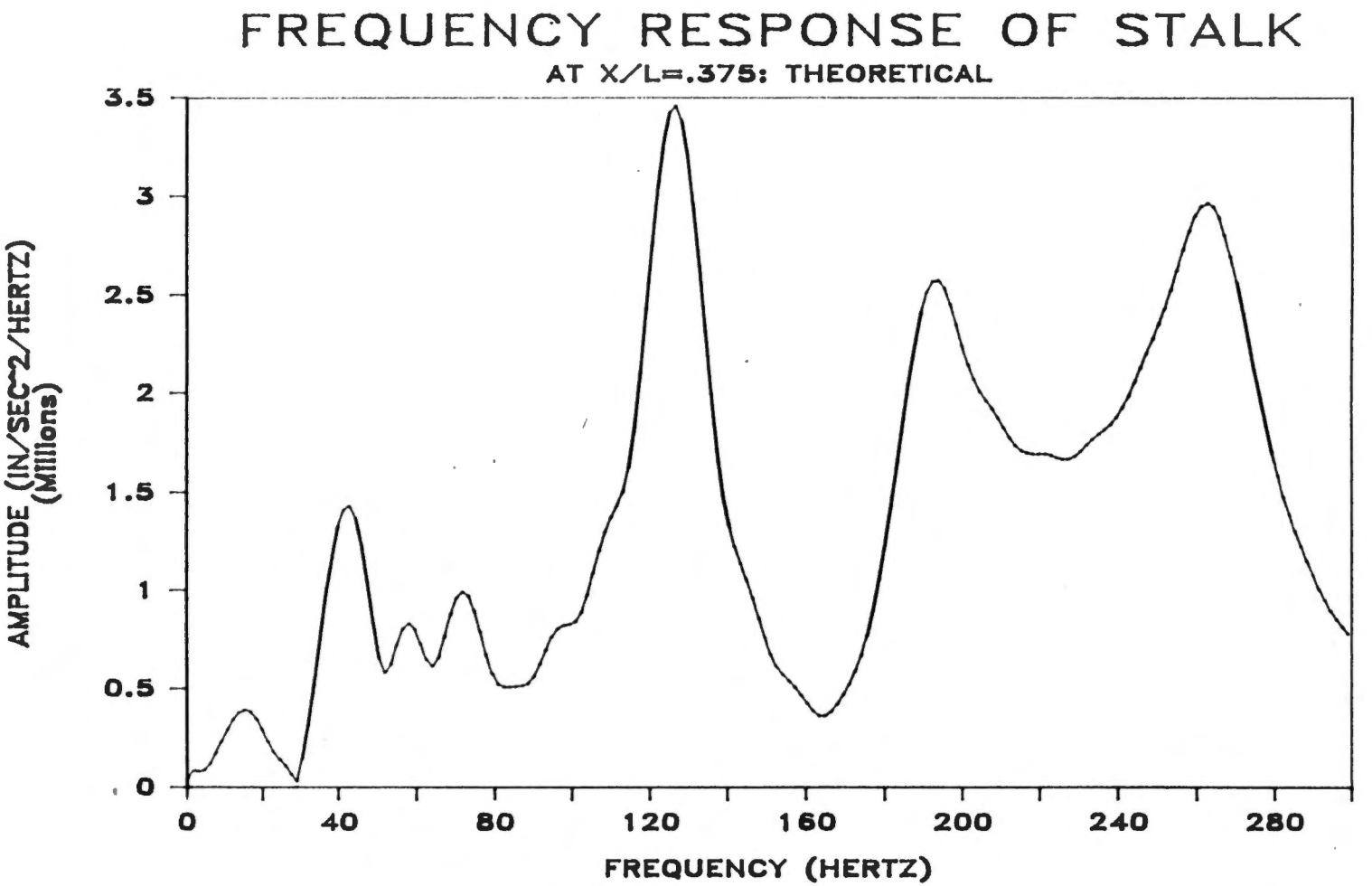

Figure 24. Amplitude spectrum of the theoretical impulse response of location x/L equal 0.375 on a soybean plant stalk.

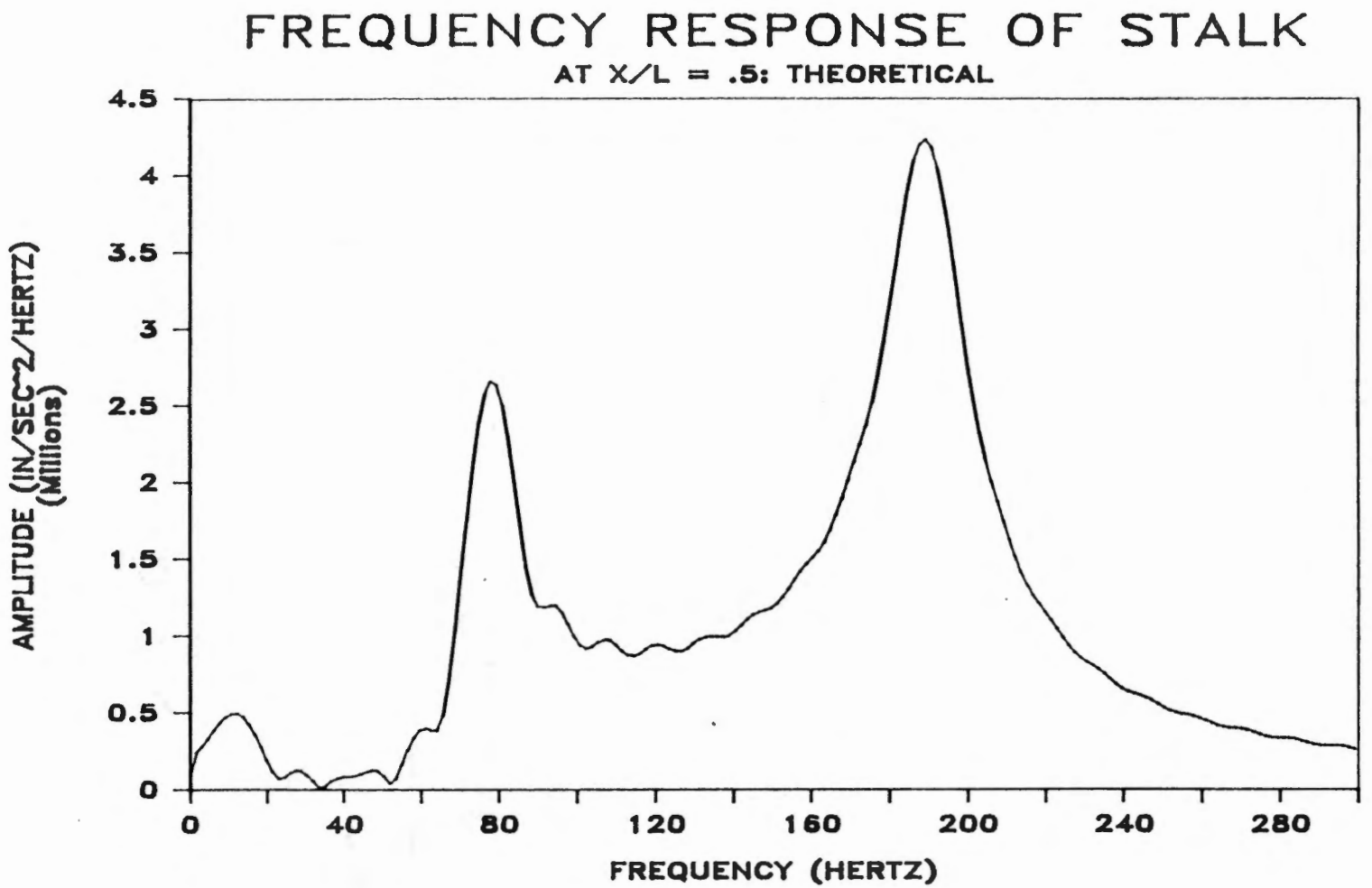

Figure 25. Amplitude spectrum of the theoretical impulse response of location x/L equal 0.50 on a soybean plant stalk.

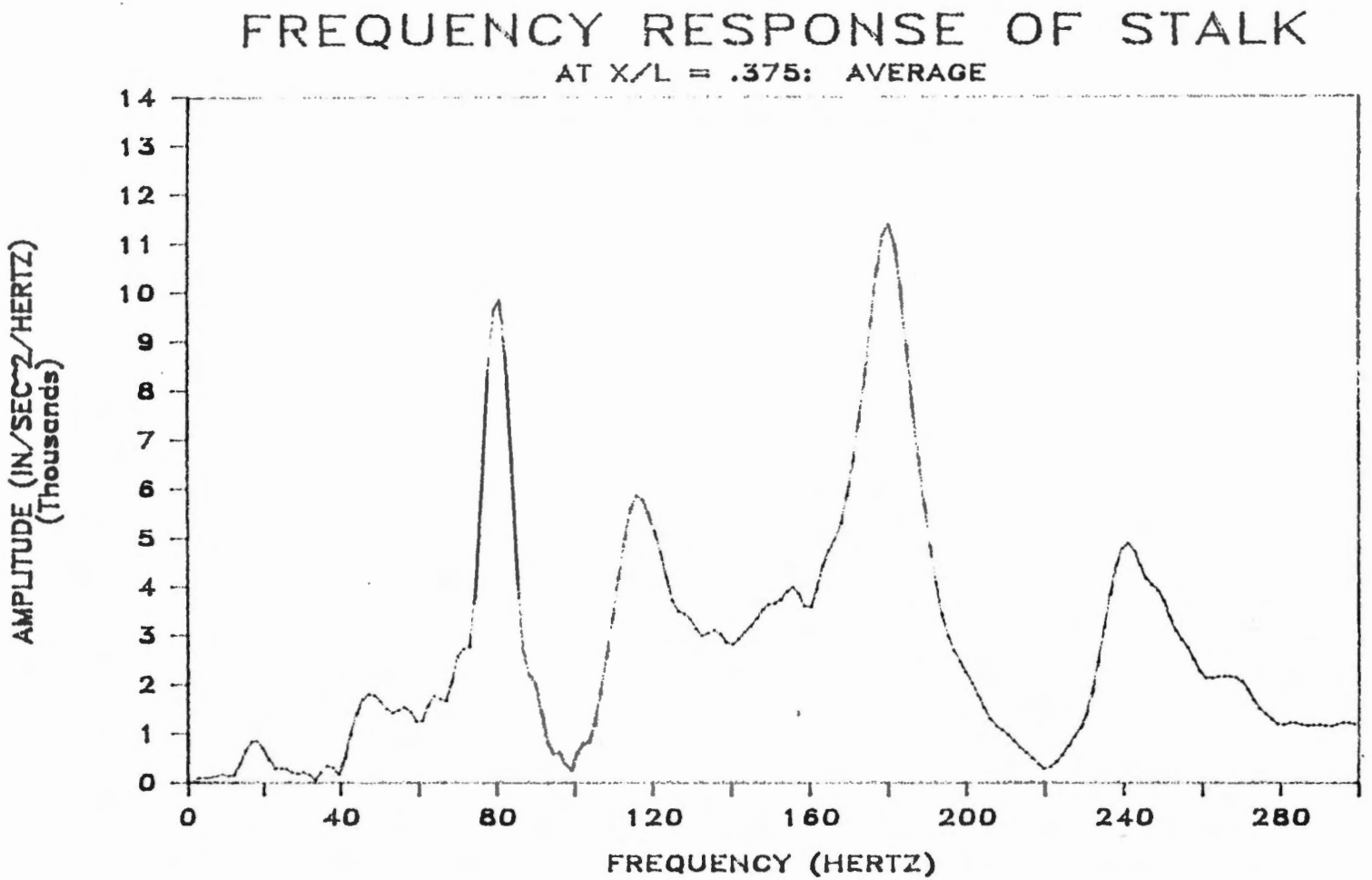

Figure 26. Amplitude spectrum of the measured impulse response of location x/L equal 0.375 on a soybean plant stalk.

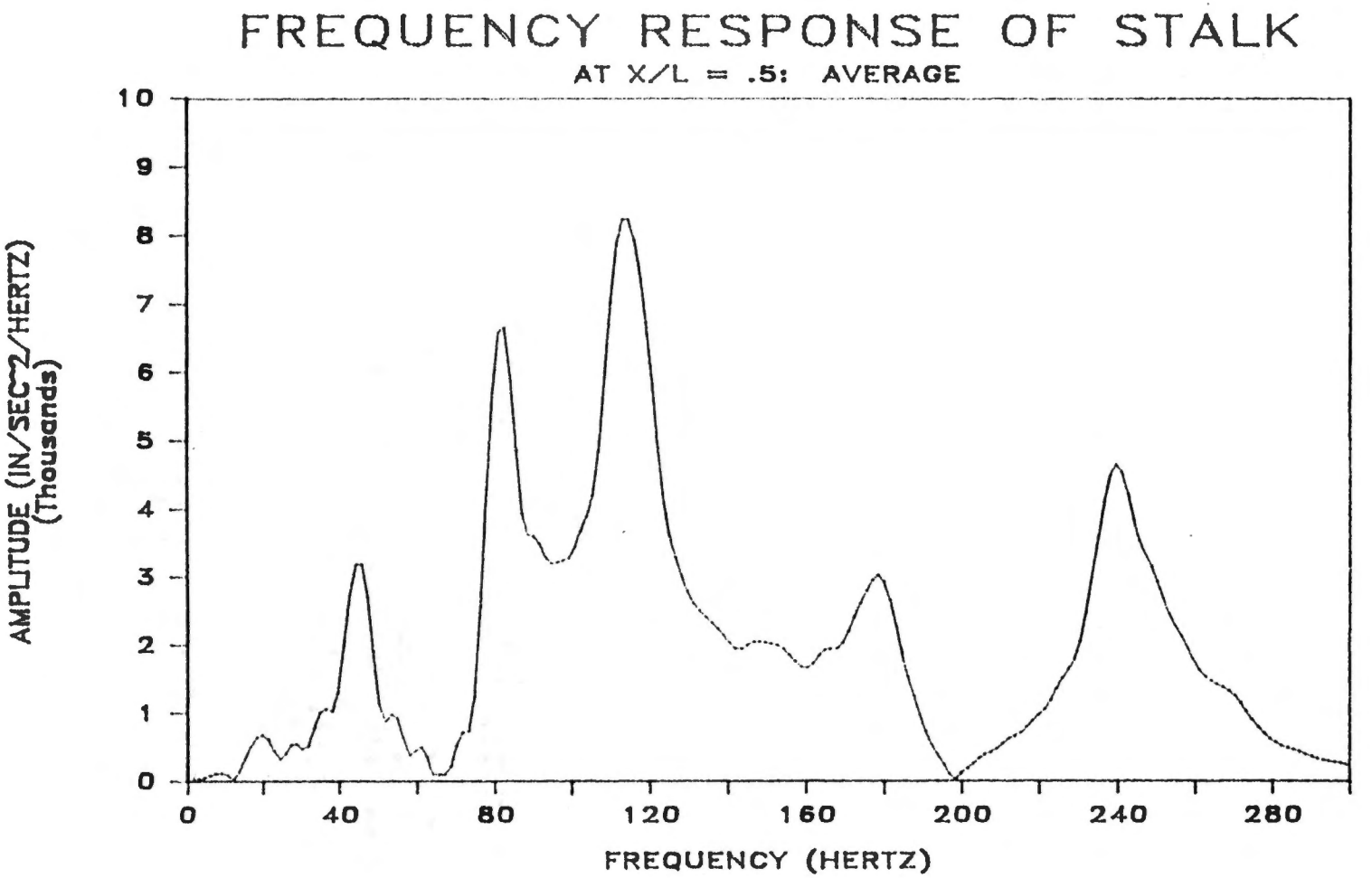

Figure 27. Amplitude spectrum of the measured impulse response of location x/L equal 0.50 on a soybean plant stalk.

One reason for the poor agreement between experimental and theoretical results was the presence of the instrumentation. The experimental data is actually a measurement of the "stalk plus instrumentation" response rather than the response of the stalk alone. Figure 28 depicts the response of the same stalk measured at x/L equal 0.5 both with and without another accelerometer attached at x/L equal 0.375. The differences in the two measured responses reflect the effect of the presence of the additional accelerometer and cable. The addition of the mass, stiffness, and degrees of freedom of the additional instrumentation affects both the locations of the natural frequencies and the amplitudes of vibration at those frequencies.

The effect of the instrumentation on the natural frequencies of the stalk is more clearly illustrated by the results listed in Table 1,

TABLE 1. Ratios of Higher Natural Frequencies With the Second Natural Frequency for the Experimental and Theoretical Results Shown in Figures 25, 27, and 28.

Natural Frequency Ratio	Figure 27 Two Accelerometers	Figure 28 One Accelerometer	Figure 25 Theoretical
/	2.32	2.97	2.80
/	4.38	4.81	5.49
/	6.16	7.62	9.07
/	9.73	11.51	13.58
/	12.97	15.57	18.89
/	-----	20.00	25.28

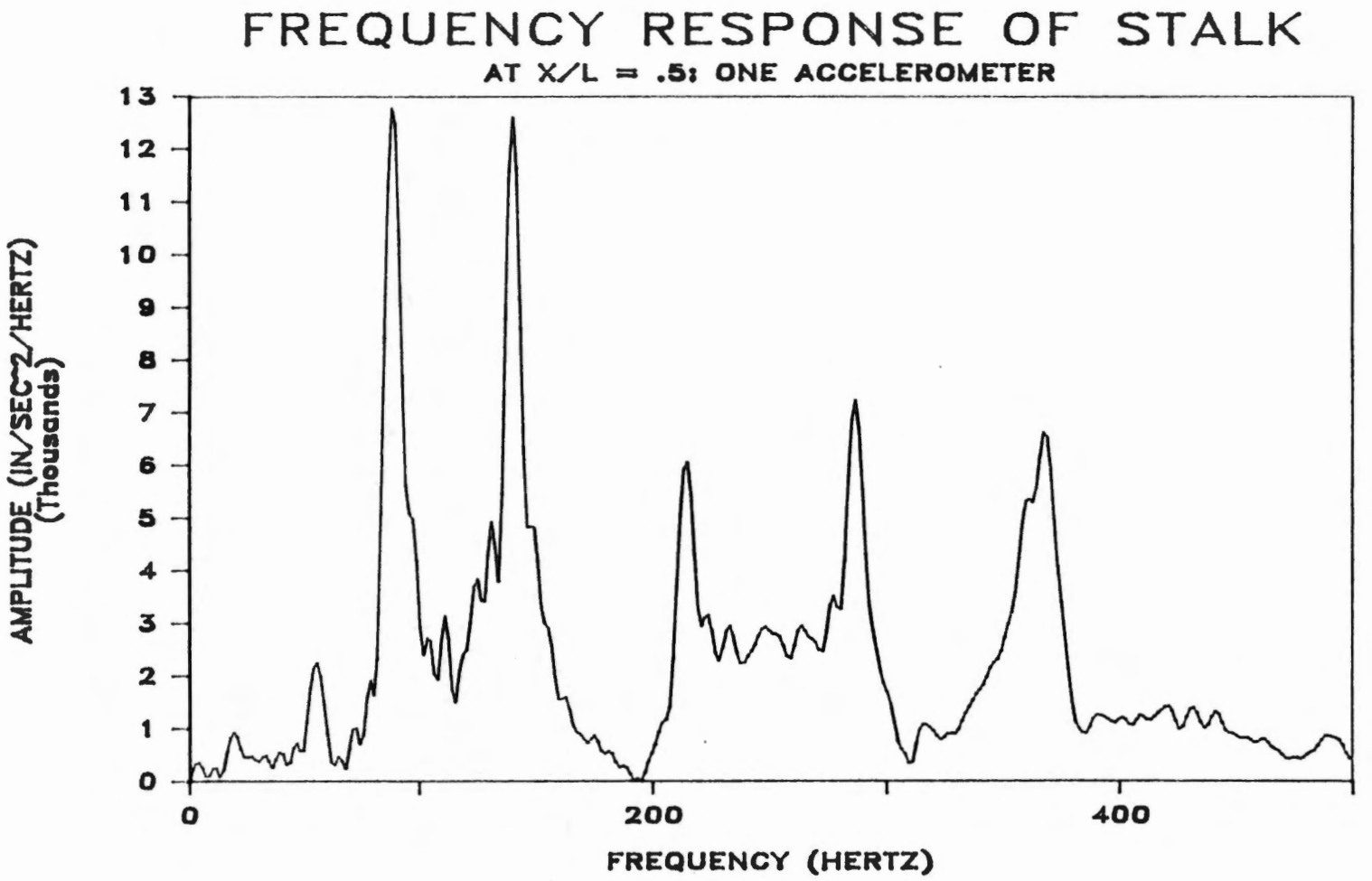

Figure 28. Amplitude spectrum of the measured impulse response of location x/L equal 0.50 on a soybean plant stalk with no other accelerometers present.

where the ratios of each natural frequency to the second natural frequency have been calculated for the data shown in Figures 25, 27, and 28. The effect of the instrumentation is to reduce these ratios below their values as predicted by Euler beam theory, implying that the higher natural frequencies have been reduced. This effect is less for one accelerometer present than for two; therefore, it might be inferred that experimental results for the stalk alone (if they could be obtained) would be even closer to theory. However, the effect of the rotary inertia of the stalk is also to reduce the natural frequencies below their values as predicted by Euler beam theory, particularly the higher frequencies. Therefore, exact agreement between experimental results and the Euler beam model might never be realized.

Despite the degrading effect of the instrumentation on the quality of the data, the beam-like nature of the stalk is still evident. The stalk does possess modes of vibration, a fact that is further substantiated by high speed photography. Because these modes did not appear to be inconsistent with the predicted modes of vibration (equation 5-9), and because it was believed that the natural frequencies of the actual stalk without accelerometers attached would approach predicted values, the Euler-Bernoulli beam was considered to be an acceptable mathematical model for predicting stalk dynamics.

Mathematical Model of the Pod

Model Selection

Mathematically modeling the dynamics of plant fruit is not a new idea. The use of vibratory fruit harvesters, in particular, motivated several efforts to model the motion of a variety of fruits.

The work of Cooke and Rand (1969) is a notable example. They developed a linearized, three-degree-of-freedom pendulum model of a fruit-stem system to investigate fruit dynamics during harvesting. Using the natural frequencies and mode shapes of their model, they predicted optimum frequency ranges for harvesting fruits either with or without stems. They reported "excellent agreement" with experimental data for fruits for which such information was available. In subsequent work, Rand and Cooke (1970) extended their analysis to include nonlinear effects. The nonlinear analysis served primarily to determine the maximum amplitude of fruit motion for which linear analysis was valid.

A pendulum model was also used in this study. The pod was modeled as a simple pendulum pinned to the stalk at the point of attachment. A torsional spring acting between the stalk and pod was used to account for the stiffness of the pedicel. Thus, the model pod had one degree of freedom: rotation about the pin in the plane of stalk motion. A drawing of this model is shown in Figure 29.

The equation describing the nonlinear free vibration of the pod with the stalk fixed can be found in standard texts (Tse et al., 1978):

$$mp^2\ddot{\theta} + mpg\sin\theta + k\theta = 0 \qquad (5\text{-}14)$$

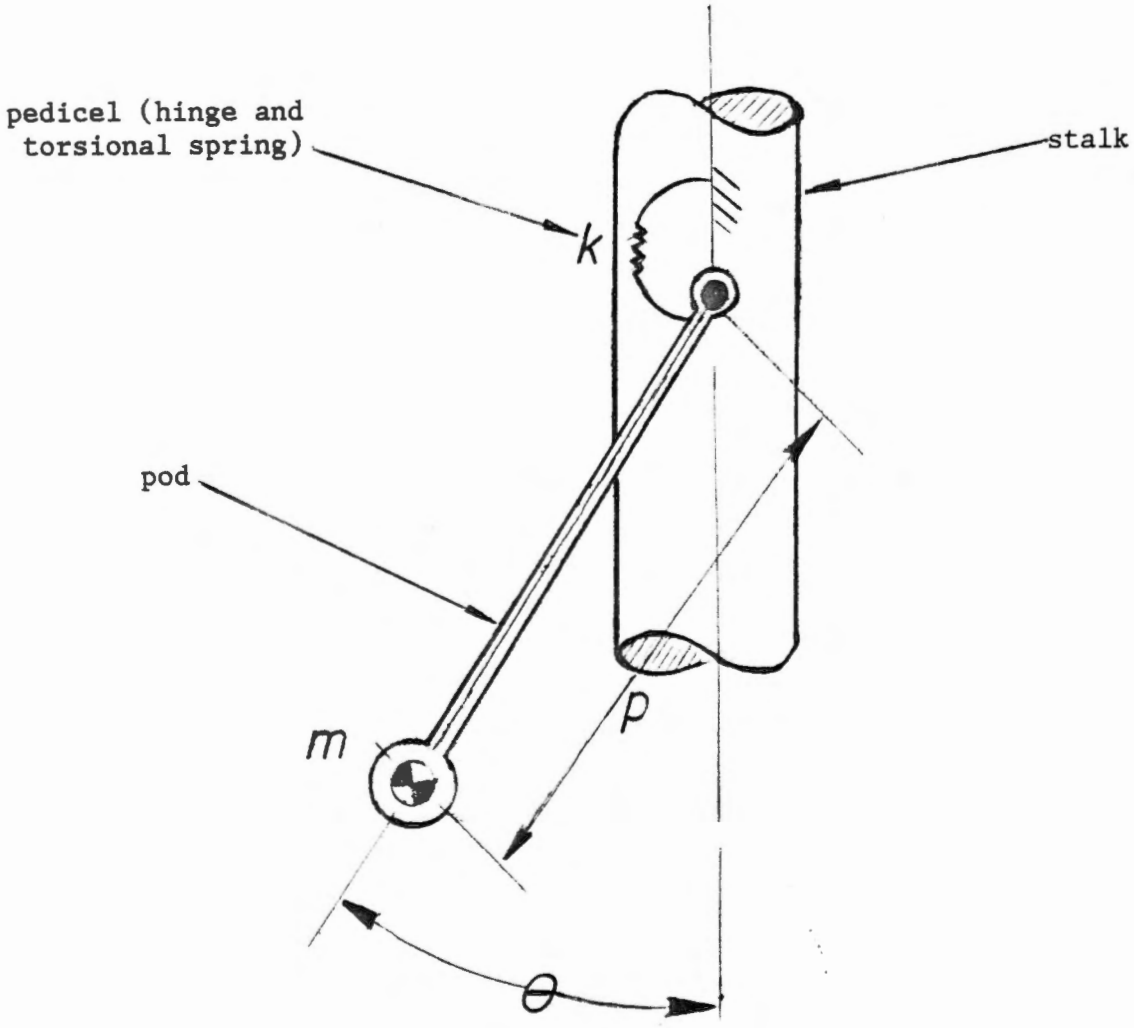

Figure 29. Geometry used to derive the equation of motion for the model pod.

where: m = the mass of the pod,

p = the distance between the pod center of mass and the point of attachment to the stalk (hinge),

g = gravitational acceleration,

k = the torsional stiffness of the pedical that connects the pod to the stalk,

θ = the rotation of the pod relative to a fixed vertical axis, and

and $\ddot{\theta}$ = the angular acceleration of the pod.

Considering only small angular deflections of the pod for which sine θ and θ are approximately equal, the linearized equation of the pod's free vibration can be written as

$$mp^2\ddot{\theta}+(mpg+k)\theta=0 \tag{5-15}$$

Natural Frequency of the Pod

The pendulum model was chosen because it was a simple system having approximately the same geometry as a pod and was capable of exhibiting similar dynamics. Because the model possessed only one degree of freedom, the motion of which was already known to be similar to that of a pod, an evaluation of the model reduced to comparing its natural frequency to that of an actual pod.

The natural frequency of the model pod is

$$f_n=\frac{1}{2\pi}\sqrt{\frac{mgp+k}{mp^2}} \tag{5-16}$$

For a particular pod, values for m, p, and k were estimated to be

$$m = 2.8 \times 10^{-6} \text{ lbf-sec /in},$$

$$p = 8.8 \times 10^{-1} \text{ in, and}$$

$$k = 1.56 \times 10^{-3} \text{ in-lbf/rad}.$$

These values result in a predicted natural frequency of the pod of 5.4 hz. The actual value was between four and six hz. Quick (1974) measured natural frequencies for three-bean Amsoy pods in the range of four to seven hz, which also compares well with the predicted value. Therefore, the mathematical model chosen for the pod was considered satisfactory.

Mathematical Model of a Stalk-Single Pod System

Review of Literature

Experimental results show that the motion of the stalk and even a single pod cannot be considered separately. That is, each affects the motion of the other. Mathematically, this interdependence can be accounted for by considering the "coupled" equations of motion of the stalk and a single pod.

The vibrations of dynamical systems consisting of a beam and various combinations of springs, masses, and dampers have been analysed by several investigators. Young (1948) determined the natural frequencies for vibrating systems consisting of a cantilever beam and: an attached mass; several masses; or a spring, mass, and damper.

Lee and Saibel (1952) derived the frequency equation for the vibration of a constrained beam and any combination of concentrated and

sprung masses. Weissenburger (1968) also considered the vibration of beam-concentrated mass and beam-sprung mass systems.

Dowell (1979) summarized the effects of mass and stiffness addition to a dynamical system on the locations of the natural frequencies of the system.

Finally, Thomson (1954,1981) also considered the vibration of constrained structures. Thomson's analysis procedure, as well as the procedures of all of the investigators mentioned, determined the normal modes of vibration of the constrained beam in terms of the normal modes of the unconstrained beam.

Impulse Response of the Stalk-Single Pod System

Following the analysis procedure of Thomson and others, and referring to Figure 30, the equations of motion for a stalk-single pod system subjected to an impulse at x equal b can be written. For the stalk (neglecting damping),

$$M\ddot{y}(x,t)+EIy''''(x,t)=mp\ddot{\Theta}\delta(x-a)-m\ddot{y}(a,t)\delta(x-a) \qquad (5\text{-}17)$$
$$+\lim_{\epsilon\to 0} k\left[\Theta-y(a,t)\right]\left[\frac{\delta(x-a-\epsilon)-\delta(x-a)}{\epsilon}\right]-\delta(t)\delta(x-b)$$

The first term on the right-hand side of equation 5-17 is due to the addition of the pod's mass to the beam, the second and third terms are due to the motion of the pod, and the last is the applied force. For the pod,

$$mp^2\ddot{\Theta}+(mpg+k)\Theta=ky'(a,t)+mp\ddot{y}(a,t) \qquad (5\text{-}18)$$

The stalk deflection can be expressed in terms of the normal modes

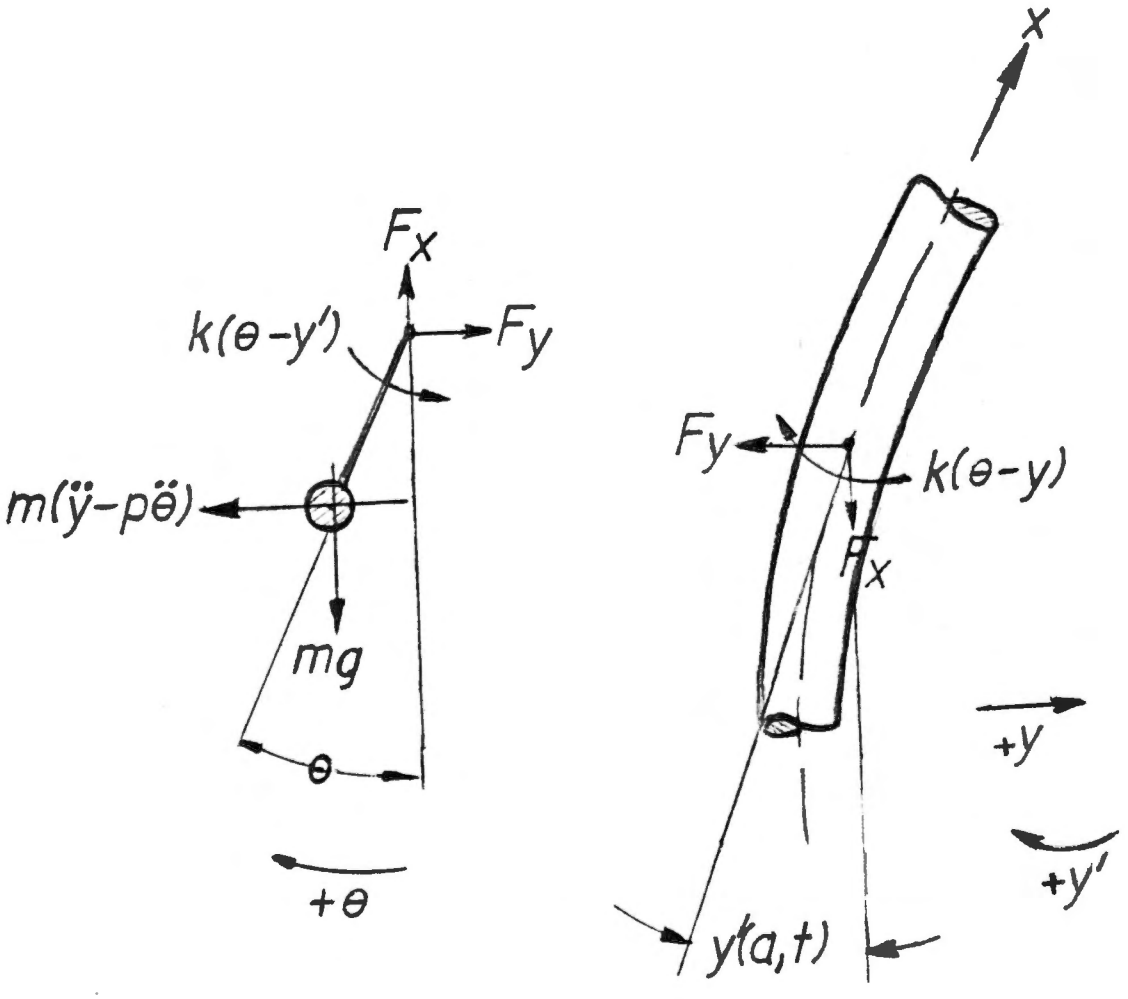

Figure 30. Free-body diagrams of the stalk and pod.

of an Euler-Bernoulli cantilever beam:

$$y(x,t)=\sum_{i=1}^{\infty} q_i(t)\phi_i(x) \tag{5-19}$$

Substituting equation 5-19 into equation 5-17 and exploiting the orthogonality of the normal modes:

$$\int_0^L M\sum_i \ddot{q}_i\phi_i\phi_j dx+\int_0^L EI\sum_i q_i\phi_i''''\phi_j dx=\int_0^L mp\ddot{\Theta}\delta(x-a)-\delta(t)\delta(x-b) \tag{5-20}$$
$$-m\sum_i \ddot{q}_i\phi_i(a)\delta(x-a)+\lim_{\epsilon\to 0}k\left[\Theta-\sum_i q_i\phi_i'(a)\right]\left[\frac{\delta(x-a-\epsilon)-\delta(x-a)}{\epsilon}\right]\phi_j dx$$

Performing the integrations in equation 5-20 yields

$$M\alpha_i\ddot{q}_i+EI\beta_i^4\alpha_i q_i=mp\ddot{\Theta}\phi_i(a)-m\phi_i(a)\sum_j \ddot{q}_j\phi_j+\delta(t)\phi_i(b)+ \tag{5-21}$$
$$k\Theta\phi_i'(a)-k\phi_i'(a)\sum_j q_j\phi_j'(a) \qquad i,j=1,2,\ldots\infty$$

For the purposes of this analysis, only the first six normal modes of the unconstrained beam will be used. Thus, equation 5-21 becomes

$$M\alpha_i\ddot{q}_i+EI\beta_i^4\alpha_i q_i=mp\ddot{\Theta}\phi_i(a)-m\phi_i(a)\sum_j \ddot{q}_j\phi_j+\delta(t)\phi_i(b)+ \tag{5-22}$$
$$k\Theta\phi_i'(a)-k\phi_i'(a)\sum_j q_j\phi_j'(a) \qquad i,j=1,2,\ldots 6$$

These equations (including equation 5-18, the equation of motion of the pod) can be written in matrix form as

$$[M][\ddot{Q}]+[K][Q]=[F] \tag{5-23}$$

where: $[M]$ = the generalized mass matrix,

$[K]$ = the generalized stiffness matrix,

$[F]$ = the vector of generalized forces,

$[Q]$ = the vector of generalized coordinates, and

$[\ddot{Q}]$ = the vector of generalized accelerations.

The complete matrix equation 5-23 is shown in Figure 31.

The generalized coordinates can be related to the principal coordinates using the modal matrix:

$$[Q]=[U][P] \tag{5-24}$$

where: $[U]$ = the modal matrix, and

$[P]$ = the vector of principal coordinates.

Substituting equation 5-24 into equation 5-23 yields

$$[M][U][\ddot{P}]+[K][U][P]=[F] \tag{5-25}$$

The system of equations can be uncoupled using the modal matrix. Premultiplying each term of equation 5-25 by the transpose of the modal matrix:

$$[U]^T[M][U][\ddot{P}]+[U]^T[K][U][P]=[U]^T[F] \tag{5-26}$$

results in

$$[\mathcal{M}][\ddot{P}]+[\mathcal{K}][P]=[N] \tag{5-27}$$

where: $[\mathcal{M}]$ = the diagonalized mass matrix,

$[\mathcal{K}]$ = the diagonalized stiffness matrix, and

$[N]$ = the transformed generalized forces.

$$\begin{bmatrix} M\alpha_1 + mp\phi_1^2(a) & mp\phi_1(a)\phi_2(a) & \cdots & -mp\phi_1(a) \\ & M\alpha_2 + mp\phi_2^2(a) & \cdots & -mp\phi_2(a) \\ & & \ddots & \vdots \\ & \text{SYM.} & & mp^2 \end{bmatrix} \begin{bmatrix} \ddot{q}_1 \\ \ddot{q}_2 \\ \vdots \\ \ddot{\theta} \end{bmatrix} + \begin{bmatrix} EI\beta_1^4\alpha_1 + k\phi_1'^2(a) & k\phi_1'(a)\phi_2'(a) & \cdots & -k\phi_1(a) \\ & \ddots & & \vdots \\ & \text{SYM.} & & mgp+k \end{bmatrix} \begin{bmatrix} q_1 \\ \vdots \\ \theta \end{bmatrix} = \delta(t) \begin{bmatrix} \phi_1(b) \\ \vdots \\ \phi_6(b) \\ 0 \end{bmatrix}$$

Figure 31. Equations of motion of the soybean plant stalk-single pod system in matrix form.

Because both $[M]$ and $[K]$ are diagonal matrices, the system of equations is uncoupled and each may be solved independently. Using the convolution theorem, the principal coordinates can be obtained. For example, for the first principal coordinate:

$$p_i = \frac{1}{m_{ii}\omega_{n_i}} \int_0^t N_i(t-\tau) \sin\omega_{n_i}\tau \, d\tau \qquad (5\text{-}28)$$

where: m_{11} = the first row first column element of $[M]$,

= k_{11}/m_{11} and k_{11} is the first row first column element of $[K]$,

N_1 = the first transformed generalized force, and

p_1 = the first principal coordinate.

The other principal coordinates can be obtained similarly.

The generalized coordinates can be retrieved using equation 5-24 and the deflection of the stalk is obtained with equation 5-19 (using only the first six modes). Differentiating equation 5-19 twice with respect to time yields the acceleration of the stalk due to the impulse. The angular deflection of the pod is the seventh generalized coordinate, as can be seen in Figure 31. The angular acceleration of the pod is obtained by differentiating the angular deflection twice with respect to time, and the linear acceleration of the center of mass of the pod can be calculated knowing this and the acceleration of the point of attachment of the pod with the stalk:

$$a_p = y(a,t) - p\ddot{\theta} \qquad (5\text{-}29)$$

where: a_p = the linear acceleration of the pod (as shown in Figure 30),

$y(a,t)$ = the acceleration of the point of attachment, and

$\ddot{\theta}$ = the angular acceleration of the pod.

The impulse response of a theoretical stalk-single pod system was calculated using the values for parameters listed in the previous sections. The location of the point of attachment of the pod with the stalk was at x/L equal 0.71. The subroutines listed in Appendix C of Tse et al. (1978) were used to numerically perform the operations represented by equations 5-24 through 5-28. The results were then used to generate time series for which spectra could be computed.

Amplitude spectra for the theoretical accelerations of two locations on the stalk of the stalk-single pod system are shown in Figures 32 and 33. The corresponding experimental results are shown in Figures 34 and 35. Again, agreement between theoretical and experimental results is poor, partly due to the presence of the instrumentation and partly beacuse damping was neglected. However, high speed film of the pod also revealed that its displacement exceeded the small angle assumption made in the development of the mathematical model. Furthermore, the pod appeared to have more than the single rotational degree of freedom assumed for its model. The additional degrees of freedom included a twisting mode as well as a translational mode which appeared to be due to the elasticity of the pedicel, a factor that could not be accounted for by the simple hinge point model assumed for the pedicel.

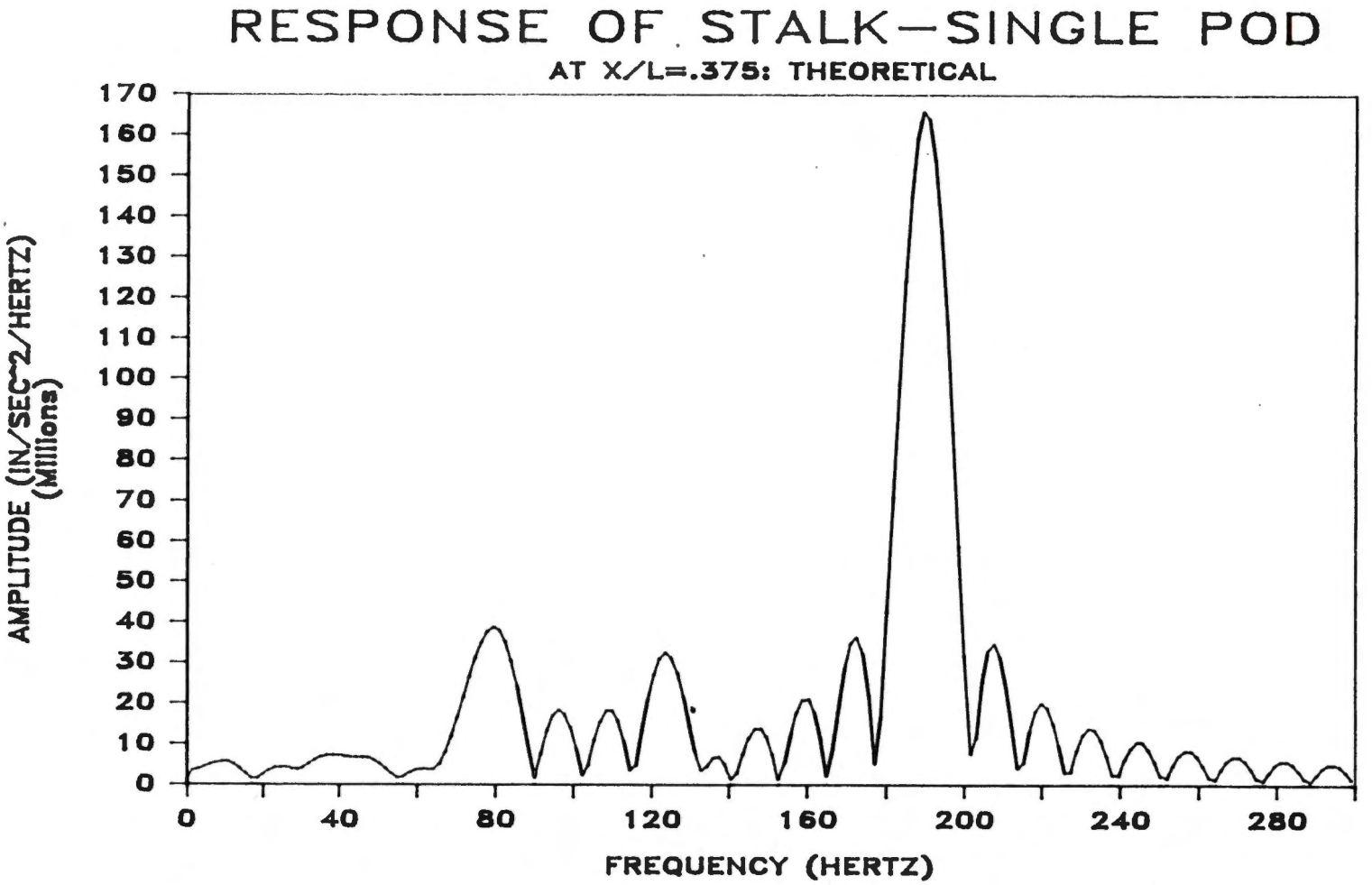

Figure 32. Amplitude spectrum of the theoretical impulse response of location x/L equal 0.375 on a stalk-single pod system.

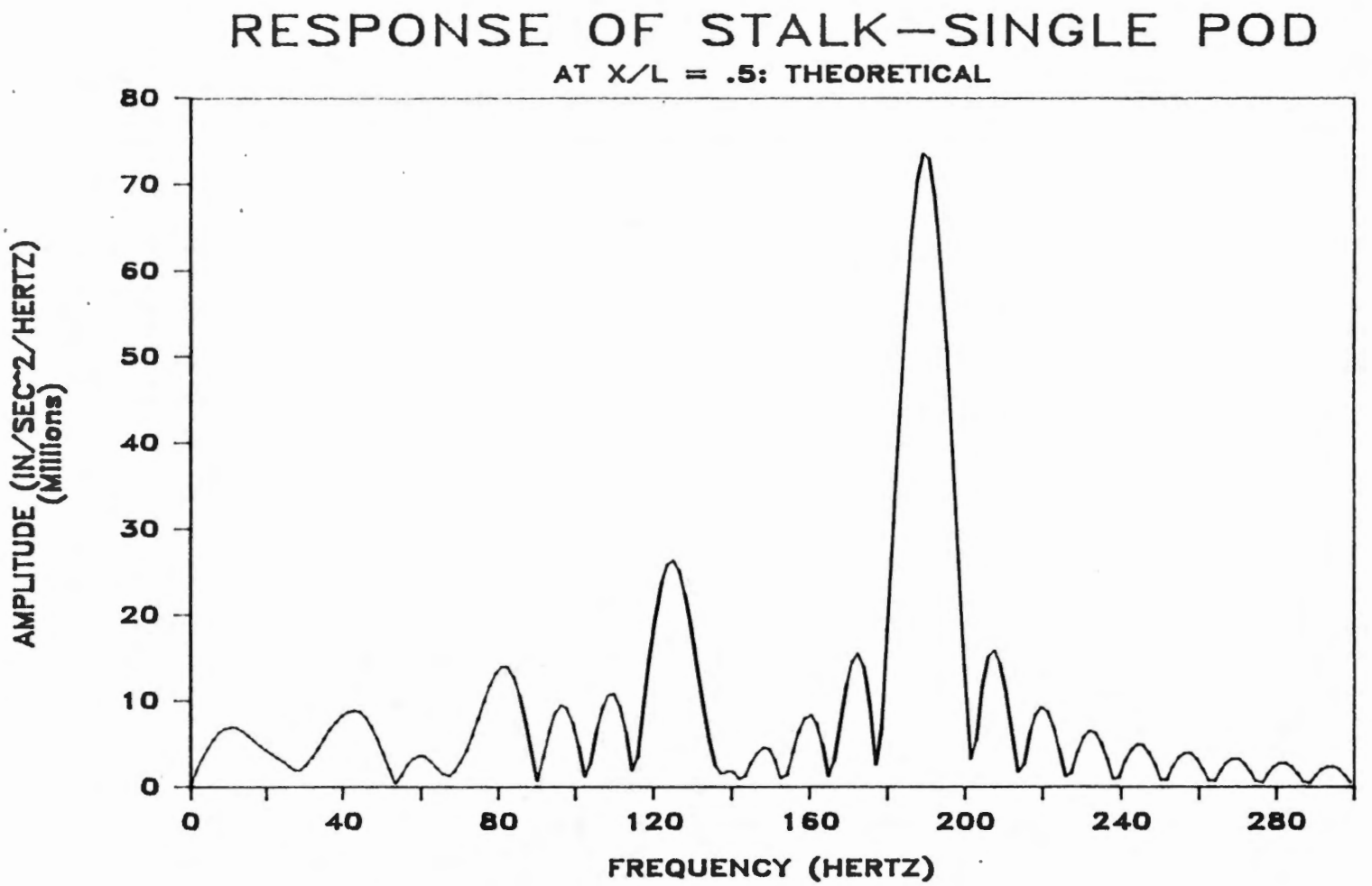

Figure 33. Amplitude spectrum of the theoretical impulse response of location x/L equal 0.50 on a stalk-single pod system.

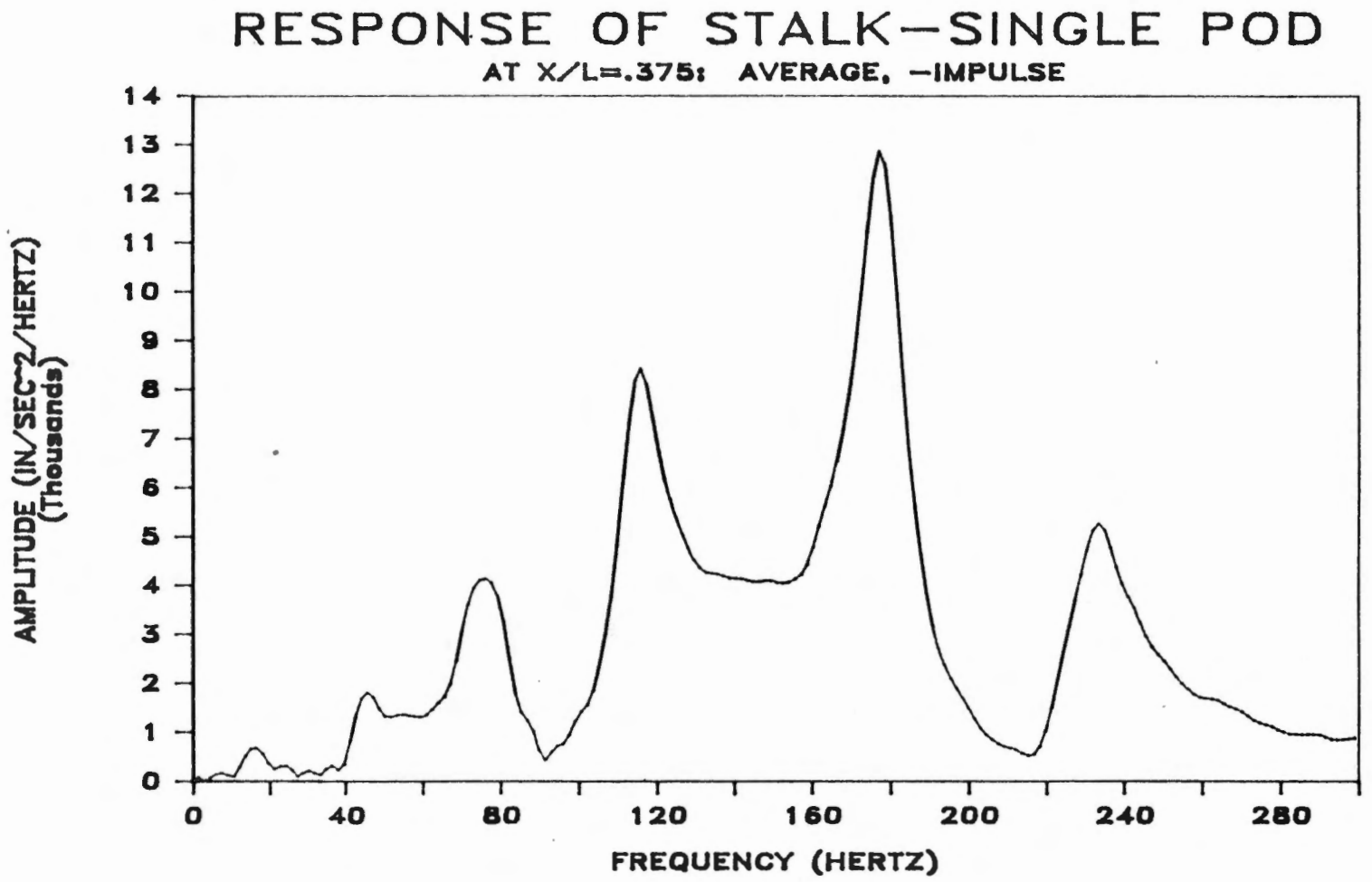

Figure 34. Amplitude spectrum of the measured impulse response of location x/L equal 0.375 on a stalk-single pod system.

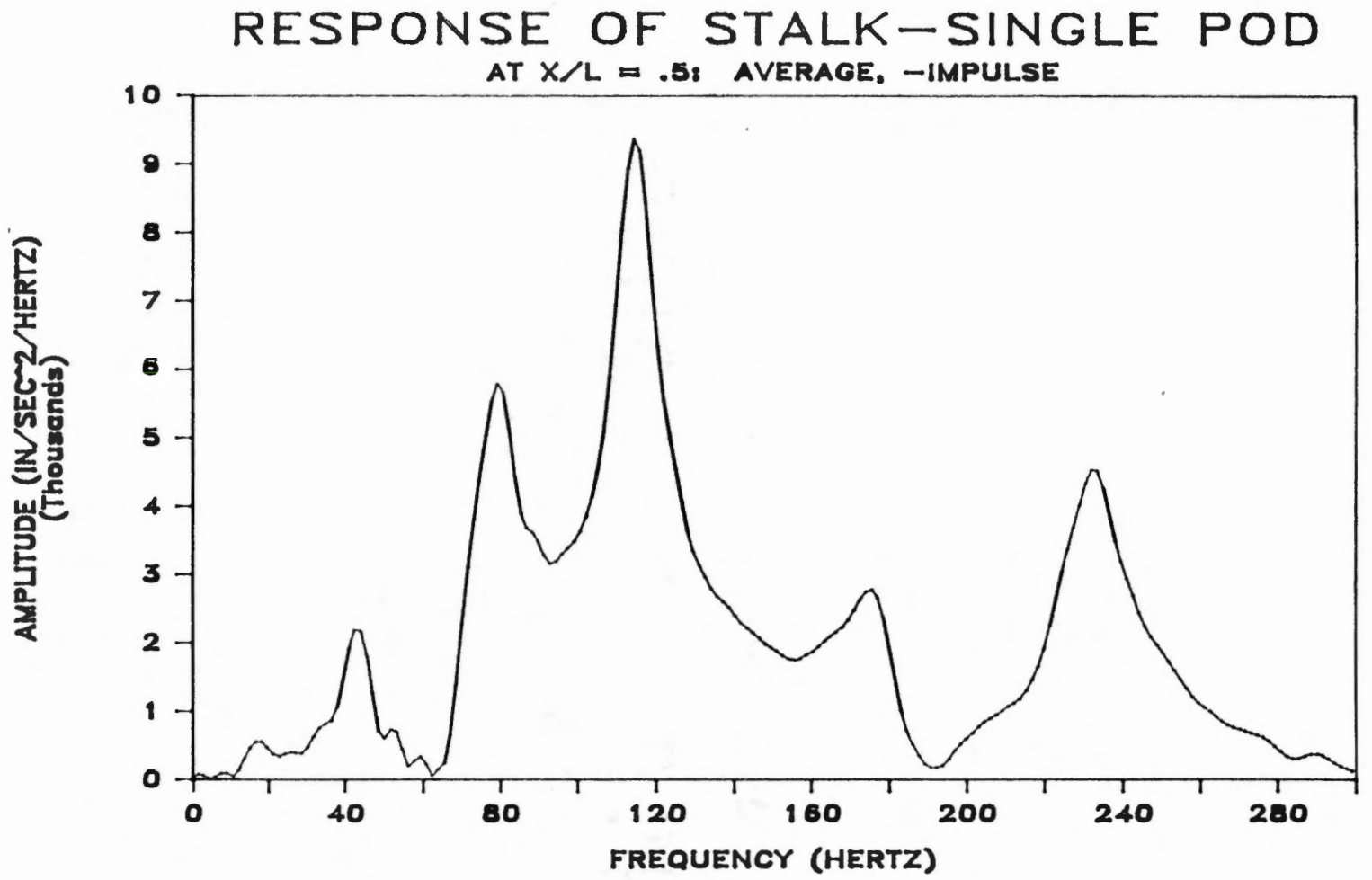

Figure 35. Amplitude spectrum of the measured impulse response of location x/L equal 0.50 on a stalk-single pod system.

Despite these discrepancies, the two most important aspects of the relative motion between the pod and the stalk were effectively modeled. These two aspects of stalk-pod motion are:

1. For vibration of the stalk at frequencies lower than the natural frequency associated with the pod, the stalk and pod tend to move in phase. In contrast, at higher frequencies the stalk and pod tend to move out of phase.
2. The amplitude of pod motion depends on the frequency at which the stalk is vibrating as well as the amplitude of stalk vibration.

The first characteristic of pod-stalk motion can be deduced by comparing the theoretical acceleration of the stalk at the point of attachment to the theoretical linear acceleration of the pod's center of mass:

$$y(a,t) = (1.0)\sin 6.65t + (13.1)\sin 42.3t + (91)\sin 90.1t - (690)\sin 247t + (1257)\sin 483t + (539)\sin 798t - (5448)\sin 1198t$$

$$a_p = (1.0)\sin 6.65t - (3.7)\sin 42.3t - (7.3)\sin 90.1t + (5.3)\sin 247t - (1.2)\sin 483t - (2.0)\sin 798t + (2.5)\sin 1198t$$

The coefficients of the sine terms in each acceleration have been divided by the same constant for ease of comparision. Note that, with the exception of the first term, the signs of the corresponding sine terms in the two accelerations are opposite. Thus, the motions of the pod and stalk at each frequency except the first are out of phase.

The second characteristic of stalk-pod motion is evident in

Figure 36, where the amplitude spectra of the linear acceleration of the pod's center of mass and of the acceleration of the point of attachment are shown.

The similarity between the motion of the pod predicted by this analysis and the vibration of one-degree-of-freedom systems in general is worth noting. As a specific example, consider the simple pendulum with its hinge point subjected to sinusoidal motion. The amplitude and phase spectra for this system are shown in Figure 37 (Tse et al., 1978). The simple pendulum also exhibits a region of high response (resonance), the response then dropping off at higher frequencies. The frequency dependent in-phase out-of-phase characteristic of the pendulum motion is evident in the phase spectrum as well.

Several researchers have proposed that shatter losses are caused by high inertial forces acting on the pods that cause pod failure. They theorize that these high pod accelerations are transmitted from the stalk which undergoes high accelerations during cutting (Nave and Hoag, 1974, Hummel and Nave, 1974, Hummel, 1982, and Hall et al., 1983). These researchers have also used measurements of "mean peak accelerations" of one location of the stalk to evaluate the shatter-causing tendencies of various cutting devices. In light of the results of this study; that is, that the amplitude of pod acceleration cannot be correlated to the amplitude of stalk acceleration without also considering the frequency at which those accelerations occur, one has to question at least this method of evaluation, if not the premise that high <u>inertial</u> forces acting on the pod are the cause of shatter.

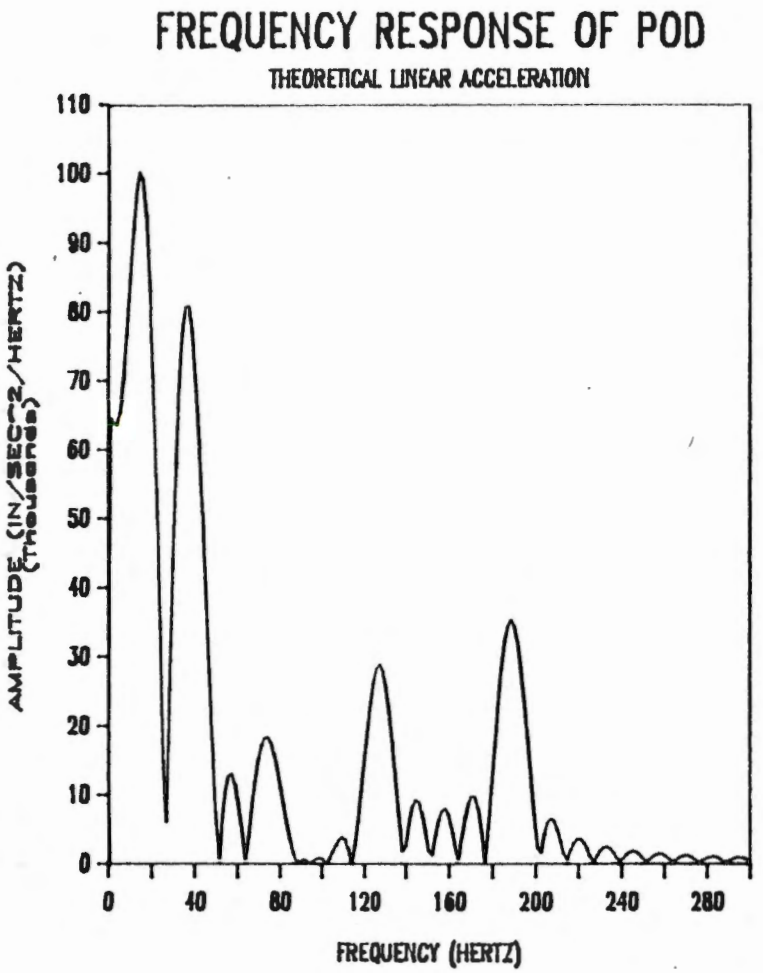

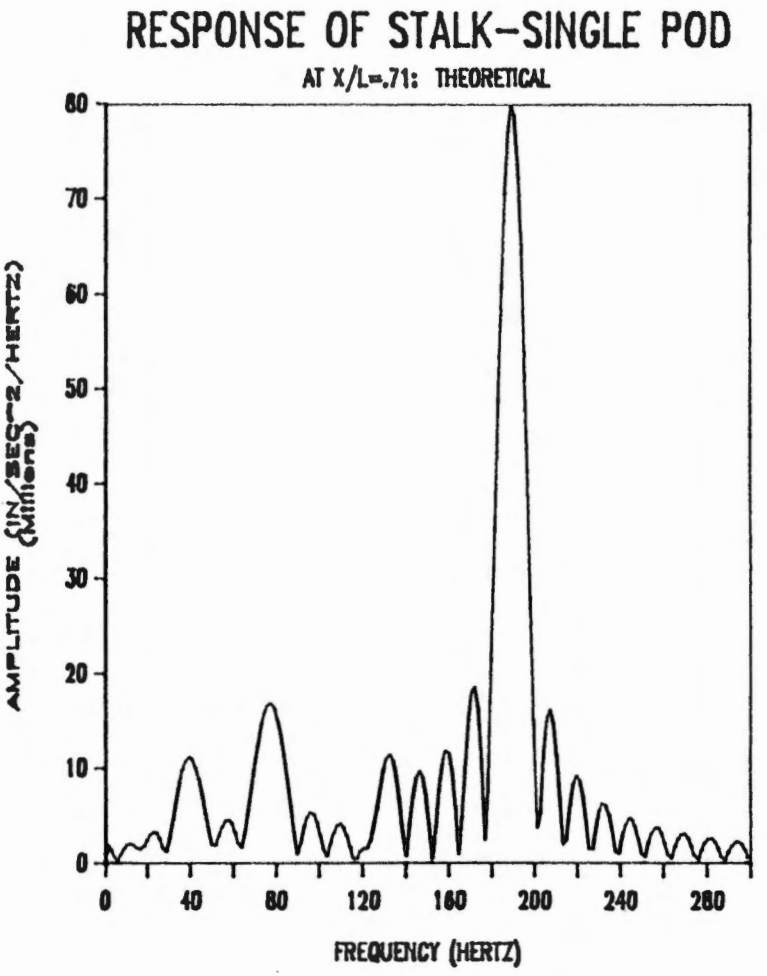

Figure 36. Amplitude spectra of the theoretical impulse responses of the center of mass of the pod and of the stalk at the point of attachment with the pod.

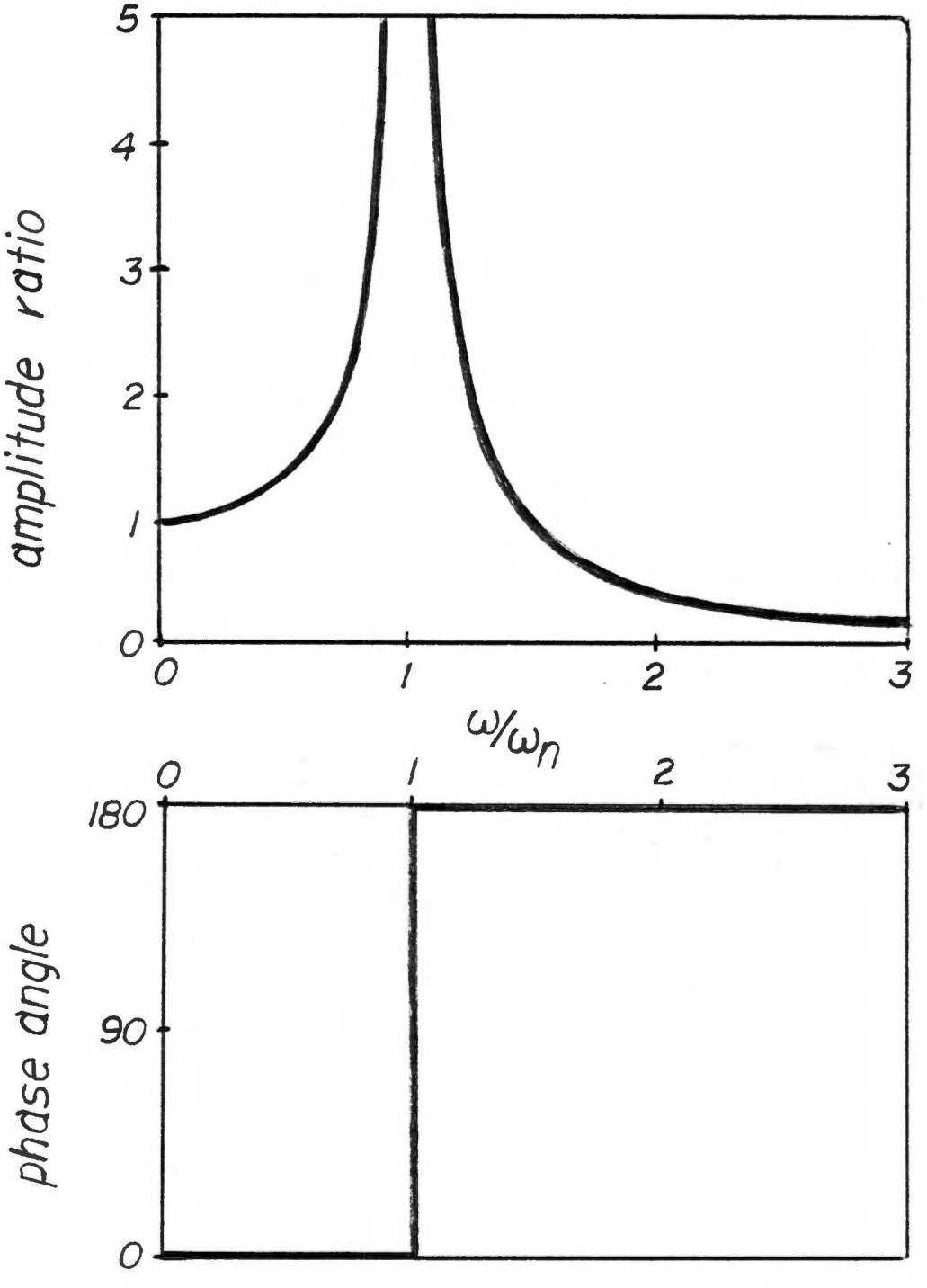

Figure 37. Amplitude and phase spectra of the motion of a simple pendulum with its hinge point subjected to sinusoidal motion (Tse et al., 1978).

Impact Damping: Collisions Between the Pod and Stalk

The fact that pods and the stalk tend to move out of phase for vibrations at most frequencies naturally leads one to wonder if, at some times during their relative motion, collisions might occur between the two. Furthermore, if collisions do occur, is it possible that the resulting impact forces exerted on the pod during some of these collisions are of sufficient magnitude to cause shatter?

Certainly this last question can only be answered by careful experimentation. However, some pertinent literature concerning this phenomenon should be mentioned. The concept of an "acceleration damper" or "impact damper" first appeared in the literature in 1944 (Lieber and Jensen, 1944). The device was described as a mass particle that was free to move within a container. The container was fixed to a body undergoing forced harmonic motion. By properly specifying the dimensions of the box and the size of the mass particle, the particle could be made to impact each side of the container once during each cycle of the body's motion. The result was a significant reduction in the amplitude of the motion of the body.

Grubin (1956), who extended the theoretical analysis of the acceleration damper, described it as "a device for reducing the vibration amplitude of a mechanical system through the mechanism of momentum transfer by collision and the conversion of mechanical energy to heat." Masri and Caughey (1966) analysed the stability of the impact damper. Their stability analysis was limited to the cases for which two-impact-per-cycle motion of the system occurred, one impact on each side of the container.

Reed and Duncan (1967) analysed an impact damper consisting of chains hanging within a container attached to a structure such as a stack, tower, erected lauch vehicle, or antenna. Their analysis was also for steady-state sinusoidally forced motion of the system.

Masri (1972) analysed the steady-state response of a multidegree-of-freedom system equipped with an impact damper and excited by a sinusoidal forcing function. In his work, he made mention of the large accelerations that are developed during impact.

All of these analyses were for steady-state response of a system equipped with an impact damper, whereas the impact damping that pods perform on the stalk during collisions occur as part of a transient process. Moreover, since stalk vibrations in several modes occur simultaneously, it is probable that some modes of stalk vibration would be damped by the collision, while others would be little affected or even enhanced.

Any theoretical study of stalk-pod collisions would almost certainly have to be numerical because the occurrence of a collision depends on the absolute motions of the stalk and pod, each of which is composed of contributions at several frequencies with different amplitudes, and each of which has an effect on the other.

In this study, a simple experiment was performed. In the previous section, the stalk-single pod system discussed was impulsed in a direction that initially caused the stalk and pod to move apart. For this experiment, the same stalk-single pod system was impulsed in the opposite direction, the direction that caused the stalk and pod to initially move towards each other, in an attempt to deliberately cause a collision.

Under visual observation, a collision of the stalk and pod did appear to occur. The amplitude spectra for these two impulse tests (no collision, collision) are compared in Figures 38 and 39 for the two locations on the stalk where response was measured. The amplitudes of some modes of stalk vibration do appear to have been reduced, particularly of the fifth (117 hz) and seventh (234 hz) modes.

Considering these results and the literature reviewed, the collisions of some pods with the stalk during cutting seem likely, and the possibility that such collisions might occasionally result in shatter losses appears to be worth investigation.

Whole Plant Motion

Impulse Response of a Complete Plant

The effect of the pods on the motion of the stalk has been shown to be threefold: an effect due to the addition of mass, an effect due to the motion of the pods, and an effect due to the collision of pods with the stalk. Of course, collisions and dry friction between pods are also likely, and, for cases where there are secondary stems attached to the stalk, their effect on stalk motion would also be significant.

Figures 40 and 41 depict the amplitude spectra of the impulse response of two locations on the stalk that has been used throughout this chapter. However, these spectra were obtained before the pods were removed from the stalk. Comparision of these amplitude spectra with those of the bare stalk shown in Figures 26 and 27 (pages 67 and 68) reveal the significant effect that the pods have on the motion of

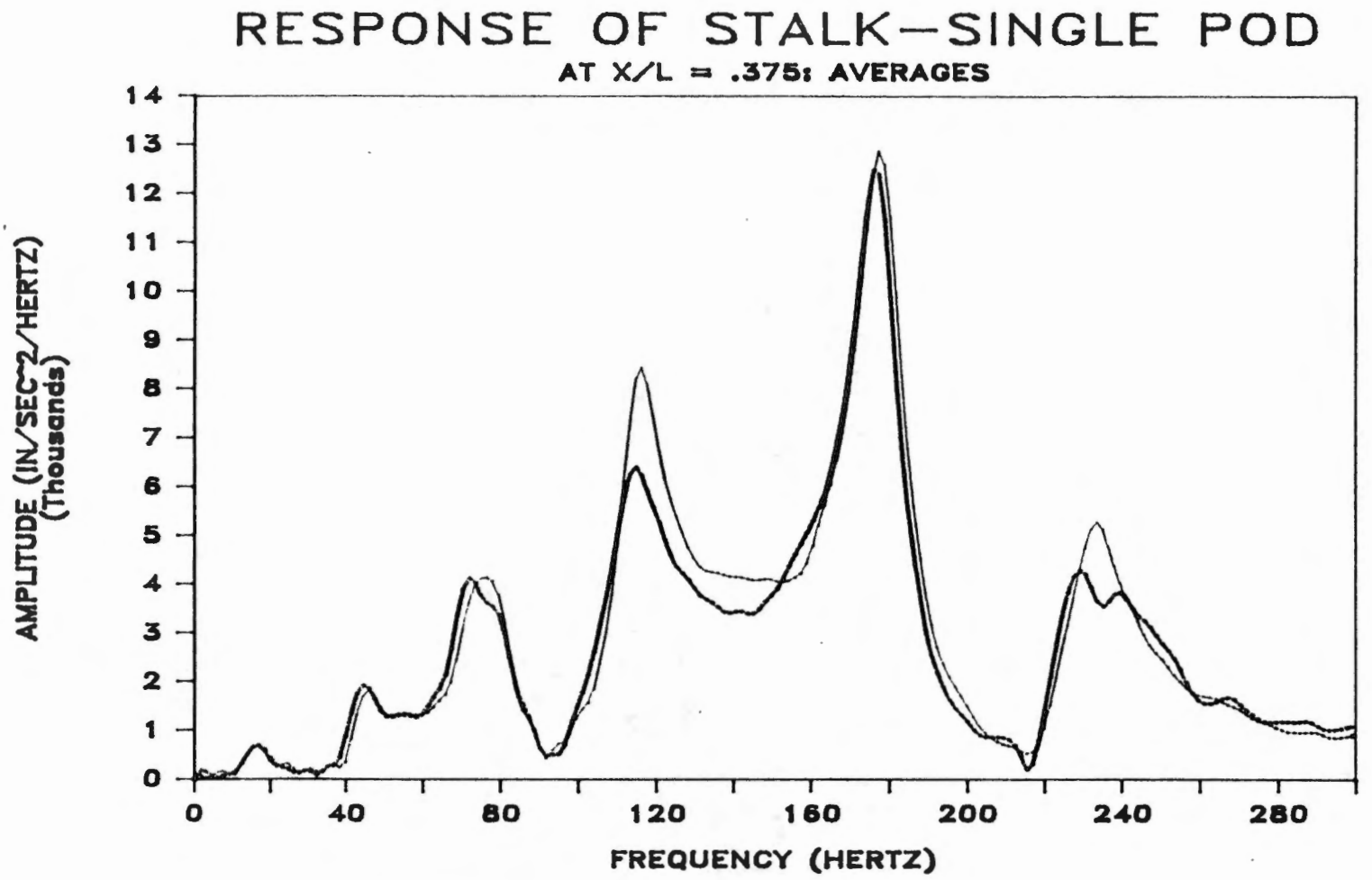

Figure 38. Amplitude spectra of the measured impulse responses of location x/L equal 0.375 on the stalk-single pod system for two cases: (1) no collision between the stalk and pod (fine curve), and (2) collision between the stalk and pod (bold curve).

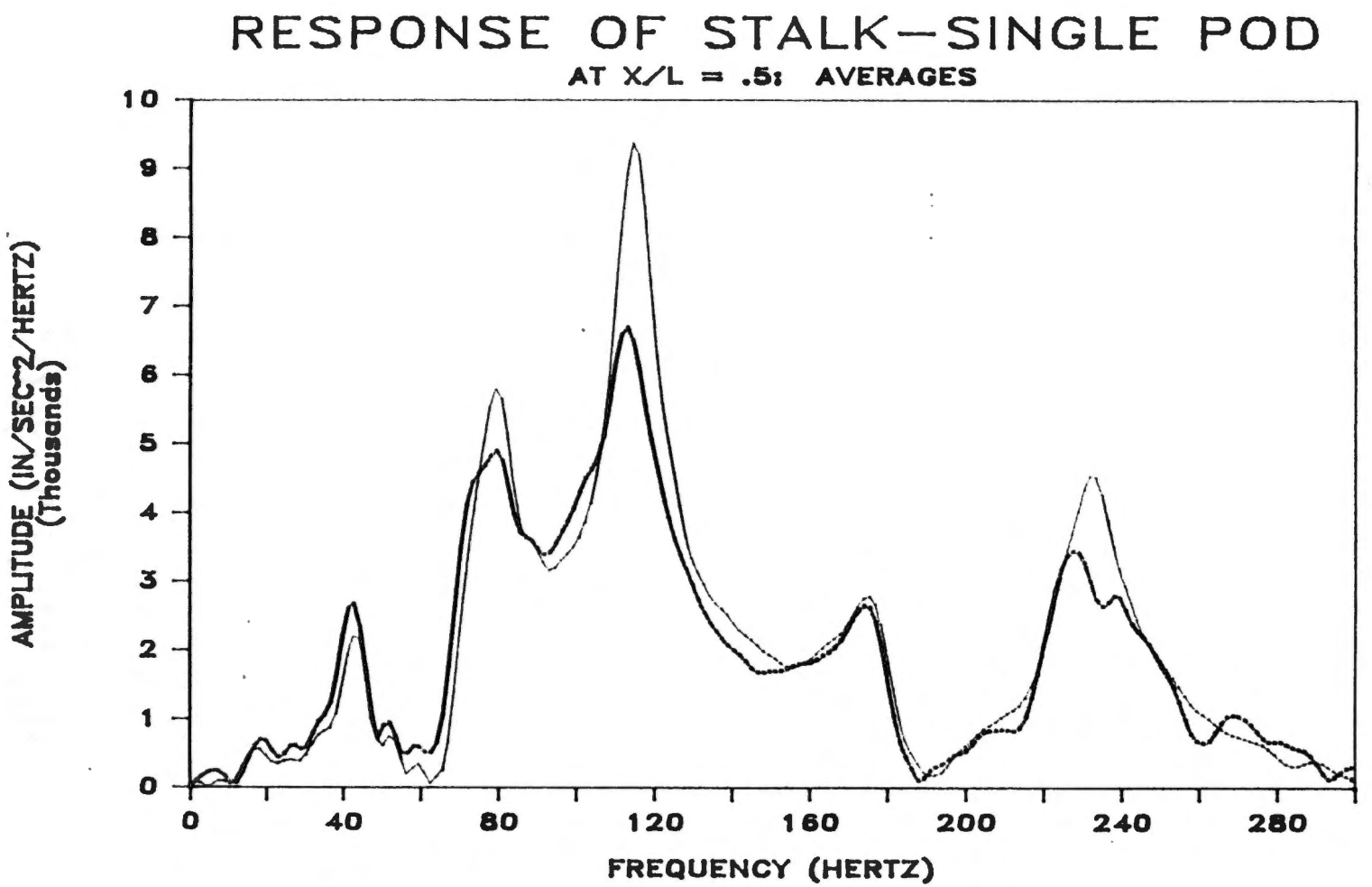

Figure 39. Amplitude spectra of the measured impulse responses of location x/L equal 0.50 on the stalk-single pod system for two cases: (1) no collision between the stalk and pod (fine curve), and (2) collision between the stalk and pod (bold curve).

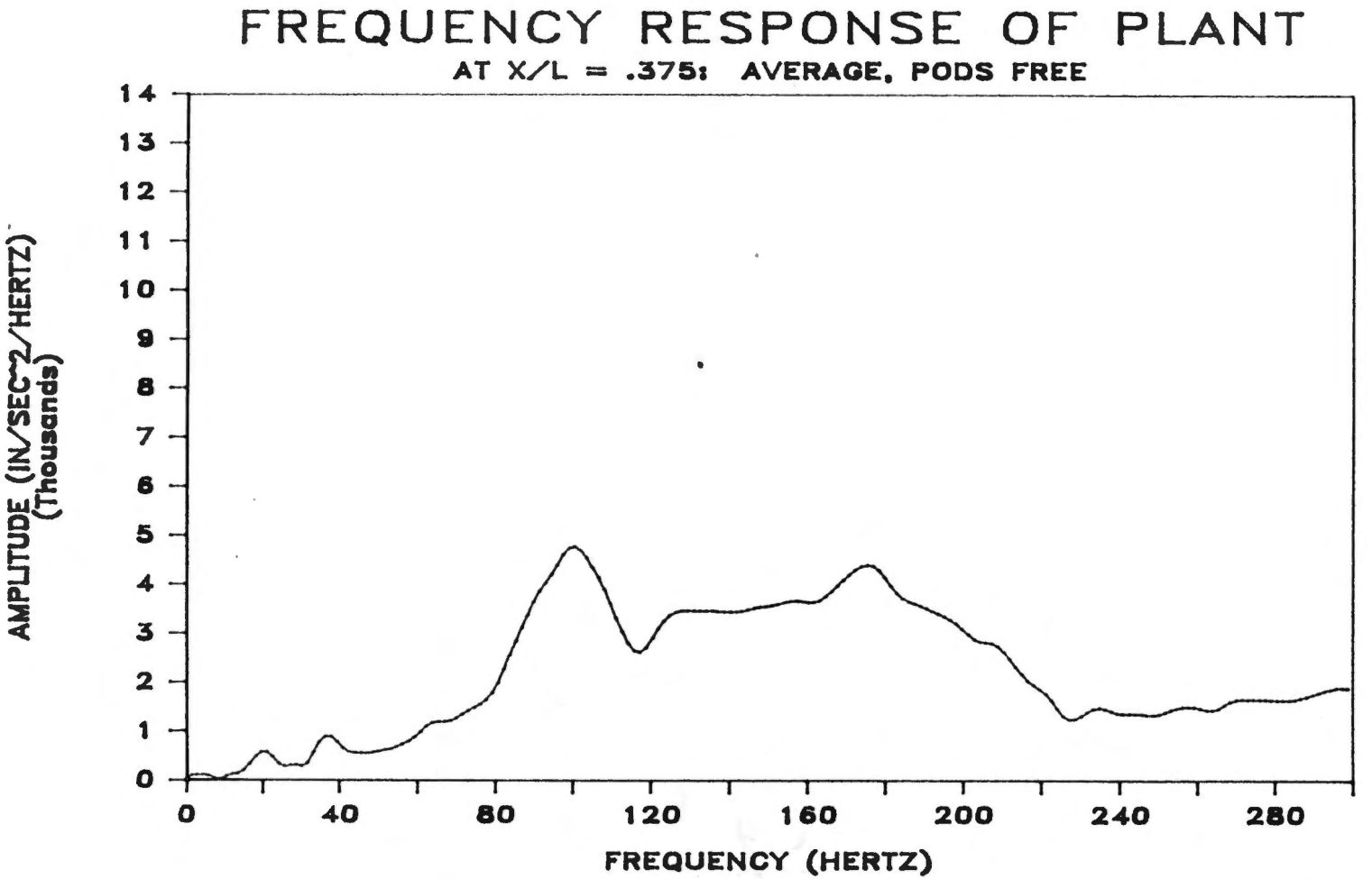

Figure 40. Amplitude spectrum of the measured impulse response of location x/L equal 0.375 on the stalk of a soybean plant with all pods attached and free to move.

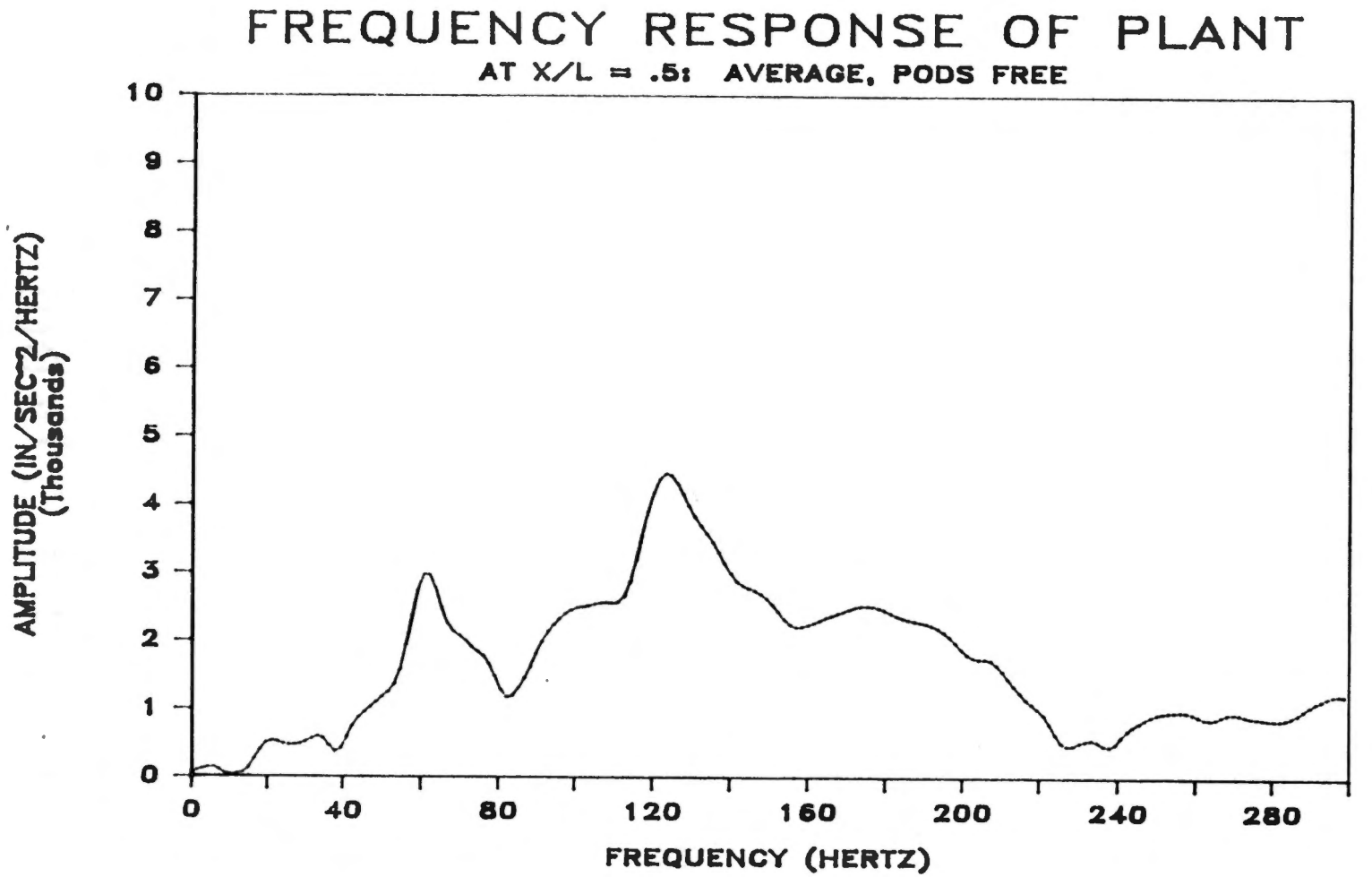

Figure 41. Amplitude spectrum of the measured impulse response of location x/L equal 0.50 on the stalk of a soybean plant with all pods attached and free to move.

the stalk. The most striking effect is the substantial reduction in stalk response caused by the presence of the pods.

Because collisions between pods and the stalk and between the pods themselves are nonlinear phenomena, the Fourier transform of the impulse responses of locations on a stalk with pods do not constitute transfer functions (recall the transfer function is a linear system concept) and therefore probably cannot be used to reliably predict the response of the plant to any excitation. This fact will become important in the succeeding chapter concerned with cutting.

Effect of the Reel on Plant Motion During Cutting

The good and bad effects of the reel on plant motion, including the effect on shatter loss, have been experimentally determined (Lamp et al., 1960). Generally, the reel is considered to aid in gathering the crop into the header as it is cut. However, the reel has been reported as a contributing cause of shatter losses under some operating conditions, as seen in Figures 42 and 43.

The role that the reel bat plays in determining plant motion during cutting and in causing or reducing shatter has never been clearly defined. Komenski (1984) suggested that, when properly adjusted, the reel had a "calming" effect on plant motion during cutting, thereby reducing shatter. This calming effect was also observed in high speed films made during this study but no accompanying shatter loss data were obtained.

In this study, it is suggested that during cutting, the reel acts as a motion-limiting device, the dynamic effects of which have been

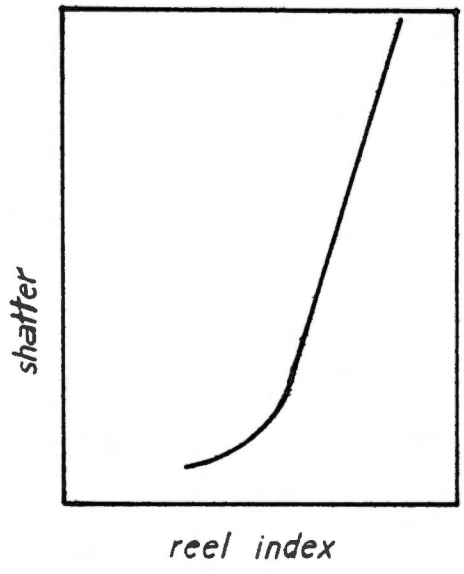

Figure 42. Effect of reel index (ratio of reel speed to harvester forward speed) on shattered loss (Lamp et al., 1960).

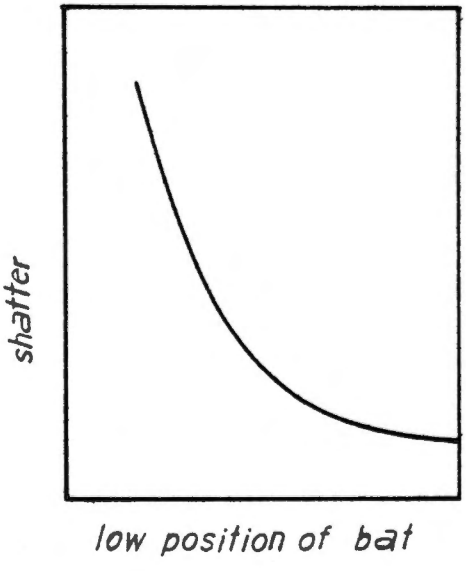

Figure 43. Relationship of reel height adjustment to shattered loss (Lamp et al., 1960).

investigated for other applications such as limiting the vibrations of pipes (Masri et al., 1981).

Considering the plant deflected by the reel near its tip, the stalk can be modeled as a clamped-pinned Euler beam. If, due to the application of an impulse at x/L equal b, the stalk begins to vibrate, then at some point in time the stalk and reel may separate. While the two are separated, the appropriate model of the stalk would be a clamped-free beam with the displacement and velocity at the time of separation as initial conditions. Later, the stalk and reel would again come into contact, an impact load probably occurring at the location of contact. This process might repeat several times before the stalk vibration damped out.

For this case of excitation due to an impulse, no energy is added to the system after the impulse is applied. However, the action of the collisions between the stalk and bat is to redistribute the energy among the modes of the stalk's vibration. This redistribution tends to favor the modes more equally than the distribution caused by the initial impulse because the stalk-bat collisions occur near the free end where the values of the modes (the O (x)'s in equation 5-3) are nearly equal. Collisions between the stalk and bat also disorganize the motions of the pods, enhancing energy dissipation by friction and pod collision.

During cutting, of course, the manner in which the stalk and reel bat interact is probably much more complex, but the same events still occur. Summarizing then, the calming effect of the reel on plant motion is suggested to be due to the motion-limiting role of the reel

bat, the more equal redistribution of energy among modes of stalk vibration, and the accompanying enhancement of energy dissipation.

Figure 44 depicts the impulse response of a location on the stalk of a plant with its end free. Figure 45 depicts the impulse response of the same location but with a stationary bat deflecting the end of the plant. The differences between the two time series are significant, particularly at 18 milliseconds, where collisions between the stalk and bat appear to have occurred (Figure 45).

Figure 46 shows the amplitude spectra of these impulse responses. In contrast to the response of the plant with its end free, the peak responses of the plant with the bat present have been substantially limited, and the amplitudes of all modes of the stalk are more nearly equal.

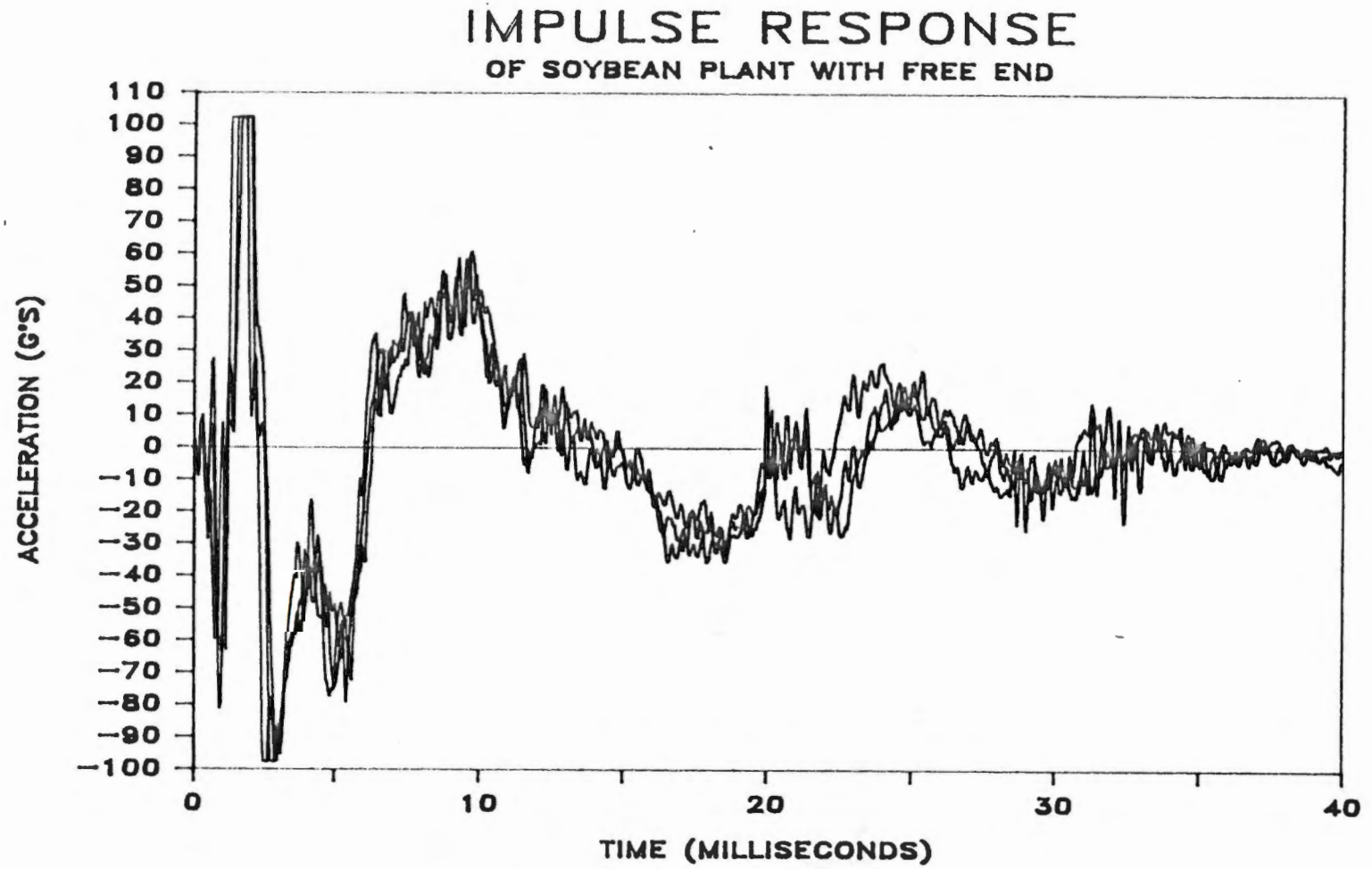

Figure 44. Measured impulse response of a location on the stalk of a soybean plant not deflected by a reel bat.

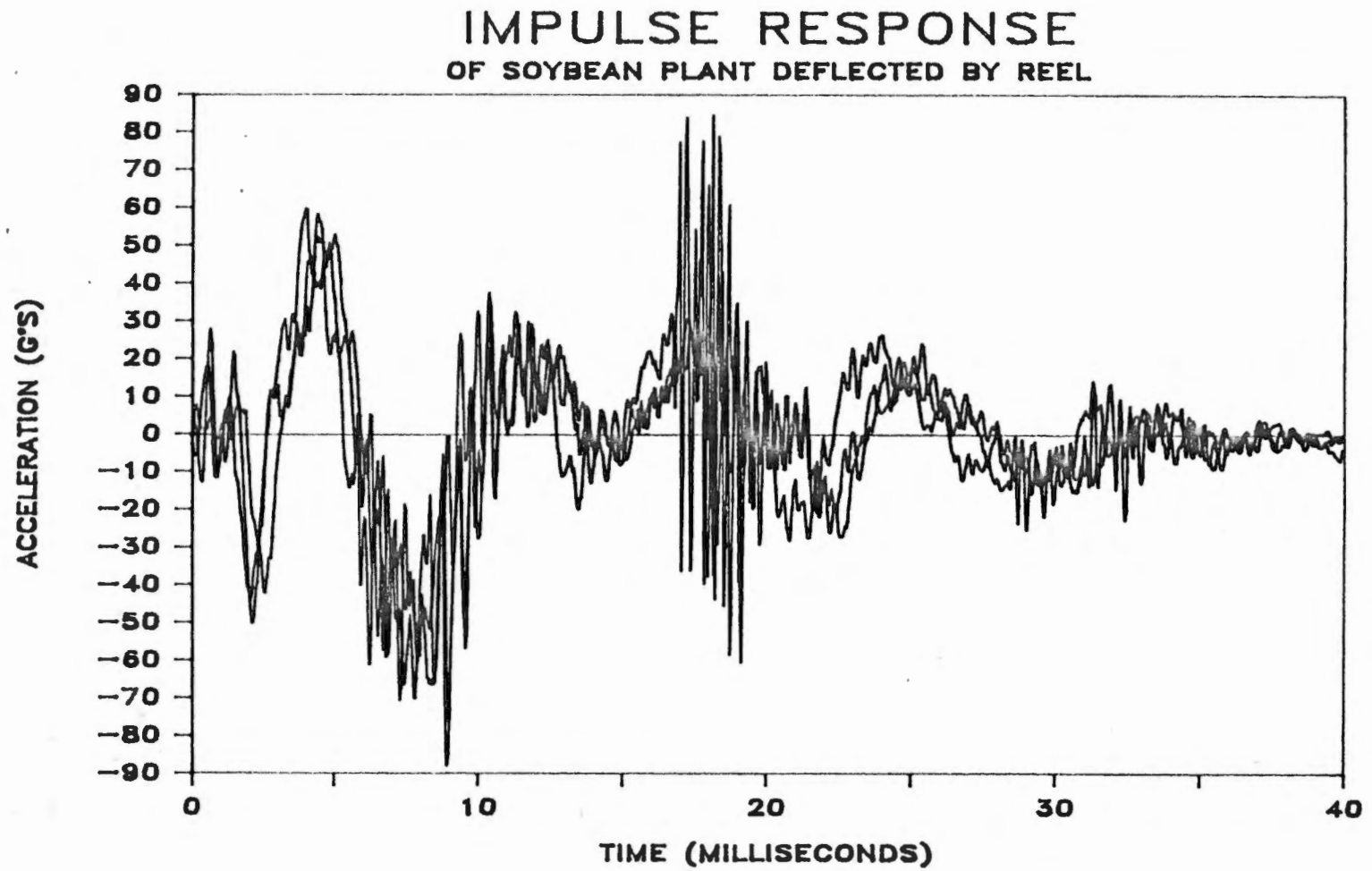

Figure 45. Measured impulse response of a location on the stalk of a soybean plant deflected by a reel bat.

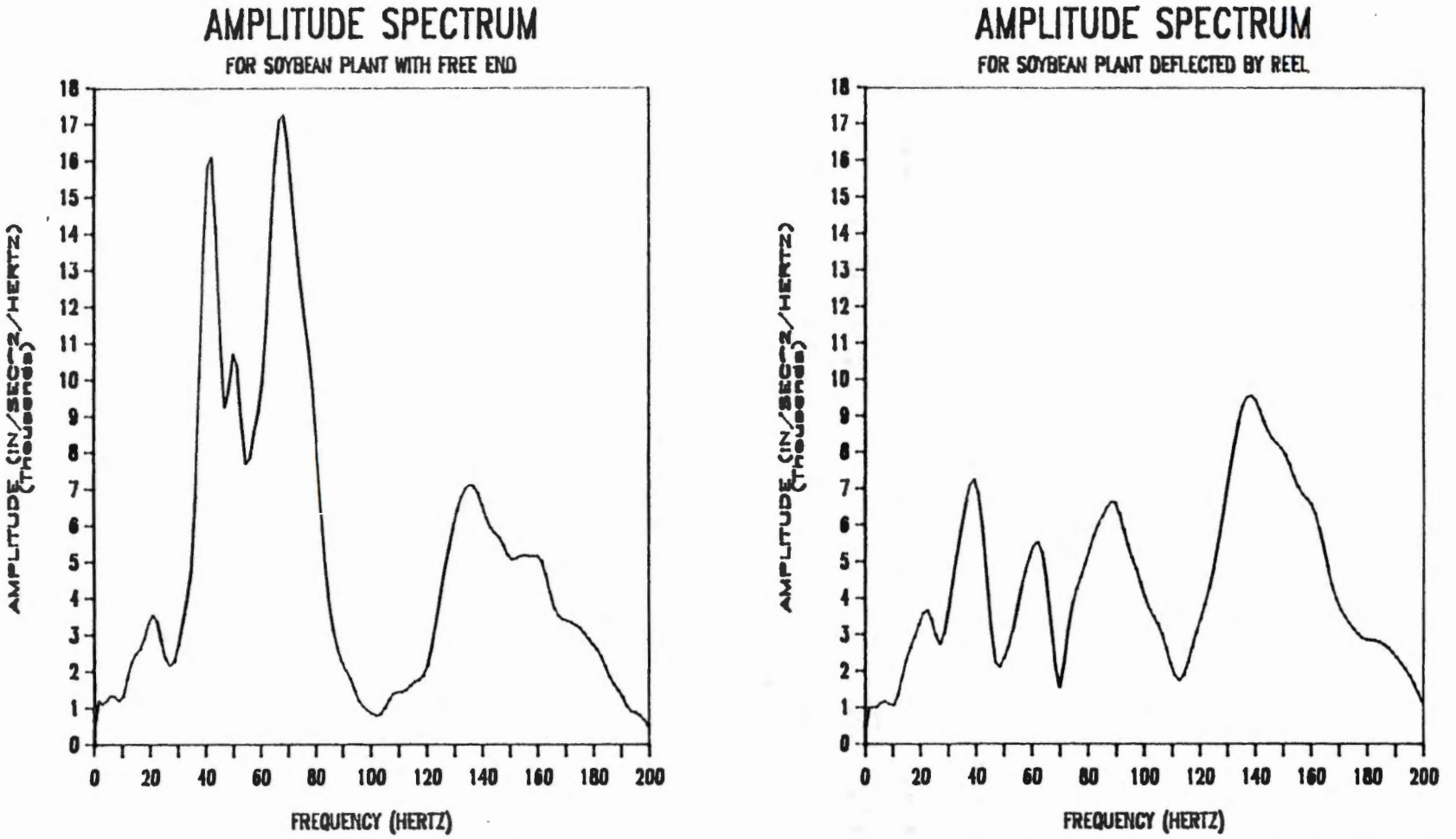

Figure 46. Amplitude spectra of impulse responses of a location on the stalk of a soybean plant for two cases: (1) not deflected by a reel bat, and (2) deflected by a reel bat.

CHAPTER VI

THE CUTTING FUNCTION

Cutting of the stalk is a complex process involving failure and separation of plant material. While the mechanisms by which failure occurs during cutting have been investigated, the approach taken in this study was to concentrate on the effects of cutting on the plant rather than on the cutting process itself. With regard to shatter losses, the important effect of cutting is the resulting motion that the rest of the plant undergoes because it is this motion that somehow results in the shattering of pods.

The cutting function that is computed and discussed in this study might therefore be considered to be a hypothetical forcing function which, when applied to the stalk, causes the same plant motion that cutting does.

The advantage of this approach is that it allows for a simple but meaningful representation of cutting that is both measurable and compatible with current vibration analysis techniques. The use of the cutting function for the design and evaluation of cutting devices and for optimizing operating parameters is especially promising. However, it is possible to imagine theoretical cutting functions that are not physically realistic because no corresponding method of cutting the stalk exists. Therefore, the intelligent use of the cutting function concept for design purposes must be guided by experimental knowledge. It is also worth noting that the concept of a cutting function need not be limited to soybean harvesting; it may be applicable to other crops as well.

Specifically concerning soybean harvesting, the ability to evaluate the shatter-causing tendencies of cutting devices depends on: (1) the ability to determine the cutting function, and (2) knowledge of what aspects of the cutting function cause motion of the plant that results in shatter. The previous chapter dealt with motion of the plant, but, as discussed there, the exact mechanism of shatter and the particular aspects of plant motion that promote shatter have still not been conclusively determined. This lack of knowledge presents the greatest impediment to the effective evaluation of cutting devices for harvesting soybeans. In this chapter, a cutting function is obtained for the multi-tooth circular blade and problems associated with cutting function determination are discussed.

Multi-Tooth Blade Cutting Function

Because of the high speeds used in cutting with multi-tooth circular blades, the cutting function might first be imagined to be a sequence of impulses, or "impulse train," one impulse occuring each time a tooth passes through the stalk. The Fourier transform of an impulse train is also a sequence of impulses, as shown in Figure 47.

However, upon further consideration, the finite amount of time that each tooth is in contact with the stalk is significant. Thus, rather than an impulse train, the cutting function might be imagined as a pulse train. An example of such a pulse train, consisting of seven pulses, is shown in Figure 48. Figure 49 depicts the amplitude spectrum of the Fourier transform of the pulse train, where the reduction in high frequency content due to finite pulse durations is

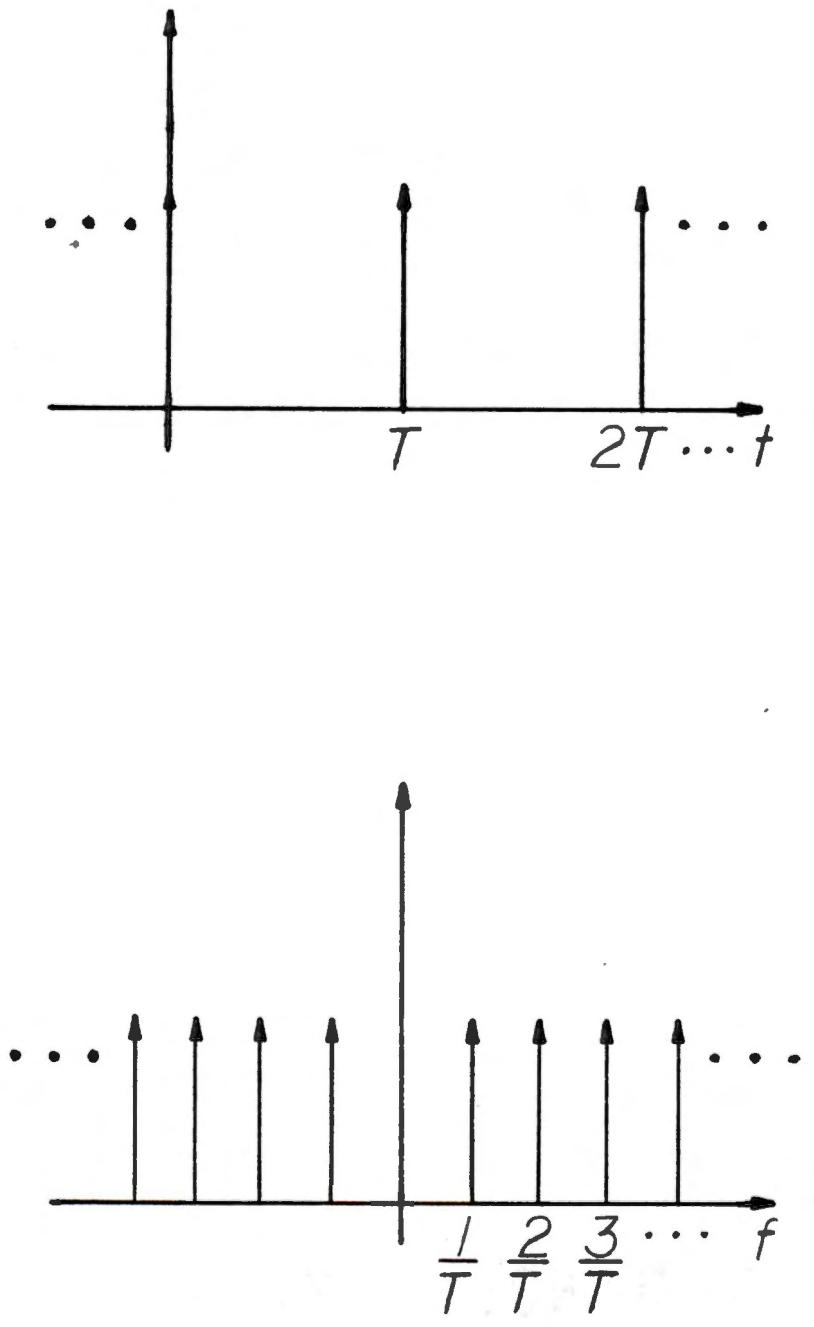

Figure 47. Graphical representation of an impulse train and its Fourier transform, which is also an impulse train (Brigham, 1974).

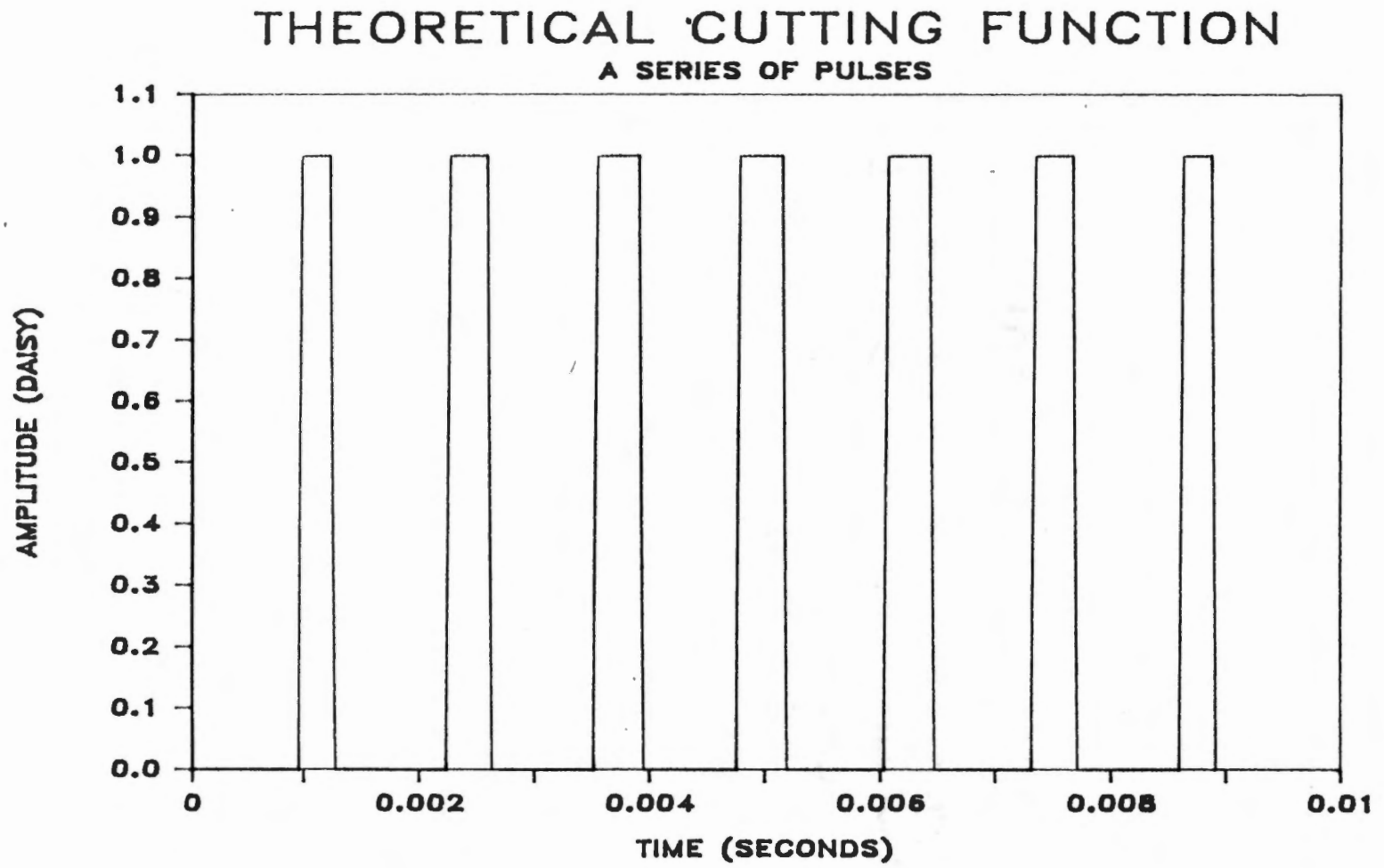

Figure 48. Theoretical cutting function: a pulse train consisting of seven pulses.

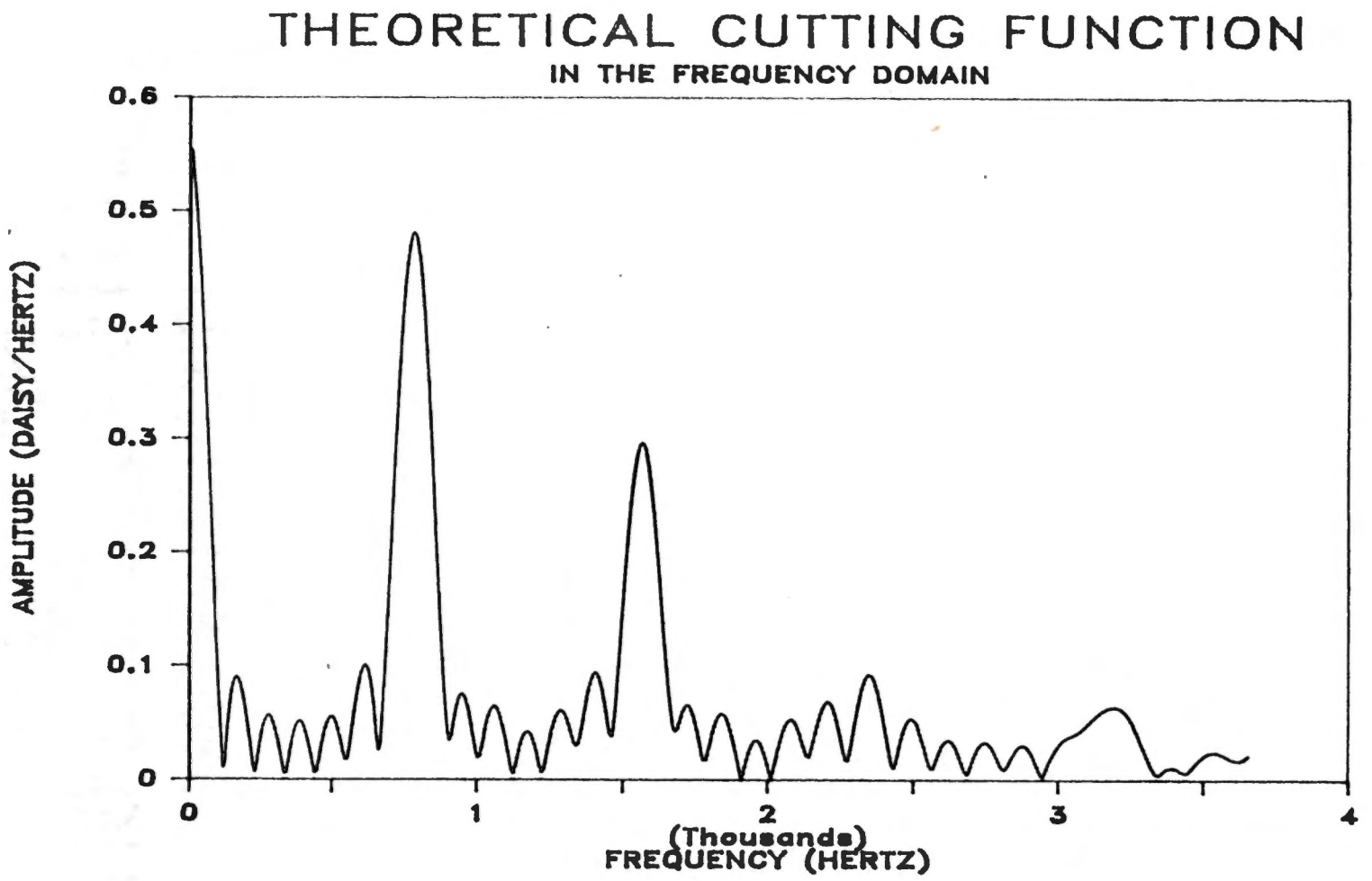

Figure 49. Amplitude spectrum of the pulse train.

evident. In reality, cutting is sufficiently complex that much hypothesizing without experience is pointless. The primary reason for discussing these imagined cutting functions is to gain familiarity with the pulse train and its Fourier transform.

The response of a bare stalk to cutting by a circular saw blade is shown in Figures 50 and 51 for two locations on the stalk. The blade speed at the time of cutting was approximately 30 revolutions per second which, for 26 teeth around the circumference of the blade, resulted in a cutting frequency of 780 hz. The excitation of the stalk at this frequency (approximately 0.0013 milliseconds per cut) is evident in both responses.

Two estimates of the Fourier transform of the cutting function, one for each location on the stalk, were computed using equation 4-9 and their amplitude spectra are shown in Figures 52 and 53. The amplitude spectrum of the average of these estimates is shown in Figure 54.

No recognizable signal is evident beyond approximately 3300 hz. In fact, the twin "spikes" that occur between 3000 and 3300 hz are undoubtedly due at least in part to the poor coherence of the impulse response data used to compute the cutting function (Figures 14-16, pages 42-44). Unfortunately, even the amplitude of the spike at 780 hz is subject to question because of poor coherence at this frequency. The lack of signal beyond 3300 hz may be explained by considering the duration of the pulses caused by the blade teeth as they passed through the stalk. The duration of each pulse varied as cutting progressed (because of the circular shape of the stalk cross-section), but 0.2 to

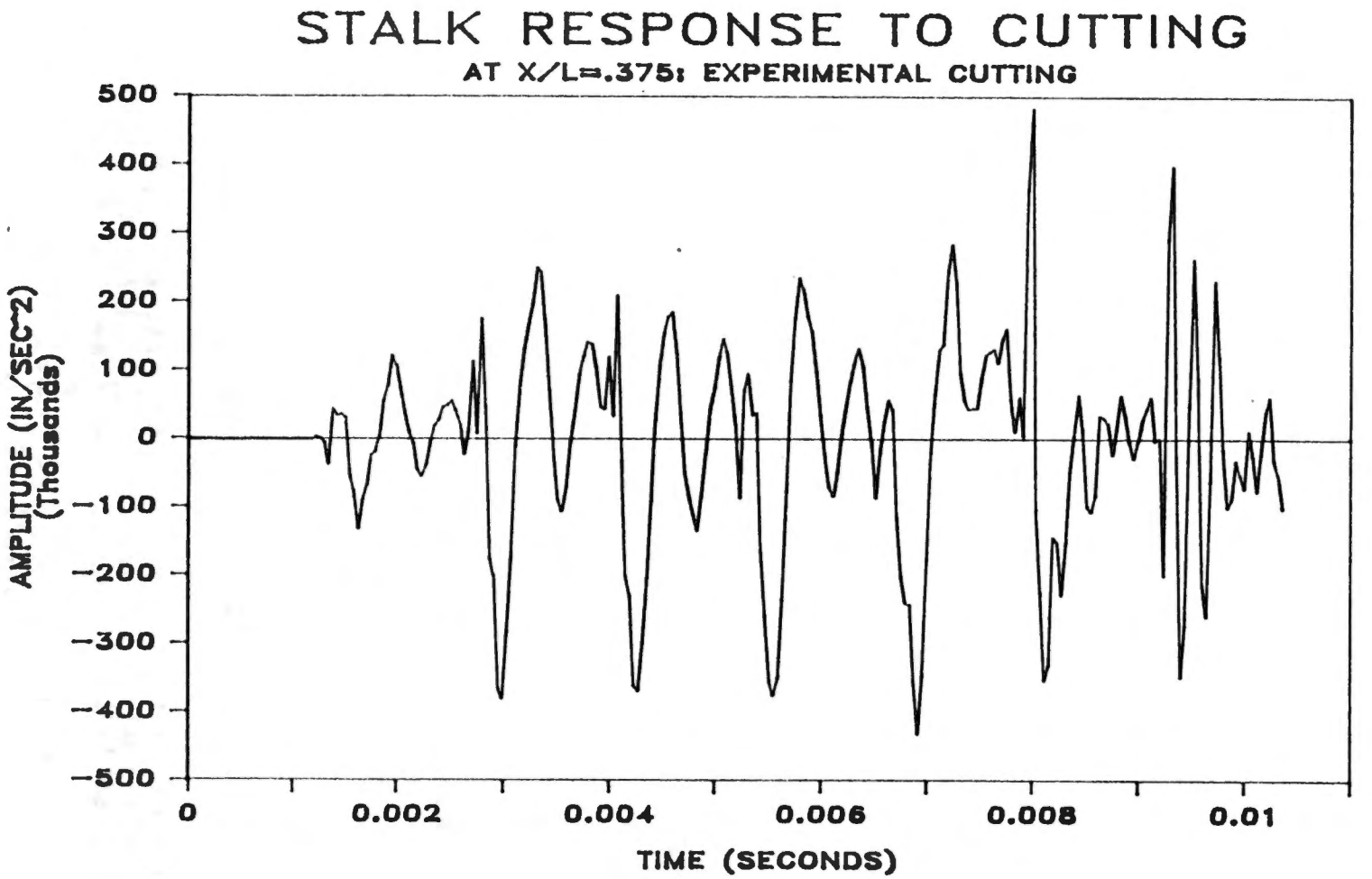

Figure 50. Measured response to cutting of location x/L equal 0.375 on the bare stalk of a soybean plant.

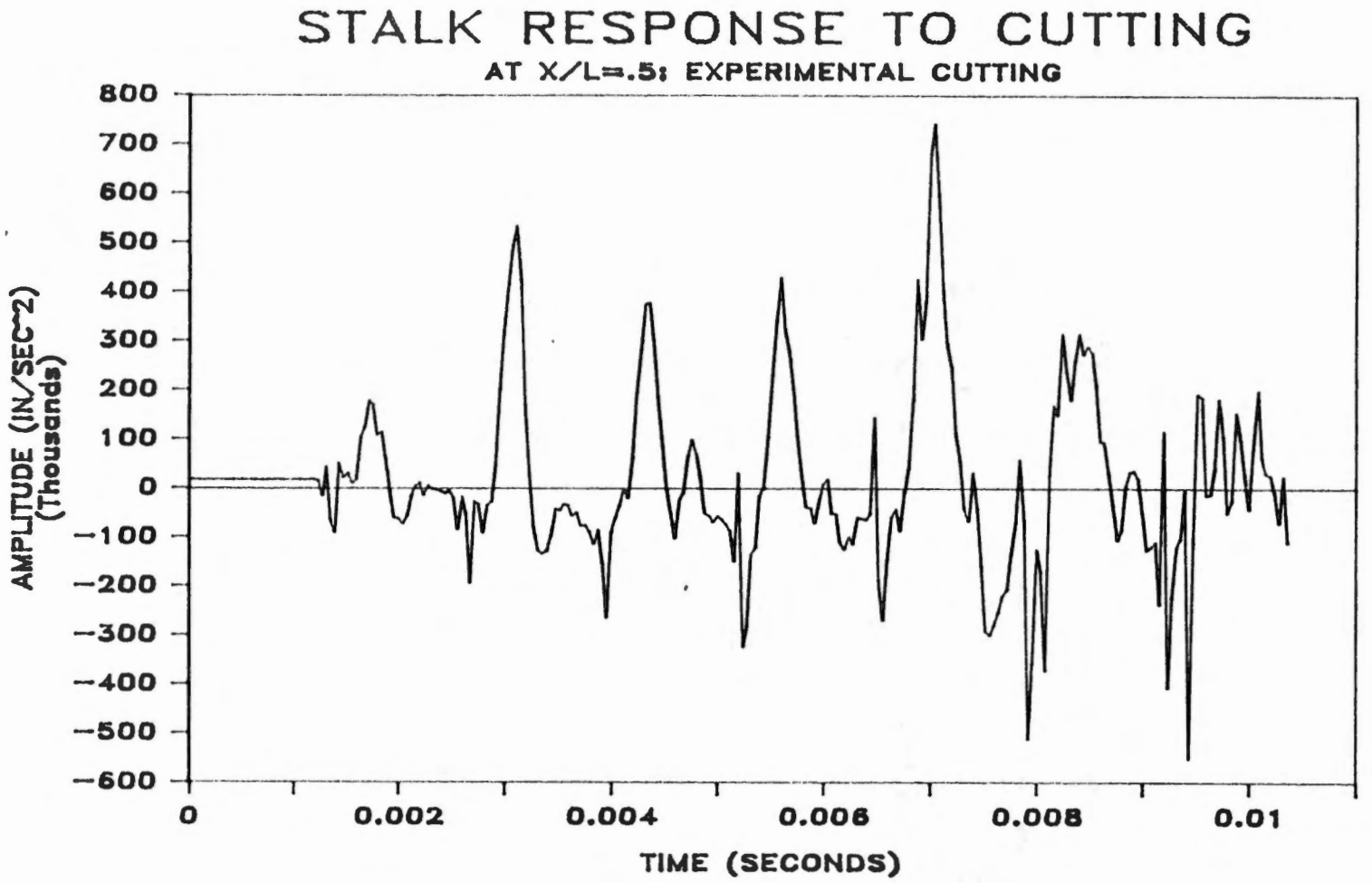

Figure 51. Measured response to cutting of location x/L equal 0.50 on the bare stalk of a soybean plant.

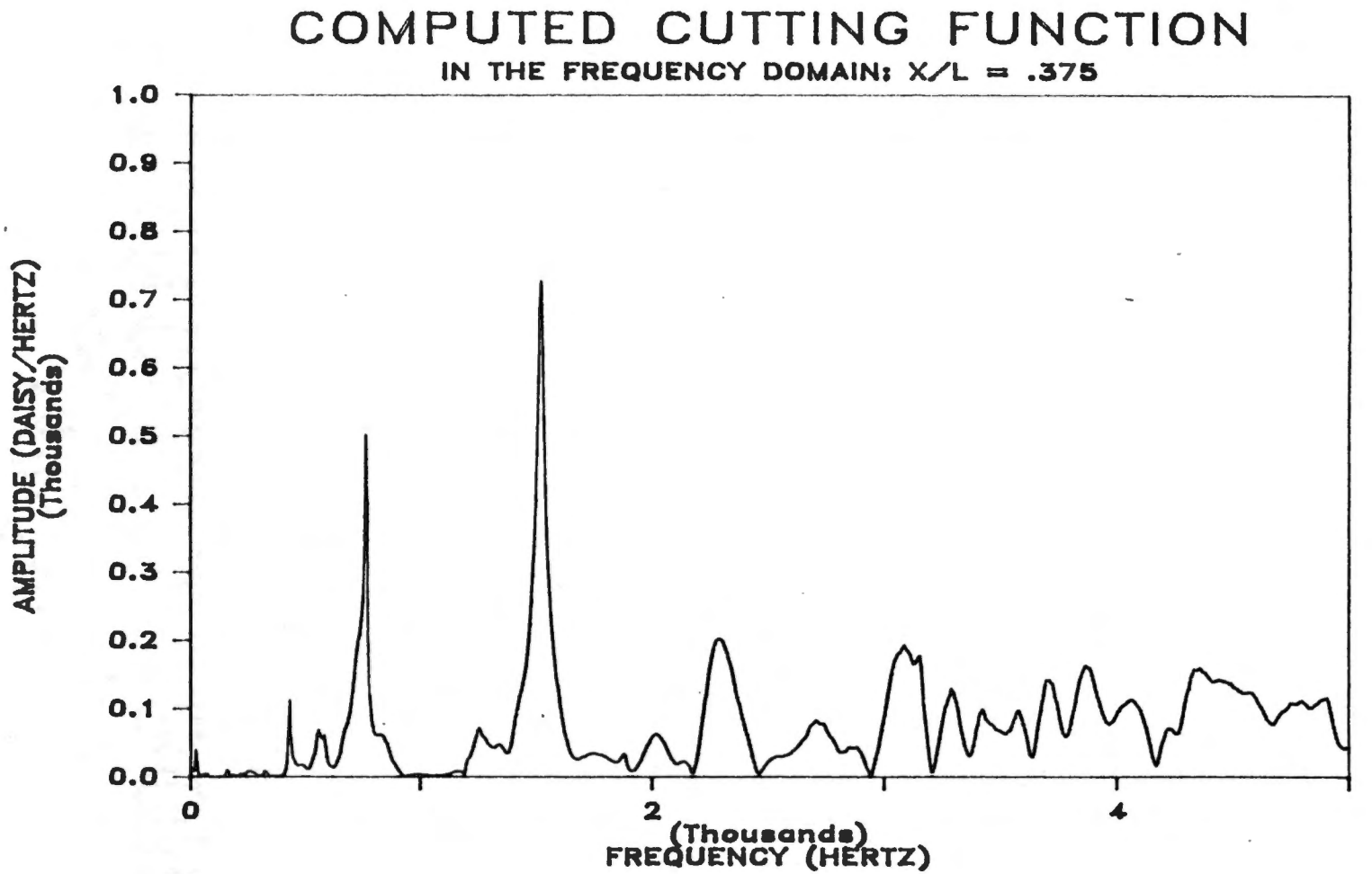

Figure 52. Amplitude spectrum of a cutting function computed using the measured impulse response and cutting response of location x/L equal 0.375 on the bare stalk of a soybean plant.

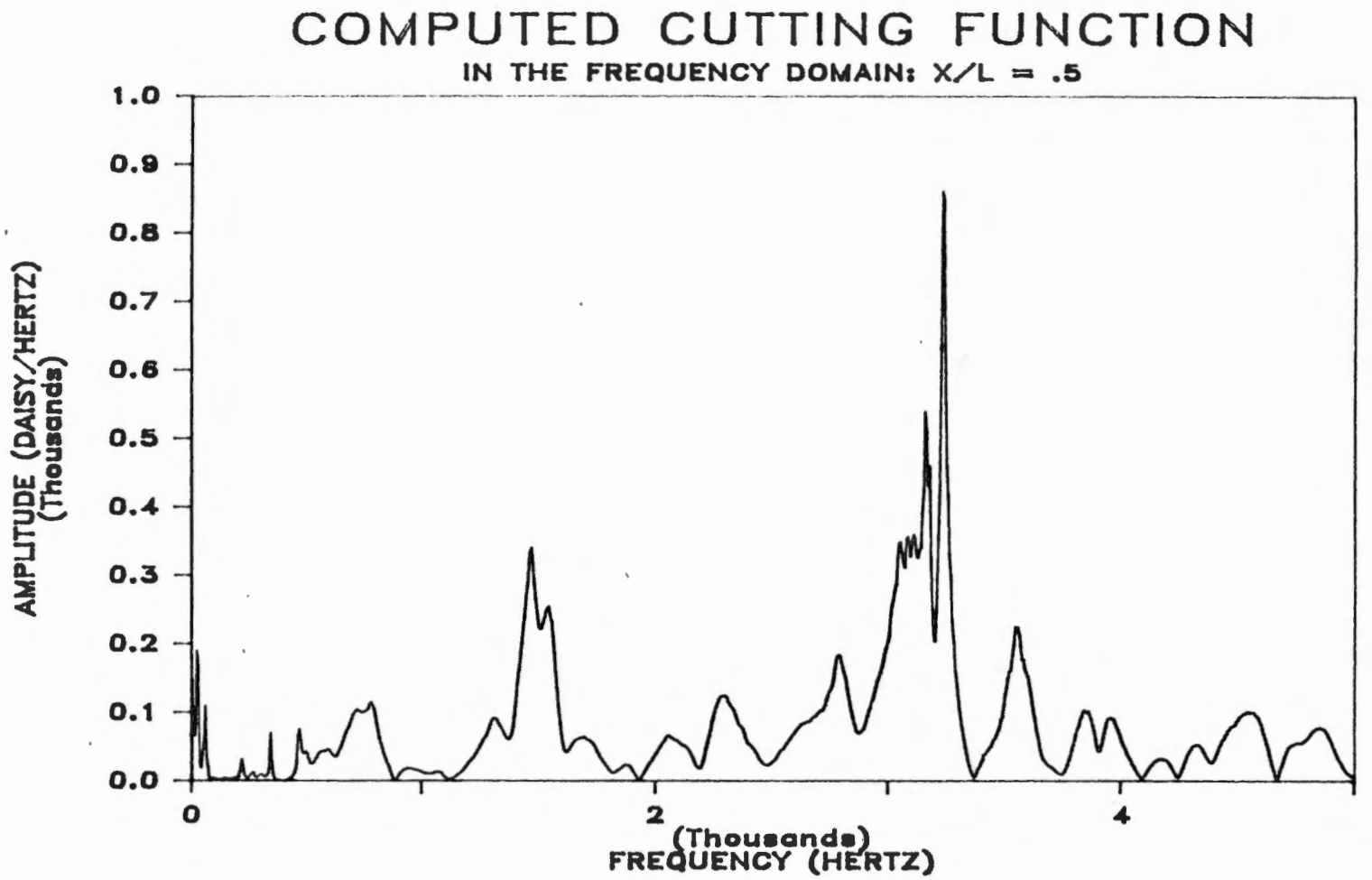

Figure 53. Amplitude spectrum of a cutting function computed using the measured impulse response and cutting response of location x/L equal 0.50 on the bare stalk of a soybean plant.

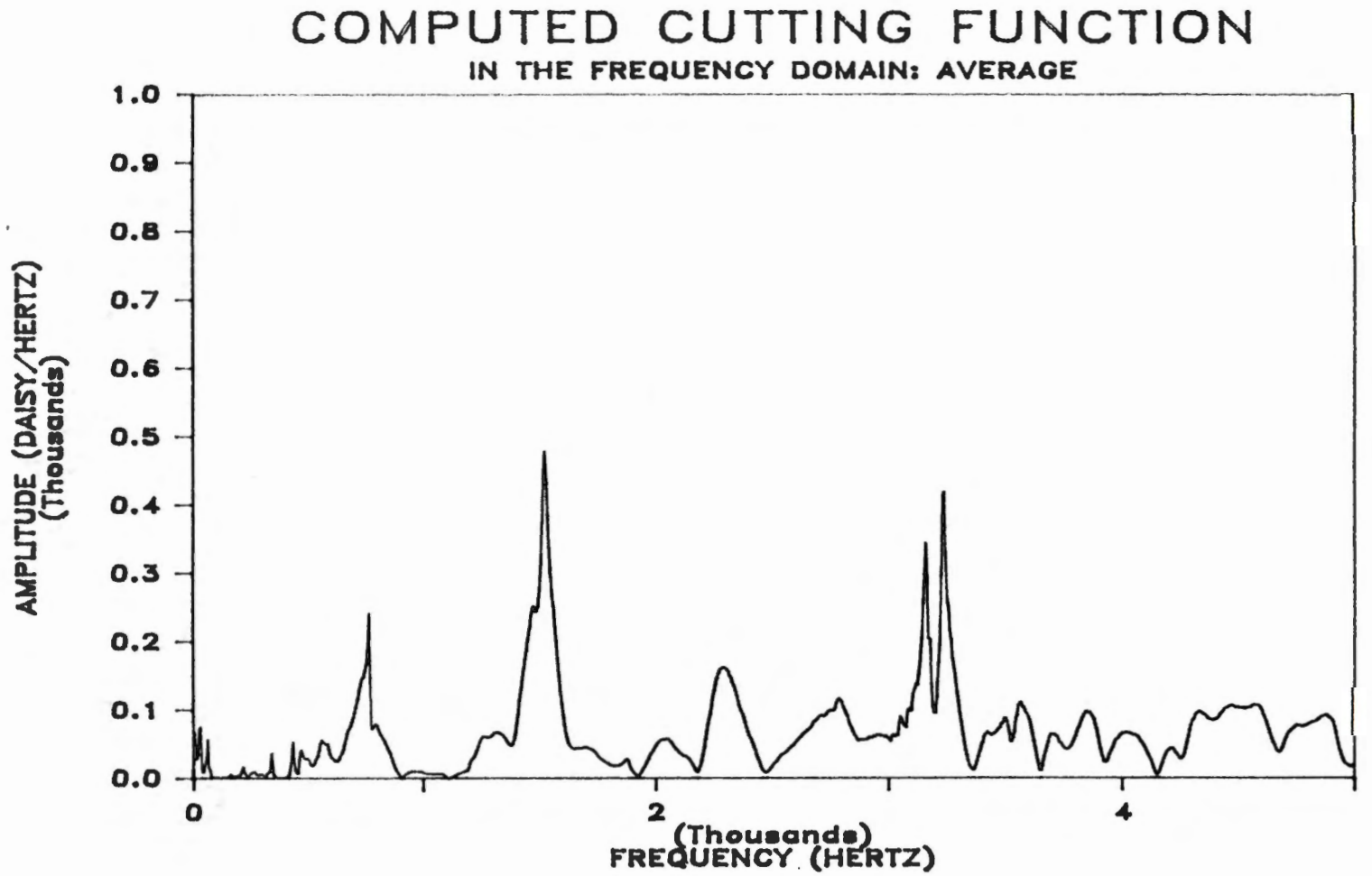

Figure 54. Amplitude spectrum of a cutting function computed by averaging the Fourier transforms of two estimates of the cutting function.

0.4 milliseconds was probably typical. The cutoff frequency for such pulses is approximately 3300 hz.

The periodic nature of the computed cutting function is obscured somewhat by the poor resolution of the spectrum (6.1 hz) depicted in Figure 54. The same amplitude spectrum obtained with a 1.5 hz resolution transform is shown in Figure 55, where a spike at 37 hz is now visible. While a considerable degree of noise is present, the amplitude spectrum of the computed cutting function does begin to resemble the amplitude spectrum of the theoretical pulse train shown in Figure 49. Some of the differences may be due to error introduced by wallowing of the plant in the soil during cutting. Despite several attempts, this could never be completely prevented.

Problem Associated with Cutting Function Determination

While experimental results for a bare stalk are encouraging, the unprofitability of harvesting bare stalks is motivation to experiment with whole plants. An additional reason for using whole plants is that for cutting devices, such as the cutter bar, which significantly deflect the plant before cutting occurs the inertia of the plant helps determine the forces applied to the stalk by the device. Thus, removing pods alters the mass of the plant and changes the applied forces. However, leaving the pods on the stalk free to move results in collisions during plant motion, a nonlinearity that degrades the reliability of the data for cutting function computation purposes.

An attempt was made to compromise between these two considerations by leaving the pods on the stalk but constraining their motion with a

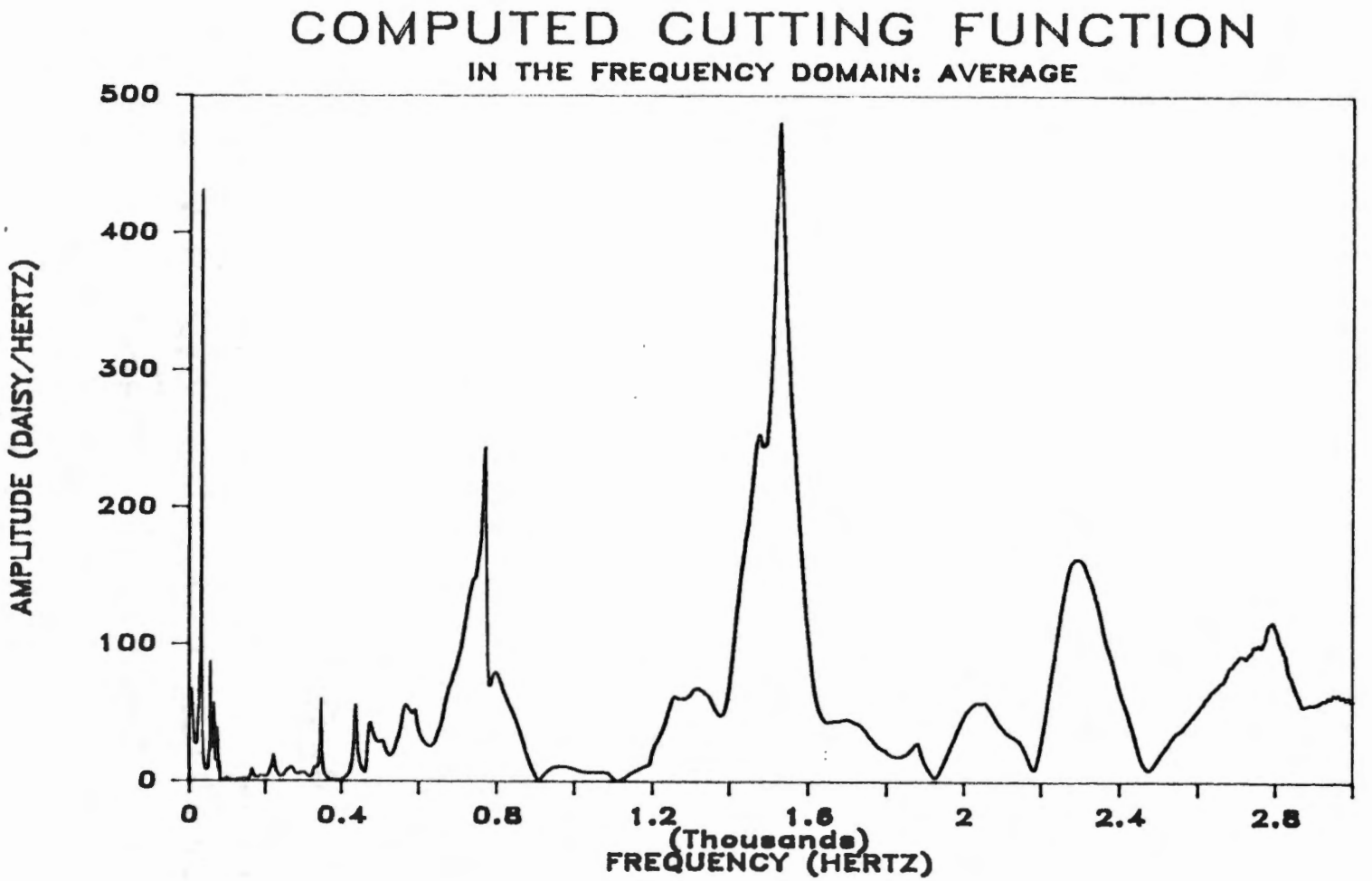

Figure 55. Amplitude spectrum of a cutting function computed by averaging the high resolution Fourier transforms of two estimates of the cutting function.

light adhesive tape. The coherence of the impulse response data for this case was shown earlier in Figure 17 (page 46).

The amplitude spectrum of the average cutting function for this case is shown in Figure 56. The blade speed for this test was the same as for the previous (bare stalk) test. Comparison of Figure 56 with Figure 54 is somewhat disappointing because there does not appear to be a clearly recognizable cutting function depicted in Figure 56. A possible explanation for these poor results is that the tape constrained the pods sufficiently during excitation by an impulse but did not adequately constrain them during the greater excitation of cutting. If this was the case, then the cutting response data was unreliable and, when used to compute a cutting function, yielded unreliable results.

It is, perhaps, ironic that this study ends almost where it began--with an inability to control the motion of the pods during cutting. Pod movement hindered the determination of a cutting function and it is pod movement that results in shatter losses. It does not seem unjustified, therefore, to hope that future study of the first problem will ultimately lead to the solution of the second.

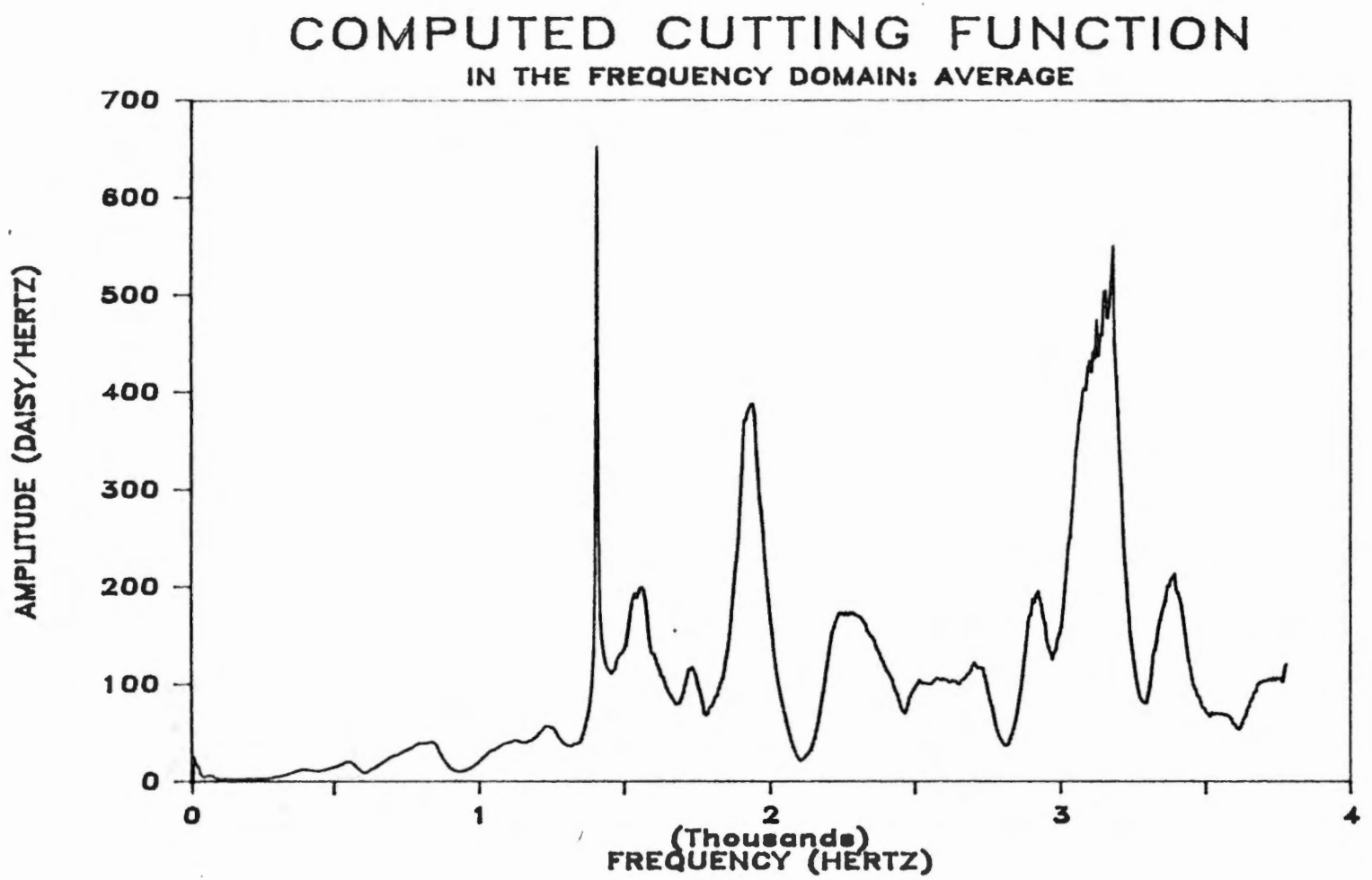

Figure 56. Amplitude spectrum of a cutting function computed using the measured impulse responses and cutting responses of two locations on the stalk of a soybean plant with restrained pods.

CHAPTER VII

SUMMARY AND CONCLUSIONS

Summary

Shatter losses of soybeans are still a substantial percentage of potential profits despite extensive research of the problem. Previous efforts have tended to be concerned with the design and operating aspects of harvesting machinery rather than the dynamic characteristics of the plant. In fact, the exact mechanism of pod shattering is still uncertain.

This research was a study of the dynamic behavior of soybean plants. Specifically, the objectives were: (1) determine appropriate mathematical models for the dynamic behavior of the soybean plant during cutting, (2) determine appropriate mathematical models for the forces applied to the soybean plant by the cutting device that cause motion of the plant, and (3) determine appropriate methods for obtaining the experimental data necessary to develop and verify these mathematical models.

Mathematical models were developed for the components of the soybean plant: the stalk and pod. The Euler-Bernoulli beam appeared to be a satisfactory model for the stalk, predicting modes of vibration with corresponding natural frequencies. The simple pendulum with a torsional spring was adequate for modeling some aspects of pod motion, although the actual pod possessed more than the single degree of freedom of this model. The coupled stalk-single pod model showed the

effect of the pod on the stalk to be due to: the added mass of the pod, the motion of the pod, and collisions between the pod and stalk. The model also predicted that the pod and stalk tend to move out of phase for vibration at most frequencies, and that the response of the pod to stalk vibration is frequency dependent, the most significant pod response occurring at lower frequencies.

These results raised questions about the experimental methods of other researchers working on shatter loss reduction. The theory that collisions between the pods and stalk might be a mechanism of shatter was also suggested.

The notion of a cutting function was introduced to represent the aspects of cutting that cause motion of the plant. For the type of cutting device used in this study, a multi-tooth circular saw blade, a sequence of pulses appeared to be an adequate mathematical model cutting function.

Experimental determination of cutting functions for bare stalks appears very possible although problems with the soil around the base of the stalk being too pliable (to represent field conditions) were encountered in this study. For stalks with pods attached, however, the nonlinearities caused by collisions and friction prevented the determination of a cutting function.

Data collection was accomplished with accelerometers mounted on the stalk of the plant and an analog-to-digital data acquisition system. The physical presence of the accelerometers and cables affected the response of the plant. For this reason, and because the instrumentation would very likely be damaged by severe plant motion,

another method of sensing plant response (an optical method, for example) would be more appropriate.

Digital signal analysis using Fast Fourier Transform methods proved to be an effective method of data analysis. With the proper instrumentation, the application of this technology to the study of crop dynamics appears as promising as it has been for other areas of vibration research.

Conclusions

1. The Euler beam equation is an adequate mathematical model of the stalk of the soybean plant.
2. The simple pendulum model is capable of predicting some aspects of pod motion, but in its linear one-degree-of-freedom form would be inadequate for accurately predicting pod dynamics during cutting.
3. The use of a cutting function to represent the effect of cutting on plant motion shows promise as a method of evaluating and designing cutting devices.
4. Further research is needed in the area of obtaining cutting functions for plants with the pods attached to the stalk.
5. The lack of detailed knowledge about the mechanics of pod shattering is hindering the solution of the problem of shatter losses.
6. The intelligent use of digital signal analysis and Fast Fourier Transform methods for investigating the dynamics of crops is a promising application of this technology.

LIST OF REFERENCES

LIST OF REFERENCES

Barnhart, Jr., K. E. and W. Goldsmith. 1957. Stresses in beams during transverse impact. Journal of Applied Mechanics 24:440-446.

Beauchamp, K. and C. Yuen. 1979. Digital methods for signal analysis. George Allen & Unwin, Boston, 316 p.

Bledsoe, B. L. 1969. The design and experimental analysis of a rotary sickle for cutting and trajecting plant stems. Unpublished Doctoral Dissertation, Oklahoma State University, Stillwater.

Boddiford, Jr., J. K. and C. B. Richey. 1974. Development of a puller-header for combining soybeans. Transactions of the ASAE 18(6):1003-1005, 1010.

Boley, B. A. 1955. An approximate theory of lateral impact on beams. Journal of Applied Mechanics 22:69-76.

Brigham, O. E. 1974. The fast fourier transform. Prentice-Hall, Inc., Englewood Cliffs, New Jersey, 252 p.

Caughey, T. K. 1960. Classical normal modes in damped linear dynamic systems. Journal of Applied Mechanics 27:269-271.

Caughey, T. K. and M. E. J. O'Kelly. 1965. Classical normal modes in damped linear dynamic systems. Journal of Applied Mechanics 32:583-588.

Chen, J. C. and B. K. Wada. 1975. Criteria for analysis-test correlation of structural dynamic systems. Journal of Applied Mechanics 42:471-477.

Chen, Y. 1963. On the vibration of beams or rods carrying a concentrated mass. Journal of Applied Mechanics 30:310-311.

Chun, K. R. 1972. Free vibration of a beam wiht one end spring-hinged and the other free. Journal of Applied Mechanics 39:1154-1155.

Collins, J. D. and W. T. Thomson. 1969. The eigenvalue problem for structural systems with statistical properties. AIAA Journal 7(4):642-648.

Colton, J. D. and G. Herrmann. 1975. Dynamic fracture process in beams. Journal of Applied Mechanics 42:435-439.

Conway, H. D.,E. C. H. Becker and J. F. Dubil. 1964. Vibration frequencies of tapered bars and circular plates. Journal of Applied Mechanics 31:329-331.

Conway, H. D. and J. F. Dubil. 1965. Vibration frequencies of truncated-cone and wedge beams. Journal of Applied Mechanics 32:932-934.

Cooke, J. R. and R. H. Rand. 1969. Vibratory fruit harvesting: a linear theory of fruit-stem dynamics. Journal of Agricultural Engineering Research 14(3):195-209.

Doebelin, E. O. 1980. System modeling and response theoretical and experimental approaches. John Wiley & Sons, New York, 587 p.

Dowell, E. H. 1971. Free vibrations of a linear structure with arbitrary support conditions. Journal of Applied Mechanics 38:595-600.

Dowell, E. H. 1972. Free vibrations of an arbitrary structure in terms of component modes. Journal of Applied Mechanics 39:727-732.

Dowell, E. H. 1979. On some general properties of combined dynamical systems. Journal of Applied Mechanics 46:206-209.

Dunn, W. E., W. R. Nave and B. J. Butler. 1973. Combine header component losses in soybeans. Transactions of the ASAE 16(6):1032-1035.

Fridley, R. B. and C. Yung. 1975. Computer analysis of fruit detachment during tree shaking. Transactions of the ASAE 18(3):409-415.

Gabel, R. A. and R. A. Roberts. 1980. Signals and linear systems. John Wiley & Sons, Inc. New York, 492 p.

Garland, C. F. 1940. The normal modes of vibrations of beams having noncollinear elastic and mass axes. Journal of Applied Mechanics 7:A-97--A-105.

Gillespie, B. A., T. Liang and A. L. Myers. 1975. Multiple spectral analysis for tree shaker parameter optimization. Transactions of the ASAE 18(2):227-230.

Grubin, C. 1956. On the theory of the acceleration damper. Journal of Applied Mechanics 23:373-378.

Hall, K. C., R. Smook and J. W. Hummel. 1983. Impact cutting of soybean Plants with a rotary disk mower. ASAE Paper No. 83-1588, ASAE, St. Joseph, Michigan.

Hallquist, J. and V. W. Snyder. 1973. Linear damped vibratory structures with arbitrary support conditions. Journal of Applied Mechanics 40:312-313.

Hatwal, H., A. K. Mallik and A. Ghosh. 1983. Forced nonlinear oscillations of an autoparametric system--part 1:periodic responses. Journal of Applied Mechanics 50:657-662.

Hatwal, H., A. K. Mallik and A. Ghosh. 1983. Forced nonlinear oscillations of an autoparametric system--part 2:chaotic responses. Journal of Applied Mechanics 50:663-668.

Haxton, R. S. and A. D. S. Barr. 1972. The autoparametric vibration absorber. Journal of Applied Mechanics 39:119-125.

Hibbeler, R. C. 1975. Free vibration of a beam supported by unsymmetrical spring-hinges. Journal of Applied Mechanics 42:501-502.

Hoag, D. L. 1972. Properties related to soybean shatter. Transactions of the ASAE 15(3):494-497.

Hoag, D. L. 1975. Determination of the susceptibility of soybeans to shatter. Transactions of the ASAE 18(6):1174-1179.

Hoppmann, II, W. H. 1951. Beam vibrations with time-dependent boundary conditions. Journal of Applied Mechanics 18:224-226.

Huang, T. C. 1961. The effect of rotatory inertia and of shear deformation on the frequency and normal mode equations of uniform beams with simple end conditions. Journal of Applied Mechanics 28:579-584.

Hummel, J. W. and W. R. Nave. 1979. Impact cutting of soybean plants. Transactions of the ASAE 22(1):35-39.

Hummel, J. W. 1983. Impact cutting of soybeans using flexible cutting systems. Transactions of the ASAE 26(5):1315-1319.

Hunt, K. H. and F. R. E. Crossley. 1975. Coefficient of restitution interpreted as damping in vibroimpact. Journal of Applied Mechanics 42:440-445.

Hussain, A. A. M., G. E. Rehkugler and W. W. Gunkel. 1975. Tree limb response to a periodic discontinuous sinusiodal displacement. Transactions of the ASAE 18(4):614-617.

Hycam intruction manual, 400 ft. model. Red Lake Laboratories, Inc., Santa Clara, California.

Hyzer, W. G. April 2, 1959. Measuring motion with high speed movies. Machine Design 27:150-158.

Idell, J. H., R. G. Holmes and E. G. Humphries. 1975. Strawberry resonance frequencies and drag coefficients in relation to an air suspension-stem vibration harvesting system. Transactions of the ASAE 18(3):427-430.

Instruction manual charge amplifiers models 2721A and 2721AM1. 1979. Endevco, Rancho Viejo Road, San Juan Capistrano, California 92675.

Instruction manual for endevco piezoelectric accelerometers. 1979. Endevco, Rancho Viejo Road, San Juan Capistrano, California 92675.

Instruction manual model 4221 power supply. 1978. Endevco, Rancho Viejo Road, San Juan Capistrano, California 92675.

Iwan, W. D. 1968. Steady-state dynamic response of a limited slip system. Journal of Applied Mechanics 35:322-326.

Klein, L. R. and E. H. Dowell. 1974. Analysis of modal damping by component modes method using Lagrange multipliers. Journal of Applied Mechanics 41:527-528.

Komenski, T. 1984. Personal communication. Allis Chalmers Corporation.

Lamp, B. J., W. H. Johnson and K. A. Harkness. 1961. Soybean harvesting losses--approaches to reduction. Transactions of the ASAE 4(2):203-205,207.

Lee, T. W. 1973. Vibration frequencies for a uniform beam with one end spring-hinged and carrying a mass at the other free end. Journal of Applied Mechanics 40:813-815.

Lieber, P. and D. P. Jensen. 1945. An acceleration damper: development, design, and some applications. Journal of Applied Mechanics 12:523-530.

Lynn, P. A. 1973. An introduction to the analysis and processing of signals. John Wiley & Sons, New York, 222 p.

Maddox, N. R. 1975. On the number of modes necessary for accurate response and resulting forces in dynamic analyses. Journal of Applied Mechanics 42: 516-517.

Masri, S. F. 1973. Steady-state response of a multidegree system with an impact damper. Journal of Applied Mechanics 40:127-132.

Masri, S. F. and T. K. Caughey. 1966. On the stability of the impact damper. Journal of Applied Mechanics 33:586-592.

Masri, S. F.,Y. A. Marlamy and J. C. Anderson. 1981. Dynamic response of a beam with a geometric nonlinearity. Journal of Applied Mechanics 48:404-410.

McRandal, D. M. and P. B. McNulty. 1978. Impact cutting behavior of forage crops. Journal of Agricultural Engineering Research 23(3): 313-338.

Mindlin, R. D. and L. E. Goodman. 1950. Beam vibrations with time-dependent boundary conditions. Journal of Applied Mechanics 17:377-380.

Nave, W. R. and D. L. Hoag. 1975. Relationship of sickle and guard spacing and sickle frequency to soybean shatter loss. Transactions of the ASAE 18(4):630-632,637.

Nave, W. R., D. L. Hoag and J. W. Hummel. 1979. Sickle and guard design for soybean harvesting. Transactions of the ASAE :30-34.

Nothmann, G. A. 1948. Vibration of a cantilever beam with prescribed end motion. Journal of Applied Mechanics 15:327-334.

Pan, H. H. 1965. Transverse vibration of an Euler beam carrying a system of heavy bodies. Journal of Applied Mechanics 32:434-437.

Paslay, P. R. and M. E. Gurtin. 1960. The vibration response of a linear undamped system resting on a nonlinear spring. Journal of Applied Mechanics 27:272-274.

Quick, G. R. 1974. A quantitative shatter index for soybeans. Experimental Agriculture 10:403-408.

Quick, G. R. and W. F. Buchelle. 1974. Reducing combine gathering losses in soybeans. Transactions of the ASAE 17(6):1123-1129.

Quick, G. R. and W. M. Mills. 1978. High capacity narrow-pitch soybean cutter. Transactions of the ASAE 21(2):277-280.

Rand, R. H. and J. R. Cooke. 1970. Vibratory fruit harvesting: a non-linear theory of fruit-stem dynamics. Journal of Agricultural Engineering Research 15(4):347-363.

Reed III, W. H. and R. L. Duncan. 1967. Dampers to suppress wind-induced oscillations of tall flexible structures. Developments in Mechanics 4:881-897.

Robinson, E. A. 1967. Multichannel time series analysis with digital computer programs. Holden-Day, San Francisco, 298 p.

Sevin, E. 1961. On the parametric excitation of pendulum-type vibration absorber. Journal of Applied Mechanics 28:330-334.

Struble, R. A. and J. H. Heinbockel. 1962. Energy transfer in a beam-pendulum system. Journal of Applied Mechanics 29:590-592.

Struble, R. A. and J. H. Heinbockel. 1963. Resonant oscillations of a beam-pendulum system. Journal of Applied Mechanics 30:181-188.

Tatara, Y. 1977. Effects of external force on contacting times and coefficients of restitution in a periodic collision. Journal of Applied Mechanics 44:773-774.

Thomson, W. T. 1954. Impulsive response of beams in the elastic and plastic regions. Journal of Applied Mechanics 21:271-278.

Tse, F. S., I. E. Morse and R. T. Hinkle. 1978. Mechanical vibrations theory and applications. Allyn and Bacon, Inc., Boston, 449 p.

User manual for Data Translation, Incorporated DT1760 series interface subsystems DT1761 DT1762 DT1764 DT1765. 1978. Data Translation, 4 Strathmore Road, Natick, Massachusetts, 01760.

Walker, J. T. 1979. Design, construction, and evaluation of a continuous band cutting mechanism for reducing shatter in soybeans. Unpublished Doctoral Dissertation. Univerisity of Tennessee, Knoxville.

Warburton, G. B. 1957. On the theory of the acceleration damper. Journal of Applied Mechanics 24:322-324.

Williams, M. M. and C. B. Richey. 1973. A new approach to gathering soybeans. Transactions of the ASAE 16(6):1017-1019,1023.

Winston, F. Z. L. and E. Saibel. 1952. Free vibrations of constrained beams. Journal of Applied Mechanics 19:471-477.

Yen, T. C. and S. Kao. 1959. Vibration of beam-mass systems with time-dependent boundary conditions. Journal of Applied Mechanics 26:353-356.

Young, D. 1948. Vibration of a Beam with concentrated mass, spring, and dashpot. Journal of Applied Mechanics 15:65-72.

Yung, C. and R. B. Fridley. 1975. Simulation of Vibration of Whole Tree Systems Using Finite Elements. Transactions of the ASAE 18(3):475-481.

APPENDIXES

APPENDIX A

DATA ACQUISITION AND ANALYSIS PROGRAMS

```
C             THIS PROGRAM CONFIGURES THE DT2782 A/D
C             BOARD TO READ DATA SEQUENTIALLY ON EIGHT
C             CHANNELS AT A RATE OF 125K SAMPLES PER
C             SECOND.  SAMPLING IS INITIATED BY AN EX-
C             TERNAL TRIGGER AND THE DATA IS STORED IN
C             A FILE ON FLOPPY DISK.................
C
C     ******* THE PROGRAM ASKS THE USER TO SPECIFY THE *******
C     ******* NUMBER OF SAMPLES TO BE TAKEN, THE FILE  *******
C     ******* NUMBER OF THE FILE THE DATA IS TO BE     *******
C     ******* PLACED IN, AND WHETHER ZERO OFFSET IS TO *******
C     ******* BE REMOVED FROM THE DATA.............. *******
C
C
      EXTERNAL BUFF,SAMPN
      DIMENSION DATA(8),CAL(8)
      INTEGER NFILE,IDATA,K,ICAL,NUMSAM
C
C     ******* GET THE NUMBER OF SAMPLES TO BE TAKEN... *******
C
      CALL ASK1(NUMSAM)
C
C     ******* GET THE FILE USED FOR DATA STORAGE (ON DISK) ***
C
      CALL ASK2(NFILE)
C
C     ******* GET WHETHER OR NOT THE DATA IS TO BE AD- *******
C     ******* JUSTED FOR ZERO OFFSET................. *******
C
      CALL ASK3(ICAL)
C
C     ******* INITIALIZE THE OFFSET VALUES............ *******
C
      CALL ZERO(CAL)
C
C     ******* IF YOU WANT TO ADJUST THE DATA (TAKE OUT  ******
C     ******* ZERO OFFSET), DO IT NOW.................. ******
C
      IF(ICAL.EQ.0) CALL OFFSET(BUFF,SAMPN,DATA,CAL,IDATA,K)
C
C     ******* NOW GET READY AND TAKE SOME DATA......... ******
C
      CALL DATSUB(BUFF,SAMPN,DATA,CAL,IDATA,K,NUMSAM,NFILE)
C
      STOP
      END
      SUBROUTINE ASK1(NUMSAM)
      INTEGER NUMSAM
      CALL PRINT ('HOW MANY SAMPLES DO YOU WANT TO TAKE?')
      CALL PRINT ('THE NUMBER MUST BE DIVISIBLE BY 8')
      READ(5,*) NUMSAM
      RETURN
```

```
      END
      SUBROUTINE ASK2(NFILE)
      INTEGER NFILE
      CALL PRINT ('WHAT IS THE # OF THE DATA STORAGE FILE ?')
      CALL PRINT ('THE FILE NUMBER=XX IN FTNXX.DAT,WHERE XX=21-99')
      READ(5,*) NFILE
      RETURN
      END
      SUBROUTINE ASK3(ICAL)
      INTEGER ICAL
      BYTE DEC
20    WRITE(5,917)
917   FORMAT(1X,'DO YOU WANT ZERO OFFSET REMOVED? (Y OR N)')
      READ(5,918,ERR=20) DEC
918   FORMAT(A1)
      IF(DEC.EQ.'Y') ICAL=0
      IF(DEC.EQ.'N') ICAL=1
      RETURN
      END
      SUBROUTINE ZERO(CAL)
      DIMENSION CAL(8)
      DO 400 I=1,8
      CAL(I)=0.
400   CONTINUE
      RETURN
      END
      SUBROUTINE OFFSET(BUFF,SAMPN,DATA,CAL,IDATA,K)
      EXTERNAL BUFF,SAMPN
      DIMENSION DATA(8),CAL(8)
      INTEGER IDATA,K
C
C     ******* GIVE THE # OF CALIBRATION VALUES THAT WILL *****
C     ******* BE TAKEN TO THE MACRO SUBROUTINE THAT SETS *****
C     ******* UP THE A/D BOARD..........................  *****
C
      CALL IPOKE(IADDR(SAMPN),9600)
      CALL DELAY
      CALL SETUP
C
C             ..... GET THE ADDRESS IN MEMORY WHERE THE ......
C             ..... FIRST CALIBRATION READING IS RESIDING ....
C
      K=IADDR(BUFF)
C
C             ..... IF YOU WANT CALIBRATION,THROW AWAY THE ...
C             ..... FIRST 1600 READINGS FOR GOOD LUCK ........
C
      DO 375 I=1,1600
      K=K+2
375   CONTINUE
C
C             ..... SUM ALL THE REMAINING READINGS FOR .......
```

```
C             ..... EACH CHANNEL ..........................
C
      DO 325 I=1,1000
      DO 350 J=1,8
      IDATA=IPEEK(K)
      DATA(J)=(IDATA/2047.)*10.
      IF(IDATA.LT.0) DATA(J)=(IDATA/2048.)*10.
      CAL(J)=CAL(J)+DATA(J)
      K=K+2
350   CONTINUE
325   CONTINUE
C
C             .....NOW TAKE THE AVERAGES AND USE THESE.....
C
      DO 300 I=1,8
      CAL(I)=CAL(I)/1000.
300   CONTINUE
      RETURN
      END
      SUBROUTINE DATSUB(BUFF,SAMPN,DATA,CAL,IDATA,K,NUMSAM,NFILE)
      EXTERNAL BUFF,SAMPN
      DIMENSION DATA(8),CAL(8)
      INTEGER NFILE,IDATA,K,NUMSAM
C
C     ******* GIVE THE NUMBER OF DATA SAMPLES THAT WILL  *****
C     ******* BE TAKEN TO THE MACRO SUBROUTINE THAT SETS *****
C     ******* UP THE A/D BOARD..........................*****
C
      CALL IPOKE(IADDR(SAMPN),NUMSAM)
      CALL DELAY
      CALL SETUP
C
C     ******* GET THE ADDRESS OF THE FIRST LOCATION IN *******
C     ******* HARDWARE MEMORY WHERE THE A/D BOARD PUT  *******
C     ******* THE DATA.................................*******
C
      K=IADDR(BUFF)
C     ******* MOVE THE DATA FROM MEMORY INTO A FILE ON *******
C     ******* FLOPPY DISK..............................*******
C
      CALL PRINT ('THE DATA IS BEING TRANSFERRED TO DISK FILE NOW...')
      OPEN(UNIT=NFILE)
C
C             .....WANT TO WRITE 8 VALUES PER LINE....
C
      LOOP=NUMSAM/8
      DO 200 I=1,LOOP
      DO 100 J=1,8
      IDATA=IPEEK(K)
C
C             .....SUBTRACT THE OFFSET AND CONVERT IT TO VOLTS.....
C
```

```
      DATA(J)=((IDATA/2047.)*10.)-CAL(J)
      IF(IDATA.LT.0) DATA(J)=((IDATA/2048.)*10.)-CAL(J)
C
C             .....INCREMENT ADDRESS SO WILL LOOK....
C             .....AT THE NEXT DATUM THE NEXT TIME...
C
      K=K+2
100   CONTINUE
C
C             .....NOW WRITE THESE EIGHT DATA........
C             .....INTO THE SPECIFIED DATA FILE......
C
      WRITE(NFILE,930) (DATA(J),J=1,8)
930   FORMAT(8F10.5)
C
C             .....KEEP LOOPING UNTIL YOU GET ALL....
C             .....OF THE DATA.......................
C
200   CONTINUE
C
C             .....YOU'RE DONE.TIDY UP,CLOSE THE.....
C             .....SHOP,AND SAY GOOD-BYE.............
C
      CLOSE(UNIT=NFILE)
      END FILE NFILE
      CALL PRINT ('DATA TRANSFER IS COMPLETE')
      RETURN
      END
      SUBROUTINE DELAY
      DO 1 I=1,1000
1     CONTINUE
      RETURN
      END
```

```
      .TITLE INTERRUPT SERVICE ROUTINES,NON-INTERRUPT PRINT
      .TITLE THANX ROB
      ADCSR=  170400                  ; A/D control status register
      ADBUF=  170402                  ; A/D data buffer
      DMAWCR= 170404                  ; DMA word count register
      DMACAR= 170406                  ; DMA current address register
      INTVEC=    400                  ; base (interrupt) vector
      ERRVEC=    404                  ; A/D error/TIME-OUT error vector
      PRIO7=     340                  ; priority seven (highest)
      .GLOBL  OUT
      .MACRO  PRINT   DUM
      MOV     R1,-(SP)
      MOV     DUM,R1
      CALL    OUT
      MOV     (SP)+,R1
      .ENDM
      .NLIST BEX
      .ENABLE LC
      .MCALL .EXIT
;
;     set up read error (a/d error), bus error (time-out error),
;     and data collection completed (a/d done) interrupts.......
;
SETUP::       MTPS    #200                    ; disable interrupts
      MOV     #ISR,@#INTVEC           ; first word of interrupt vector
      MOV     #PRIO7,@#INTVEC+2       ; second word of interrupt vector
      MOV     #ESR,@#ERRVEC           ; first word of error vector
      MOV     #PRIO7,@#ERRVEC+2       ; second word of error vector
      MOV     SAMPN,R1                ; this is the number of samples
 to get
      NEG     R1                      ; take the two's complement of it
      MOV     R1,@#DMAWCR             ; _load it in the word count
 register
      MOV     #BUFF,@#DMACAR          ; load current address register
;
;     clean the a/d control and status register out before using it
;
INIT: CLR     @#ADCSR                 ; clear the error bits
      TST     @#ADBUF                 ; clear the a/d done bit
      TST     @#ADCSR                 ; see if read error bit is clear
      BMI     INIT                    ; if no, go back and clear it
 again
      TSTB    @#ADCSR                 ; see if ad done bit is clear
      BMI     INIT                    ; if no, go back and clear it
 again
      BITB    @#ADCSR,#020            ; see if time out error bit is
 clear
      BNE     INIT                    ; if no, go back and clear it
 again
      BIS     #40000,@#ADCSR          ; allow error interrupts
      BISB    #7,@#ADCSR+1            ; load the channel address
```

```
      MOVB    #176,@#ADCSR            ; allow a/d done interrupts,
 allow
                                      ; external triggering,increment
 mode,
                                      ; burst mode,and dma
      MTPS    #0                      ; enable interrupts
      PRINT   #MESS1
LOOP: BR      LOOP
END:  RETURN
ISR:  MTPS    #200
      TST     @#ADBUF
      CLR     @#ADCSR
      PRINT   #MESS2
      ADD     #2,(SP)
      MTPS    #0
      RTI
ESR:  MTPS    #200
      TST     @#ADCSR
      BPL     2$
      PRINT   #MESS3
      .EXIT
2$:   BITB    #20,@#ADCSR
      BEQ     3$
      PRINT   #MESS4
      .EXIT
3$:   PRINT   #MESS5
      .EXIT
MESS1:        .ASCII  /This is Mission Control,all systems are
 go./<12><15><200>
MESS2:        .ASCII  /Roger, Houston. We have data.../<7><12><15><200>
MESS3:        .ASCII  /Houston, we have an  a-d read error...
 /<12><15><200>
MESS4:        .ASCII  /Houston, we have an unidentified
 error.../<12><15><200>
MESS5:        .ASCII  /Houston, we have a bus time out
 error.../<12><15><200>
      .EVEN
SAMPN::       .WORD   0
BUFF::        .BLKW   16000.
      .END    SETUP
```

```
C     FFT4.FOR
C     THIS PROGRAM COMPUTES THE FAST FOURIER TRANSFORM OF A
C     REAL TIME FILE OR THE INVERSE FOURIER TRANSFORM OF A
C     FREQUENCY DOMAIN FILE.  THE AMPLITUDE SPECTRUM IS
C     ALSO CALCULATED.  THE  FILE TO BE TRANSFORMED MUST CONTAIN
C     NO MORE THAN 4096 DATA POINTS (FOR LESS THAN THIS
C     NUMBER, ZERO-FILLING IS USED).
C
C
      VIRTUAL X(4096)
      COMPLEX X
      BYTE TELL,RINT
      REAL A,B
      CALL PRINT ('WHAT IS THE NUMBER OF THE FILE TO BE FFT`ED?')
      ACCEPT *,NIN
800   CALL PRINT ('FOURIER TRANSFORM (F) OR INVERSE FFT (I)?')
      READ(5,900,ERR=800) TELL
900   FORMAT(A1)
      CALL PRINT ('WHAT IS THE FILE NUMBER THE FFT WILL BE STORED IN?')
      ACCEPT *,NFFT
      IF(TELL.EQ.'I') CALL PRINT('# OF SAMPLES IN ORIGINAL FILE?')
      IF(TELL.EQ.'I') ACCEPT *,NSCF
      IF(TELL.EQ.'I') SCF=FLOAT(NSCF)/4096.
      IF(TELL.EQ.'I') GO TO 20
      CALL PRINT ('WHAT IS THE FILE # FOR THE AMPLITUDE SPECTRUM?')
      ACCEPT *,NGAIN
      OPEN(UNIT=NFFT,INITIALSIZE=500)
      OPEN(UNIT=NGAIN,INITIALSIZE=200)
20    N=0
      IF(TELL.EQ.'I') GO TO 4
      DO 1 I=1,4096
      READ(NIN,*,END=2) A
      X(I)=CMPLX(A,0.)
      N=N+1
1     CONTINUE
2     CONTINUE
      SCF=1./FLOAT(N)
      IF(N.EQ.4096) GO TO 113
      DO 3 I=N+1,4096
      X(I)=CMPLX(0.,0.)
3     CONTINUE
113   CONTINUE
      GO TO 60
4     CONTINUE
      OPEN(UNIT=NFFT,INITIALSIZE=300)
      DO 5 I=1,4096
      READ(NIN,*,END=21) A,B
      X(I)=CMPLX(A,-B)
      N=N+1
5     CONTINUE
21    CONTINUE
      IF(N.EQ.4096) GO TO 60
```

```
      DO 6 I=N+1,4096
      X(I)=CMPLX(0.,0.)
6     CONTINUE
60    CONTINUE
      CALL FFT(X,4096,12)
      IF(TELL.EQ.'I') GO TO 9
      DO 7 I=1,4096
      X(I)=SCF*X(I)
      WRITE(NFFT,*) REAL(X(I)),AIMAG(X(I))
7     CONTINUE
      TOTPOW=0.
      CALL SPCTRM(NGAIN,NPHASE,NPSD,TOTPOW,X(1),0.)
      DO 8 I=2,2048
      CALL SPCTRM(NGAIN,NPHASE,NPSD,TOTPOW,X(I),X(4098-I))
8     CONTINUE
      CALL SPCTRM(NGAIN,NPHASE,NPSD,TOTPOW,X(2049),0.)
      CLOSE(UNIT=NFFT)
      CLOSE(UNIT=NGAIN)
25    CONTINUE
      STOP
9     CONTINUE
      DO 10 I=1,NSCF
      X(I)=SCF*X(I)
      WRITE(NFFT,*) REAL(X(I))
10    CONTINUE
      CLOSE(UNIT=NFFT)
      STOP
      END
      SUBROUTINE FFT(X,N,M)
      VIRTUAL X(N)
      COMPLEX X,U,W,T
      PI=3.14159265
      NV2=N/2
      NM1=N-1
      J=1
      DO 30 I=1,NM1
      IF(I.GE.J) GO TO 25
      T=X(J)
      X(J)=X(I)
      X(I)=T
25    K=NV2
26    IF(K.GE.J) GO TO 30
      J=J-K
      K=K/2
      GO TO 26
30    J=J+K
      DO 20 L=1,M
              LE=2**L
              LE1=LE/2
              U=CMPLX(1.0,0.0)
              W=CMPLX(COS(PI/FLOAT(LE1)),-SIN(PI/FLOAT(LE1)))
              DO 20 J=1,LE1
```

```
                    DO 10 I=J,N,LE
                    IP=I+LE1
                    T=X(IP)*U
                    X(IP)=X(I)-T
10                  X(I)=X(I)+T
20          U=U*W
      RETURN
      END
      SUBROUTINE SPCTRM(NGAIN,NPHASE,NPSD,TOTPOW,X,Y)
      COMPLEX X,Y
      A=REAL(X)
      B=REAL(Y)
      C=AIMAG(X)
      D=AIMAG(Y)
      G=(ABS(A+B))**2.+(ABS(C-D))**2.
      G=SQRT(G)
      WRITE(NGAIN,*) G
      RETURN
      END
```

```
C     FFT16.FOR
C     THIS PROGRAM COMPUTES THE FAST FOURIER TRANSFORM OF A
C     REAL TIME FILE OR THE INVERSE FOURIER TRANSFORM OF A
C     FREQUENCY DOMAIN FILE.  THE AMPLITUDE SPECTRUM IS
C     ALSO CALCULATED.  THE  FILE TO BE TRANSFORMED MUST CONTAIN
C     NO MORE THAN 16384 DATA POINTS (FOR LESS TTHAN THIS
C     NUMBER, ZERO-FILLING US USED).
C
C
      VIRTUAL X(16384)
      COMPLEX X
      BYTE TELL,RINT
      REAL A,B
      CALL PRINT ('WHAT IS THE NUMBER OF THE FILE TO BE FFT`ED?')
      ACCEPT *,NIN
800   CALL PRINT ('FOURIER TRANSFORM (F) OR INVERSE FFT (I)?')
      READ(5,900,ERR=800) TELL
900   FORMAT(A1)
      CALL PRINT ('WHAT IS THE FILE NUMBER THE FFT WILL BE STORED IN?')
      ACCEPT *,NFFT
      IF(TELL.EQ.'I') CALL PRINT('# OF SAMPLES IN ORIGINAL FILE?')
      IF(TELL.EQ.'I') ACCEPT *,NSCF
      IF(TELL.EQ.'I') SCF=FLOAT(NSCF)/16384.
      IF(TELL.EQ.'I') GO TO 20
      CALL PRINT ('WHAT IS THE FILE # FOR THE AMPLITUDE SPECTRUM?')
      ACCEPT *,NGAIN
      OPEN(UNIT=NFFT,INITIALSIZE=1000)
      OPEN(UNIT=NGAIN,INITIALSIZE=300)
20    N=0
      IF(TELL.EQ.'I') GO TO 4
      DO 1 I=1,16384
      READ(NIN,*,END=2) A
      X(I)=CMPLX(A,0.)
      N=N+1
1     CONTINUE
2     CONTINUE
      SCF=1./FLOAT(N)
      DO 3 I=N+1,16384
      X(I)=CMPLX(0.,0.)
3     CONTINUE
      GO TO 60
4     CONTINUE
      OPEN(UNIT=NFFT,INITIALSIZE=300)
      DO 5 I=1,16384
      READ(NIN,*,END=21) A,B
      X(I)=CMPLX(A,-B)
      N=N+1
5     CONTINUE
21    CONTINUE
      IF(N.EQ.16384) GO TO 60
      DO 6 I=N+1,16384
      X(I)=CMPLX(0.,0.)
```

```
6       CONTINUE
60      CONTINUE
        CALL FFT(X,16384,14)
        IF(TELL.EQ.'I') GO TO 9
        DO 7 I=1,16384
        X(I)=SCF*X(I)
        WRITE(NFFT,*) REAL(X(I)),AIMAG(X(I))
7       CONTINUE
        CALL SPCTRM(NGAIN,NPHASE,NPSD,TOTPOW,X(1),0.)
        DO 8 I=2,8192
        CALL SPCTRM(NGAIN,NPHASE,NPSD,TOTPOW,X(I),X(16386-I))
8       CONTINUE
        CALL SPCTRM(NGAIN,NPHASE,NPSD,TOTPOW,X(8193),0.)
        CLOSE(UNIT=NFFT)
        CLOSE(UNIT=NGAIN)
        STOP
9       CONTINUE
        DO 10 I=1,NSCF
        X(I)=SCF*X(I)
        WRITE(NFFT,*) REAL(X(I))
10      CONTINUE
        CLOSE(UNIT=NFFT)
        STOP
        END
        SUBROUTINE FFT(X,N,M)
        VIRTUAL X(N)
        COMPLEX X,U,W,T
        PI=3.14159265
        NV2=N/2
        NM1=N-1
        J=1
        DO 30 I=1,NM1
        IF(I.GE.J) GO TO 25
        T=X(J)
        X(J)=X(I)
        X(I)=T
25      K=NV2
26      IF(K.GE.J) GO TO 30
        J=J-K
        K=K/2
        GO TO 26
30      J=J+K
        DO 20 L=1,M
                LE=2**L
                LE1=LE/2
                U=CMPLX(1.0,0.0)
                W=CMPLX(COS(PI/FLOAT(LE1)),-SIN(PI/FLOAT(LE1)))
                DO 20 J=1,LE1
                        DO 10 I=J,N,LE
                        IP=I+LE1
                        T=X(IP)*U
                        X(IP)=X(I)-T
```

```
10                    X(I)=X(I)+T
20            U=U*W
      RETURN
      END
      SUBROUTINE SPCTRM(NGAIN,NPHASE,NPSD,TOTPOW,X,Y)
      COMPLEX X,Y
      A=REAL(X)
      B=REAL(Y)
      C=AIMAG(X)
      D=AIMAG(Y)
      G=(ABS(A+B))**2.+(ABS(C-D))**2.
      G=SQRT(G)
      WRITE(NGAIN,*) G
      RETURN
      END
```

```
C     COMPUT.FOR
C     MULTIPLICATION, DIVISION, POWER SPECTRAL DENSITY,
C     OR CROSS SPECTRAL DENSITY OF COMPLEX DATA FILES.
C     THE TWO FILES MUST BE THE SAME LENGTH.
C
      BYTE MDP
      CALL PRINT ('OUTPUT FILE #?')
      ACCEPT *,NOUT
      CALL PRINT ('MULTIPLICATION (M), DIVISION (D), POWER
     A SPECTRAL DENSITY (P), OR CROSS SPECTRAL DENSITY (C)?')
20    READ(5,900,ERR=20) MDP
900   FORMAT(A1)
      IF (MDP.EQ.'M') CALL MULT(NOUT)
      IF (MDP.EQ.'D') CALL DIV(NOUT)
      IF (MDP.EQ.'P') CALL PSD(NOUT)
      IF (MDP.EQ.'C') CALL CSD(NOUT)
      END FILE NOUT
      STOP
      END
      SUBROUTINE MULT(NOUT)
      COMPLEX X,Y,Z
      CALL PRINT ('WHAT FILE NUMBERS ARE TO BE MULTIPLIED? (#1,#2)')
      ACCEPT *,NOFIL1,NOFIL2
      DO 1 I=1,10000
      READ(NOFIL1,*,END=99) X
      READ(NOFIL2,*,END=99) Y
      Z=X*Y
      WRITE(NOUT,*) Z
1     CONTINUE
99    RETURN
      END
      SUBROUTINE DIV(NOUT)
      COMPLEX X,Y,Z
      CALL PRINT ('NUMERATOR FILE #,DENOMINATOR FILE #?')
      ACCEPT *,NOFIL1,NOFIL2
      DO 2 I=1,10000
      READ(NOFIL1,*,END=99) X
      READ(NOFIL2,*,END=99) Y
      Z=X/Y
      WRITE(NOUT,*) Z
2     CONTINUE
99    RETURN
      END
      SUBROUTINE PSD(NOUT)
      COMPLEX X,Y(4096)
      CALL PRINT ('WHAT FILE DO YOU WANT THE PSD OF?')
      ACCEPT *,NOFILE
      N=0
      DO 3 I=1,10000
      READ(NOFILE,*,END=99) X
      Y(I)=X*CONJG(X)
      N=N+1
```

```
3       CONTINUE
        KUSE=0
        X=2.*REAL(Y(1))
        WRITE(NOUT,*) X
        DO 4 I=2,N/2
        X=REAL(Y(I))+REAL(Y(I-KUSE))
        WRITE(NOUT,*) X
        KUSE=KUSE+1
4       CONTINUE
99      RETURN
        END
        SUBROUTINE CSD(NOUT)
        COMPLEX X,Y,Z
        CALL PRINT ('WHAT FILE NUMBERS DO YOU WANT THE CSD OF?(#1,#2)')
        ACCEPT *,NOFIL1,NOFIL2
        DO 1 I=1,10000
        READ(NOFIL1,*,END=99) X
        READ(NOFIL2,*,END=99) Y
        Z=CONJUG(X)*Y
        WRITE(NOUT,*) Z
1       CONTINUE
99      RETURN
        END
```

```
C     CHOP.FOR:  "CHOPS OFF" SPECIFIED PORTIONS (AT
C     THE BEGINNING AND/OR THE END) OF A DATA FILE.
C
      INTEGER OUTFIL
      BYTE DEC
      IC=0
      CALL PRINT ('WHAT IS THE # OF THE FILE TO BE CHOPPED?')
      ACCEPT *,INFILE
      CALL PRINT ('WHAT FILE # DOES THE CHOPPED FILE BECOME?')
      ACCEPT *,OUTFIL
      CALL PRINT ('CHOP OFF THE END OF THE FILE? (Y OR N)')
20    READ(5,900,ERR=20) DEC
900   FORMAT(A1)
      IF(DEC.EQ.'Y') CALL END(INFILE,OUTFIL,IC)
      IUSE=INFILE
      IF(DEC.EQ.'Y') IUSE=OUTFIL
      CALL PRINT ('CHOP OFF THE BEGINNING OF THE FILE? (Y OR N)')
30    READ(5,900,ERR=30) DEC
      IF(DEC.EQ.'Y') CALL BEGIN(IUSE,OUTFIL,IC)
      CALL PRINT ('THE NEW FILE CONTAINS THIS # OF VALUES:')
      WRITE(5,*) IC
      STOP
      END
      SUBROUTINE BEGIN(INFILE,OUTFIL,IC)
      DIMENSION X(5000)
      INTEGER OUTFIL
3     CALL PRINT ('WHAT IS THE # OF THE LAST POINT TO BE CHOPPED FROM
     1 THE BEGINNING OF THE FILE?')
      ACCEPT *,K
      DO 2 I=1,K
      READ(INFILE,*,END=99) X(1)
2     CONTINUE
      II=0
      DO 1 I=1,5000
      READ(INFILE,*,END=98) X(I)
      II=II+1
1     CONTINUE
98    CONTINUE
      DO 4 I=1,II
      WRITE(OUTFIL,*) X(I)
      IC=IC+1
4     CONTINUE
      END FILE OUTFIL
      RETURN
99    CALL PRINT('?CHOP GOOF: TRIED TO CHOP PAST END OF FILE')
      REWIND INFILE
      GO TO 3
      RETURN
      END
      SUBROUTINE END(INFILE,OUTFIL,IC)
      INTEGER OUTFIL
      CALL PRINT ('WHAT IS THE # OF THE FIRST POINT TO BE CHOPPED FROM
```

```
     1 THE END OF THE FILE?')
       ACCEPT *,K
       K=K-1
       DO 1 I=1,K
       READ(INFILE,*,END=99) X
       WRITE(OUTFIL,*) X
       IC=IC+1
1      CONTINUE
99     REWIND INFILE
       END FILE OUTFIL
       REWIND OUTFIL
       RETURN
       END
```

```
C     ADZERO:  THIS PROGRAM ADDS ZEROS TO THE
C     BEGINNING AND/OR END OF A SPECIFIED FILE.
C
      CALL PRINT ('WHAT FILE # WILL 0`S BE ADDED TO?')
      ACCEPT *,NOFILE
      CALL PRINT ('# OF ZEROS TO BE ADDED TO BEGINNING?')
      ACCEPT *,NBEGIN
      CALL PRINT ('# OF ZEROS TO BE ADDED TO END?')
      ACCEPT *,NEND
      CALL PRINT ('# OF NEW FILE WITH ZEROS ADDED?')
      ACCEPT*,NEWFIL
      X=0.
      K=0
      IF (NBEGIN.EQ.0) GO TO 10
      DO 1 I=1,NBEGIN
      WRITE(NEWFIL,*) X
      K=K+1
1     CONTINUE
10    CONTINUE
      DO 2 I=1,10000
      READ(NOFILE,*,END=3) Y
      WRITE(NEWFIL,*) Y
      K=K+1
2     CONTINUE
3     CONTINUE
      IF (NEND.EQ.0) GO TO 20
      DO 4 I=1,NEND
      WRITE(NEWFIL,*) X
      K=K+1
4     CONTINUE
20    CONTINUE
      END FILE NEWFIL
      CALL PRINT ('THE NEW FILE CONTAINS THIS # OF VALUES:')
      WRITE(5,*) K
      STOP
      END
```

```
C
C
C     SEPRAT.FOR:
C     THIS PROGRAM READS DATA FROM A DISK FILE CREATED BY THE
C     PROGRAM "SOR.FOR" AND CREATES FOUR SEPARATE DATA FILES--
C     (ONE FOR BLADE SPEED AND ONE FOR EACH OF THE THREE ACCEL-
C     EROMETERS)
C
C
      REAL A(8)
      CALL PRINT ('WHAT IS THE NUMBER OF THE FILE TO BE SEPARATED?')
      ACCEPT *,NFILEN
      CALL PRINT ('WHAT ARE THE #'S OF THE 4 FILES TO BE CREATED?
     1 (#1,#2,#3,#4)')
      ACCEPT *,NFILE1,NFILE2,NFILE3,NFILE4
      DO 1 I=1,3000
      READ(NFILEN,*,END=99) (A(J),J=1,8)
      A(4)=A(4)*1.
      A(8)=A(8)*1.
      DO 3 J=1,5,4
      A(J)=A(J)*3860.
      A(J+1)=A(J+1)*3860.
      A(J+2)=A(J+2)*3860.
3     CONTINUE
      DO 2 J=1,5,4
      WRITE(NFILE1,*) A(J)
      WRITE(NFILE2,*) A(J+1)
      WRITE(NFILE3,*) A(J+2)
      WRITE(NFILE4,*) A(J+3)
2     CONTINUE
1     CONTINUE
99    END FILE NFILE1
      END FILE NFILE2
      END FILE NFILE3
      END FILE NFILE4
      STOP
      END
```

```
C     LOOK.FOR:  THIS PROGRAM OUTPUTS SPECIFIED FILES
C     TO THE TELETYPE OR LINE PRINTER.
C     THE DATA IN THE FILES MUST BE ONE VALUE PER LINE
C
C
      DIMENSION NOFILE(10),XLO(10),XHI(10),N(10),J(10)
      BYTE B(132)
      CALL PRINT ('THE CONSOLE NUMBER IS 7, THE PRINTER NUMBER IS 6')
      CALL PRINT ('SO IF YOU WANT OUTPUT ON THE SCREEN, TYPE 7 (AND
 RETURN)
     A  IF YOU WANT OUTPUT ON THE PRINTER, TYPE 6 (AND RETURN)')
      ACCEPT *,NDEVEX
      CALL PRINT ('HOW MANY CHARACTERS ACROSS THE SCREEN OR PAGE DO YOU

     A  WANT THE GRAPH TO BE? PRINTER MAX IS 126, SCREEN MAX IS 74')
      ACCEPT *,LINE
      CALL PRINT ('HOW MANY CURVES WILL BE PUT ON THE SAME GRAPH?')
      ACCEPT *,NUMBER
      CALL PRINT ('WHAT ARE THE FILE NUMBER(S) THAT ARE TO BE
 GRAPHED?')
      DO 1 I=1,NUMBER
      WRITE(7,920) I
920   FORMAT(1X,'FILE #',I1,'?')
      ACCEPT *,NOFILE(I)
1     CONTINUE
      IF(NDEVEX.EQ.7.AND.LINE.GT.74) LINE=74
      IF(NDEVEX.EQ.6.AND.LINE.GT.126) LINE=126
      CALL GRAPH(NOFILE,XLO,XHI,N,NDEVEX,LINE,B,NUMBER)
      STOP
      END
```

```
      SUBROUTINE GRAPH(NOFILE,XLO,XHI,N,NDEVEX,LINE,B,NUM,J,SYMBOL)
      DIMENSION NOFILE(NUM),XLO(NUM),XHI(NUM),N(NUM),J(NUM)
      BYTE B(LINE),SYMBOL(NUM)
      BYTE YAXIS,BLANK,XAXIS,CEZR
      YAXIS='+'
      BLANK=' '
      XAXIS='+'
      CEZR='-'
      DO 2 I=1,NUM
      II=I+20
      CALL LOHIN(II,XLO(I),XHI(I),N(I))
2     CONTINUE
      LOOP=32766
      XLONEW=50000000.
      XHINEW=-50000000.
      DO 6 I=1,NUM
      LOOP=MIN0(N(I),LOOP)
      XLONEW=AMIN1(XLO(I),XLONEW)
      XHINEW=AMAX1(XHI(I),XHINEW)
6     CONTINUE
      RLINE=FLOAT(LINE-1)
      SCALE=XHINEW-XLONEW
      SCALE=LINE/SCALE
      IF(XLONEW.GT.0.) SCALE=RLINE/XHINEW
      IF(XLONEW.GE.0.0) IX=1
      IF(XLONEW.LT.0.0) CALL ORIGIN(XLONEW,SCALE,IX)
      WRITE(NDEVEX,90) XLONEW,XHINEW
90    FORMAT('0','MINIMUM VALUE=',F16.7,5X,'MAXIMUM VALUE=',F16.7)
      DO 1 L=1,LINE
      B(L)=YAXIS
1     CONTINUE
      WRITE(NDEVEX,92) B
92    FORMAT('0',4X,128A1)
      DO 11 L=1,LINE
11    B(L)=BLANK
      B(IX)=XAXIS
      KCOUNT=10
      LCOUNT=10
      DO 5 J2=1,LOOP
      IF(KCOUNT.EQ.J2) CALL EZREAD(B,KCOUNT,LINE,CEZR,IX)
      DO 3 I=1,NUM
      II=I+20
      READ(II,*) A
      A=SCALE*A+.5
      J(I)=INT(A)+IX
      CALL KEY(I,J(I),B(J(I)),SYMBOL,NUM)
3     CONTINUE
      LCOUNT=LCOUNT+1
      IF (LCOUNT.NE.KCOUNT) GO TO 27
      MCOUNT=KCOUNT-10
      WRITE(NDEVEX,999) MCOUNT,B
999   FORMAT(' ',I4,128A1)
```

```
      GO TO 29
27    CONTINUE
      WRITE(NDEVEX,93) B
93    FORMAT(' ',4X,128A1)
29    CONTINUE
      DO 4 I=1,LINE
      B(I)=BLANK
4     CONTINUE
      B(IX)=XAXIS
5     CONTINUE
      DO 98 I=1,NUM
      II=I+20
98    CLOSE(UNIT=II)
99    STOP
      END
      SUBROUTINE ORIGIN(XLONEW,SCALE,IX)
      USE=ABS(XLONEW)
      USE=SCALE*USE+.5
      IX=INT(USE)
      IX=IX+1
      RETURN
      END
      SUBROUTINE KEY(I,K,C,SYMBOL,NUM)
      BYTE C,SYMBOL(NUM)
      C=SYMBOL(I)
      RETURN
      END
      SUBROUTINE EZREAD(B,KCOUNT,LINE,CEZR,IX)
      BYTE B(LINE)
      BYTE CEZR
      DO 23 I=1,LINE
23    B(I)=CEZR
      B(IX)='+'
      KCOUNT=KCOUNT+10
      RETURN
      END
```

```
      SUBROUTINE LOHIN(NOFILE,XLO,XHI,N)
C
C     THIS SUBROUTINE FINDS THE MINIMUM, MAXIMUM, AND NUMBER
C     OF ENTRIES IN A FILE.
C     ---ADAPTED FROM "MULTICHANNEL TIME SERIES ANALYSIS WITH-----
C     ---DIGITAL COMPUTER PROGRAMS" BY E. A. ROBINSON, PAGE 21.---
C
C     NOFILE=NUMBER (XX) OF THE FILE FTNXX.DAT TO BE EXAMINED.
C     XLO=MINIMUM VALUE IN THE FILE.
C     XHI=MAXIMUM VALUE IN THE FILE.
C     N=NUMBER OF ENTRIES IN THE FILE.
C
      N=0
      READ (NOFILE,*,END=99) X
      N=N+1
      XLO=X
      XHI=X
      DO 1 I=1,10000
      READ (NOFILE,*,END=99) X
      N=N+1
      IF(X.LT.XLO) XLO=X
      IF(X.GT.XHI) XHI=X
1     CONTINUE
99    REWIND NOFILE
      RETURN
      END
```

APPENDIX B

TEST REPLICATION DATA

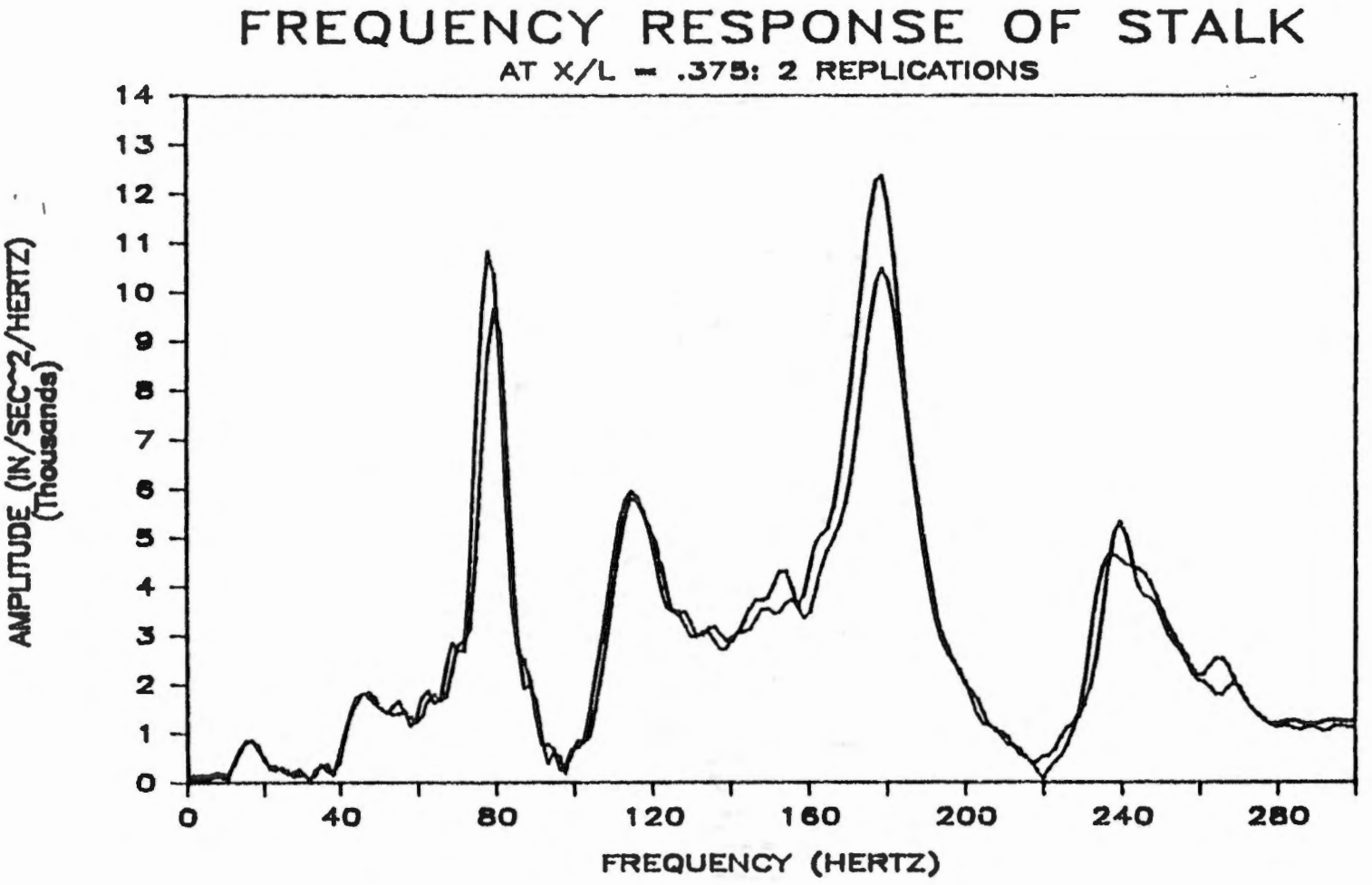
FREQUENCY RESPONSE OF STALK
AT X/L = .375: 2 REPLICATIONS
AMPLITUDE (IN/SEC**2/HERTZ)
(Thousands)
0
1
2
3
4
5
6
7
8
9
10
11
12
13
14
0
40
80
120
160
200
240
280
FREQUENCY (HERTZ)

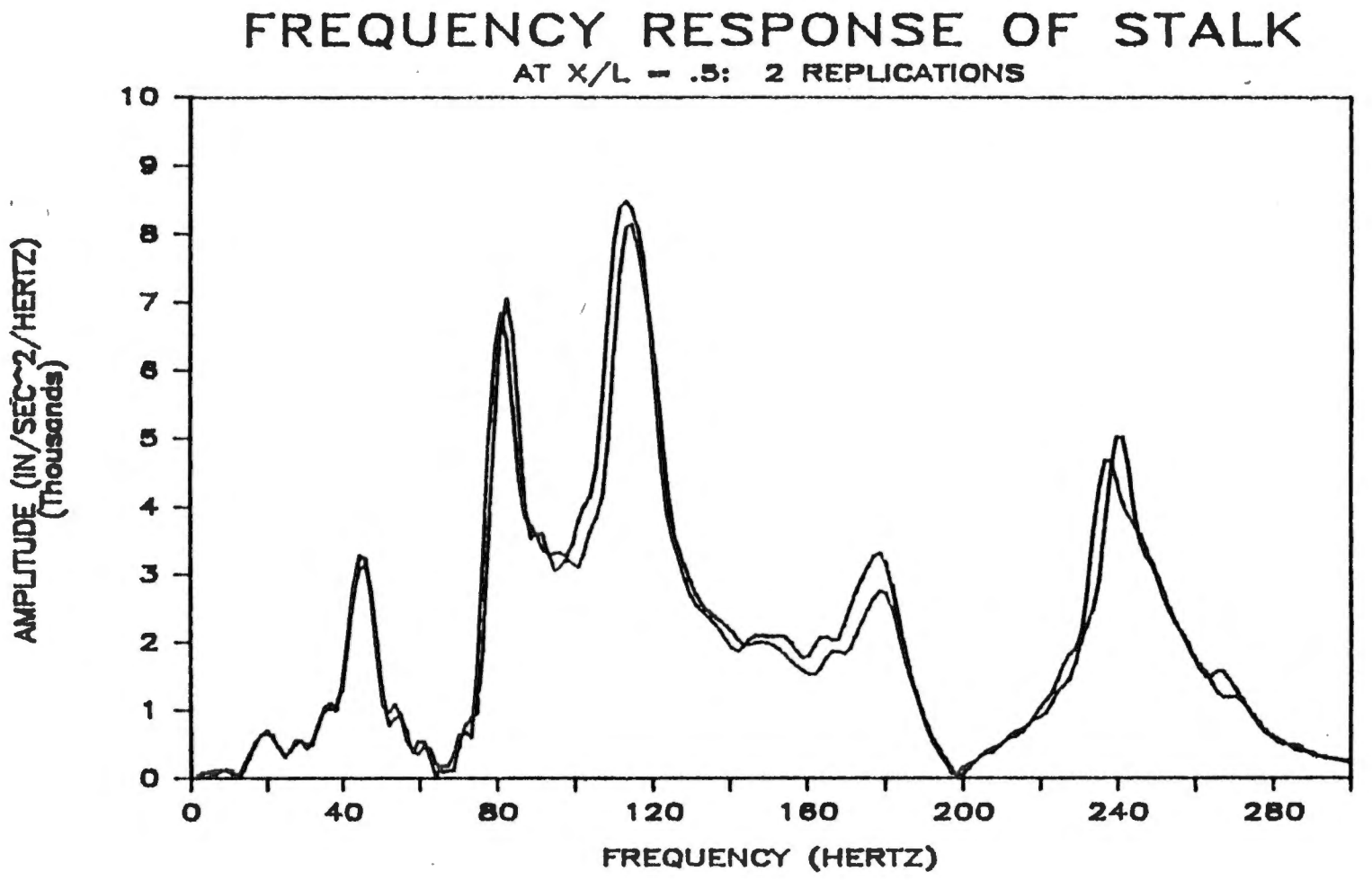
FREQUENCY RESPONSE OF STALK
AT X/L = .5: 2 REPLICATIONS
AMPLITUDE (IN/SEC**2/HERTZ)
(Thousands)
10
9
8
7
6
5
4
3
2
1
0
0
40
80
120
160
200
240
280
FREQUENCY (HERTZ)

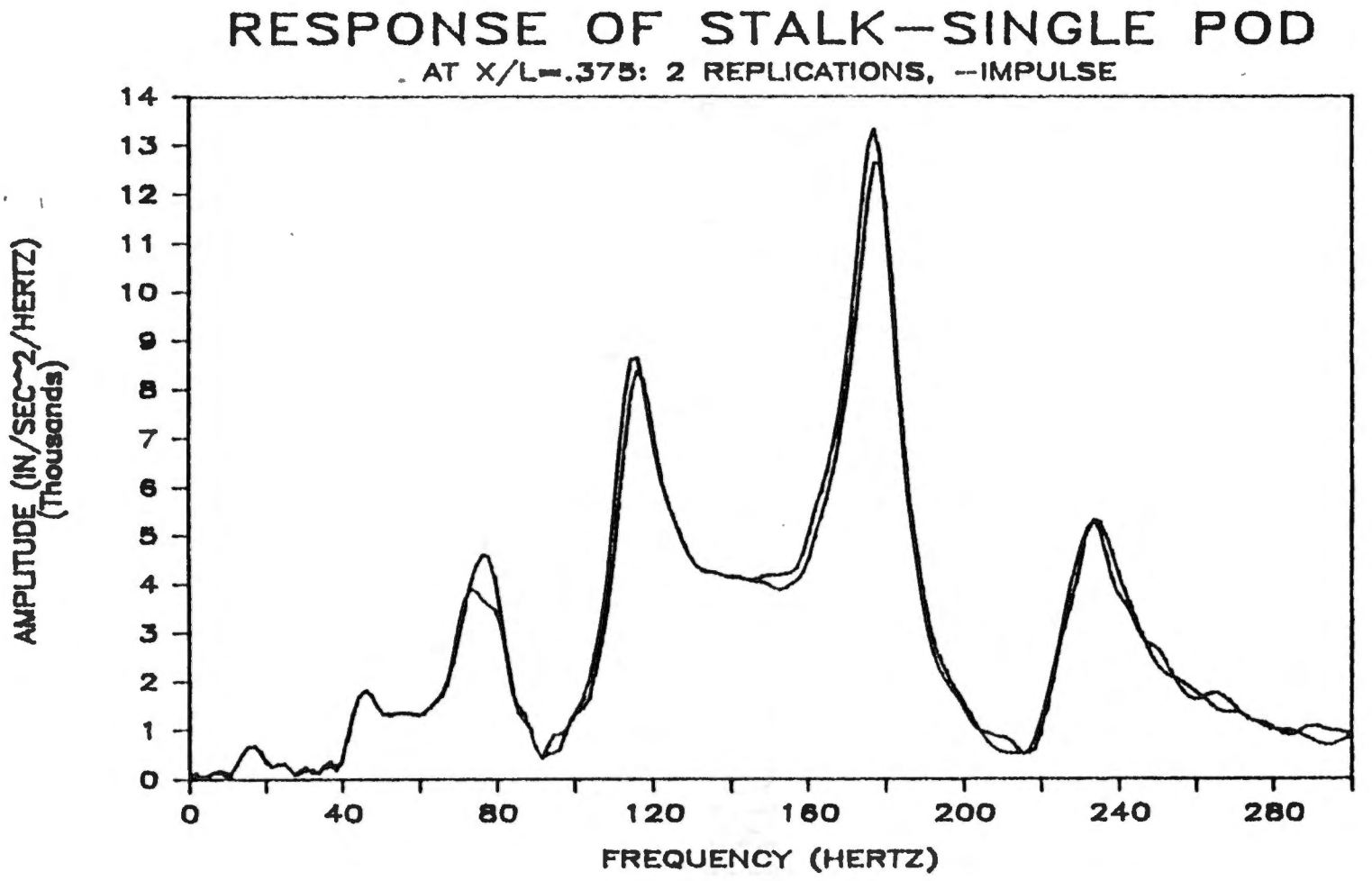
RESPONSE OF STALK—SINGLE POD
AT X/L=.375: 2 REPLICATIONS, —IMPULSE
AMPLITUDE (IN/SEC^2/HERTZ) (Thousands)
14
13
12
11
10
9
8
7
6
5
4
3
2
1
0
0
40
80
120
160
200
240
280
FREQUENCY (HERTZ)

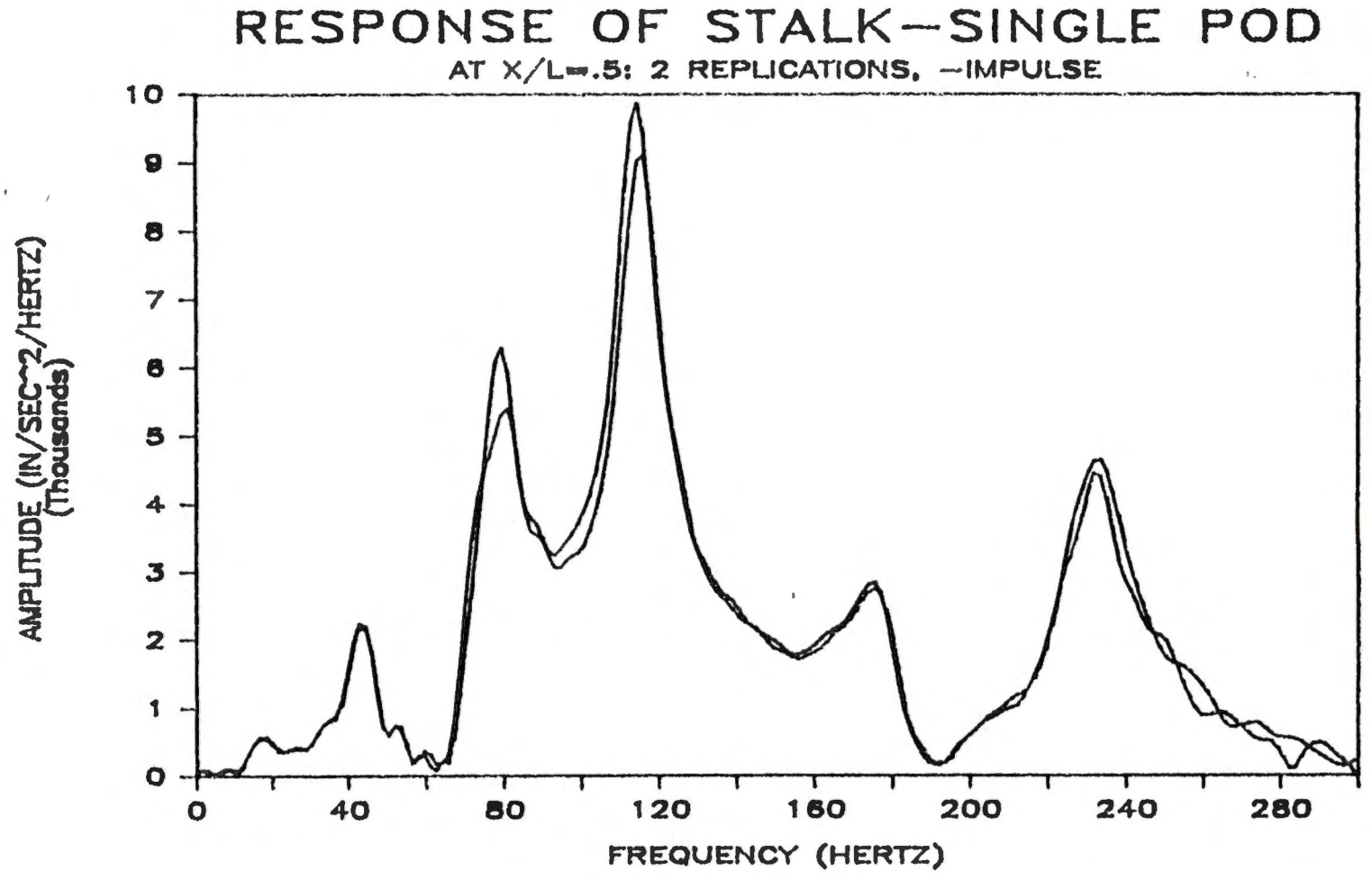
RESPONSE OF STALK—SINGLE POD
AT X/L=.5: 2 REPLICATIONS, —IMPULSE
AMPLITUDE (IN/SEC^2/HERTZ)
(Thousands)
10
9
8
7
6
5
4
3
2
1
0
0
40
80
120
160
200
240
280
FREQUENCY (HERTZ)

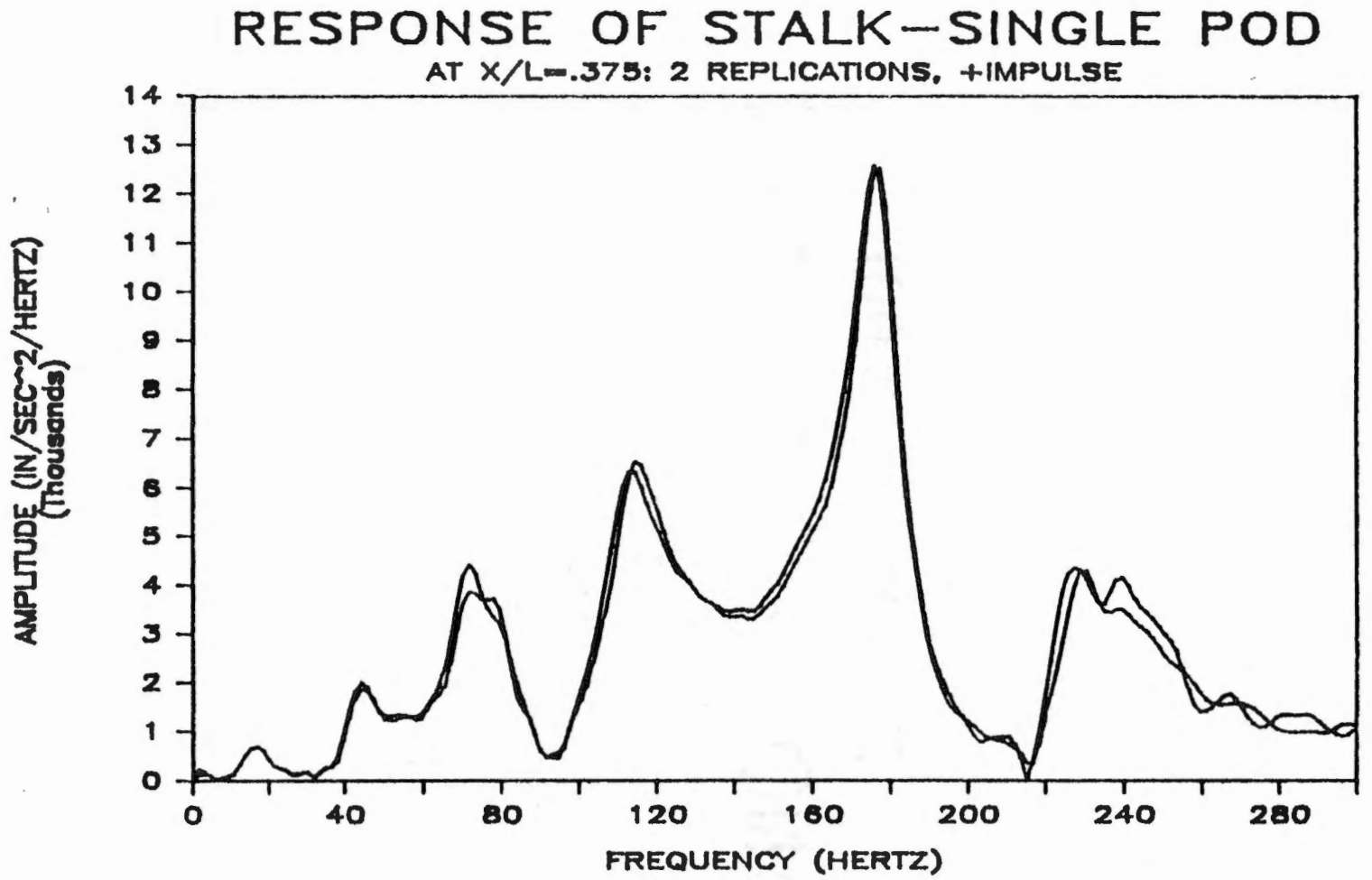
RESPONSE OF STALK—SINGLE POD
AT X/L=.375: 2 REPLICATIONS, +IMPULSE
AMPLITUDE (IN/SEC^2/HERTZ)
(Thousands)
0
1
2
3
4
5
6
7
8
9
10
11
12
13
14
0
40
80
120
160
200
240
280
FREQUENCY (HERTZ)

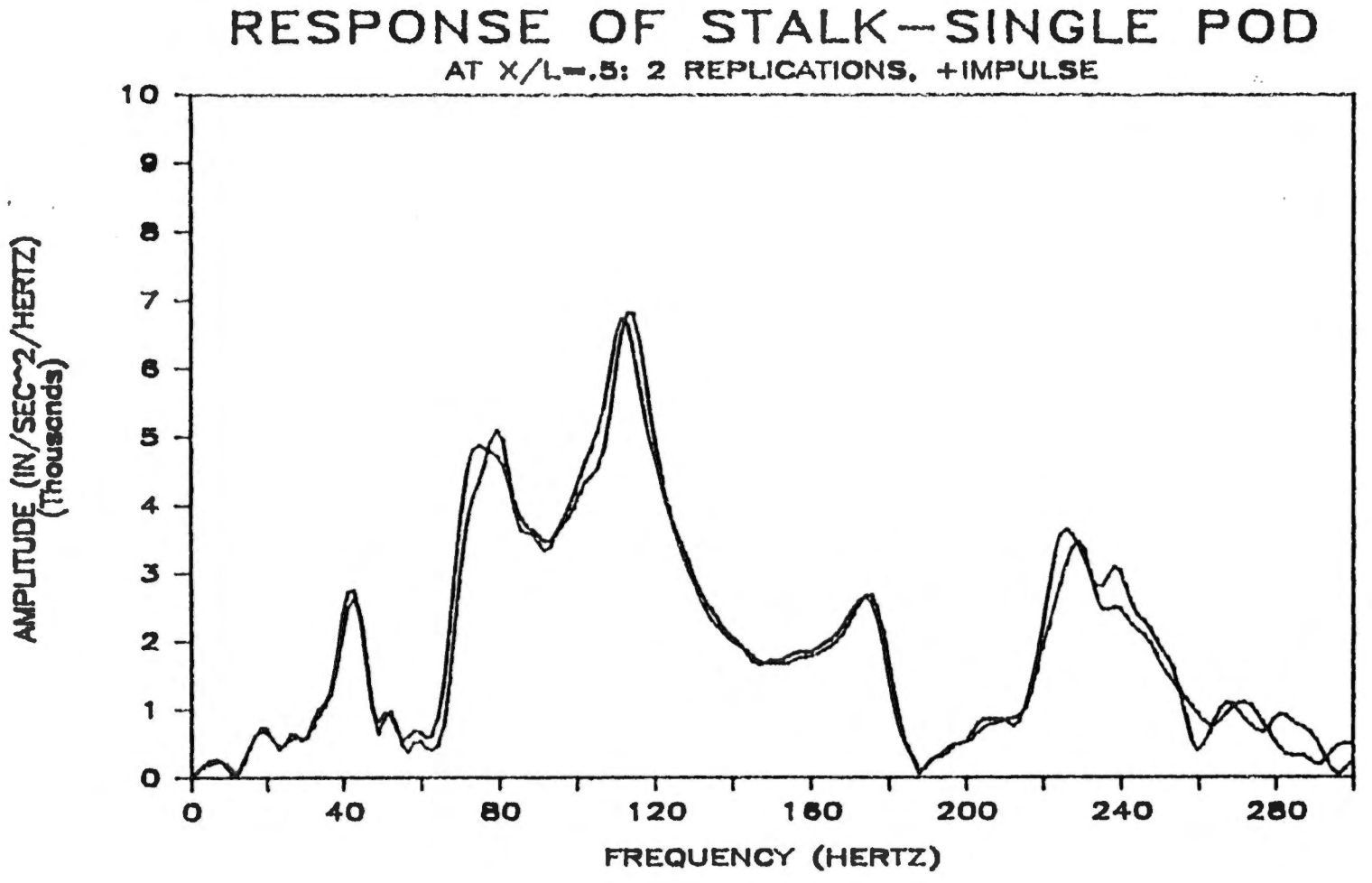
RESPONSE OF STALK—SINGLE POD
AT X/L=.5: 2 REPLICATIONS, +IMPULSE
AMPLITUDE (IN/SEC^2/HERTZ)
(Thousands)
10
9
8
7
6
5
4
3
2
1
0
0
40
80
120
160
200
240
280
FREQUENCY (HERTZ)

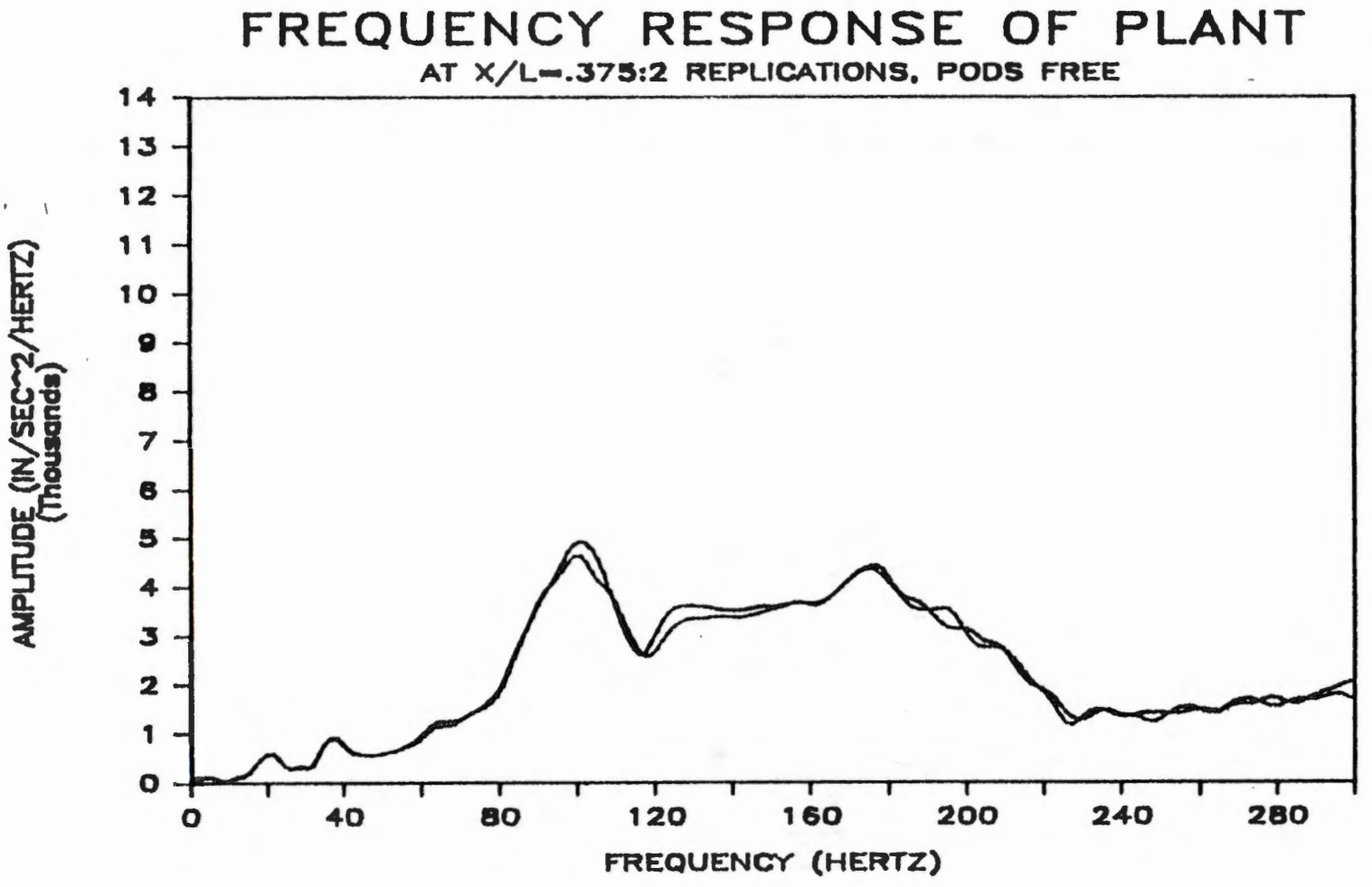
FREQUENCY RESPONSE OF PLANT
AT X/L=.375:2 REPLICATIONS, PODS FREE
AMPLITUDE (IN/SEC^2/HERTZ)
(Thousands)
14
13
12
11
10
9
8
7
6
5
4
3
2
1
0
0
40
80
120
160
200
240
280
FREQUENCY (HERTZ)

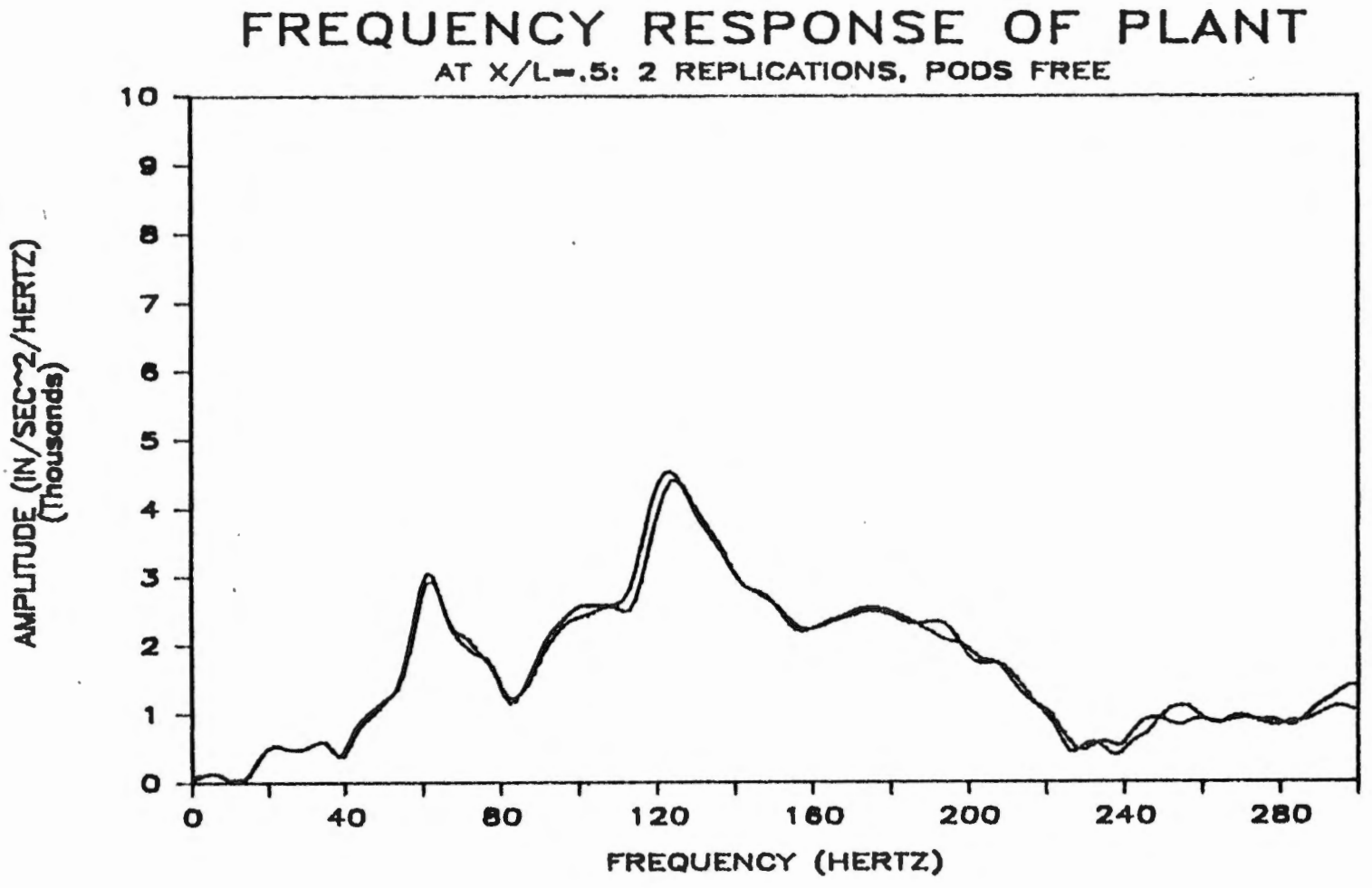
FREQUENCY RESPONSE OF PLANT
AT X/L=.5: 2 REPLICATIONS, PODS FREE
AMPLITUDE (IN/SEC**2/HERTZ)
(Thousands)
10
9
8
7
6
5
4
3
2
1
0
0
40
80
120
160
200
240
280
FREQUENCY (HERTZ)

VITA

Steve Shoulders was born in Portsmouth, Virginia on March 6, 1956. He attended elementary schools in several southeastern states and was graduated from Clarksville High School, Clarksville, Tennessee, in 1974.

In September of 1974, the author entered the University of Tennessee, Knoxville, and received a Bachelor of Science degree in Agricultural Engineering in June of 1977. The following fall, he entered the Graduate School at The University of Tennessee, Knoxville, and accepted a graduate research assistantship in the Agricultural Engineering Department. He completed his graduate studies in August of 1985 and received a Doctor of Philosophy degree with a major in Agricultural Engineering.